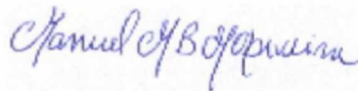


Thesis presented to the Instituto Tecnológico de Aeronáutica, in partial fulfillment of the requirements for the degree of Doctor of Science in the Graduate Program of Physics, Field of Nuclear Physics.

Ronaldo Vieira Lobato

**SGRS/AXPS AND BINARY STAR MERGERS:
ELECTROMAGNETIC AND GRAVITATIONAL
EMISSION**

Thesis approved in its final version by signatories below:



Prof. Dr. Manuel Máximo Bastos Malheiro de Oliveira

Advisor



Prof. Dr. Jorge Armando Rueda Hernández

Co-advisor



Prof. Dr. Jaziel Goulart Coelho

Co-advisor

Prof. Dr. Pedro Teixeira Lacava

Pro-Rector of Graduate Courses

Campo Montenegro
São José dos Campos, SP - Brazil
2019

Cataloging-in Publication Data
Documentation and Information Division

Vieira Lobato, Ronaldo
SGRs/AXPs and binary star mergers: electromagnetic and gravitational emission / Ronaldo
Vieira Lobato.
São José dos Campos, 2019.
114f.

Thesis of Doctor of Science – Course of Physics. Area of Nuclear Physics – Instituto Tecnológico
de Aeronáutica, 2019. Advisor: Prof. Dr. Manuel Máximo Bastos Malheiro de Oliveira.
Co-advisors: Prof. Dr. Jorge Armando Rueda Hernández and Prof. Dr. Jaziel Goulart Coelho.

1. Estrelas anãs. 2. Raios gama. 3. Estrela de nêutrons. 4. Campos magnéticos.
5. Radiofrequência. 6. Astrofísica. 7. Física. I. Instituto Tecnológico de Aeronáutica. II. Title.

BIBLIOGRAPHIC REFERENCE

VIEIRA LOBATO, Ronaldo. **SGRs/AXPs and binary star mergers: electromagnetic and gravitational emission**. 2019. 114f. Thesis of Doctor of Science – Instituto Tecnológico de Aeronáutica, São José dos Campos.


CESSION OF RIGHTS

AUTHOR'S NAME: Ronaldo Vieira Lobato

PUBLICATION TITLE: SGRs/AXPs and binary star mergers: electromagnetic and gravitational emission.

PUBLICATION KIND/YEAR: Thesis / 2019

It is granted to Instituto Tecnológico de Aeronáutica permission to reproduce copies of this thesis and to only loan or to sell copies for academic and scientific purposes. The author reserves other publication rights and no part of this thesis can be reproduced without the authorization of the author.



Ronaldo Vieira Lobato

Praça Marechal Eduardo Gomes, 50

Departamento de Física, Instituto Tecnológico de Aeronáutica – 12228900, São José dos Campos, SP

SGRS/AXPS AND BINARY STAR MERGERS: ELECTROMAGNETIC AND GRAVITATIONAL EMISSION

Ronaldo Vieira Lobato

Thesis Committee Composition:

Prof. Dr. Rubens de Melo Marinho Junior	Chairperson	-	ITA
Prof. Dr. Manuel Máximo Bastos Malheiro de Oliveira	Advisor	-	ITA
Prof. Dr. Jorge Armando Rueda Hernández	Co-advisor	-	ICRANet
Prof. Dr. Jaziel Goulart Coelho	Co-advisor	-	UTFPR
Prof. Dr. César Henrique Lenzi		-	ITA
Prof. Dr. João Braga		-	INPE
Prof. Dr. Márcio Eduardo da Silva Alves		-	UNESP

“In the vastness of space and the immensity of time, it is my joy to share a planet and an epoch with” those that I love.

Acknowledgments

To everyone that made this possible.

CNPq process 141157/2015-1 and CAPES/PDSE/88881.134089/2016-01 for financial support.

“Der Unterschied zwisch Vergangenheit, Gegenwart und Zukunft ist nur eine Illusion...” —
ALBERT EINSTEIN

Resumo

Neste trabalho, abordamos os pulsares de anãs brancas recentemente encontrados e o número crescente de anãs brancas massivas e magnéticas encontradas. Estudamos a possibilidade de alguns 'repetidores de γ -moles' (SGRs) e 'pulsares de raios-X anômalos' (AXPs) serem pulsares de anãs brancas.

Usando modelos auto-consistentes (incluindo rotação observada e equações de estado realísticas) estimamos a massa, o raio e o momento de inércia das estrelas como anãs brancas (WDs). Fazemos também uma revisão dos modelos realísticos considerando as mesmas como estrelas de nêutrons (NS). O campo magnético dipolar é então estimado para as fontes como WDs e NSs.

Investigamos também as fontes dentro do contexto de modelos de emissão eletromagnética, investigando a radiação X, gamma e rádio. A condição para produção de pares é estudada com parâmetros realísticos e as linhas de morte são obtidas para a radiação gamma e de radio. Os modelos estudados versam sobre a possibilidade de emissão gamma perto e longe das fontes e conseqüentemente a produção de radio. Mostramos que o tamanho da fonte i.e., o raio da estrela R , e a razão entre este e o cilindro de luz R_{lc} , são escalas importantes para entender a emissão eletromagnética nestes modelos. Concluimos que a emissão observada de raios gamma moles, raios X duros e a ausência de radiação rádio são melhor entendidas numa descrição das SGRs/AXPs como pulsares de anãs brancas, onde esta razão entre R_{lc} e R é 100 vezes menor do que para o caso dos magnetares. Este fato permite-nos concluir que para as SGRs/AXPs como anãs brancas o campo magnético no cilindro de luz é 100 vezes mais intenso do que como estrela de nêutrons, facilitando assim a emissão em raio X duros e raios gamma moles.

Por fim, estudamos as propriedades de sistemas binários de NS-NS, WD-NS e WD-WD, analisando o evento de ondas gravitacionais GW170817, tentando entender os mecanismos de emissão eletromagnética envolvidos. Em particular, um novo tipo de fusão de duas anãs brancas (WD-WD) foi investigada, podendo ser um progenitor de anãs brancas muito massivas, rápidas e magnéticas. Mostramos que a onda gravitacional recebida no evento GW170817, fruto de uma fusão de estrelas de nêutrons, não é compatível com a contraparte eletromagnética observada, que parece vir de uma fusão WD-WD.

Abstract

In this work, we discuss the white dwarf pulsars found recently and the massive and magnetic white dwarfs reported in the few years. We make the reference of the possibility of some soft γ repeaters (SGRs) and anomalous X-ray pulsars (AXPs) being part of this class of white dwarfs pulsars.

Using self-consistently models which consider the sources' rotation and a realistic EoS, we estimate the mass, radius and moment of inertia of these sources as white dwarfs (WD). We also review them as neutrons stars (NS) with self-consistently models estimating the radius in both cases.

We investigated these sources as WDs and NSs within of the context of high energy emission, studying hard X-ray, γ and radio band. The pair condition with realist parameters is calculated and the death lines for the electromagnetic radiation are obtained for γ production and consequently for radio emission. We have shown that the size of the source, i.e. the radius of the star R , and the ratio between it and the light cylinder R_{lc} , are important scales to understand the electromagnetic emission in these models. We conclude that the observed electromagnetic emission for soft gamma rays and the absence of radio radiation are better understood in a description of SGRs/AXPs as white dwarf pulsars, where this ratio between R_{lc} and R is 100 times smaller than in the case of magnetars. This fact, allows us to conclude that for SGRs/AXPs as white dwarfs the magnetic field in the light cylinder is 100 times more intense than as neutron stars, thus facilitating the emission in hard X-rays and soft gamma rays.

We also study the properties of binary systems composed of NS-NS, WD-NS, WD-WD analyzing the event GW170817, trying to understand the nature and mechanism of the high energy emission of this event. We analyzed in particular the electromagnetic emission of a new type of two white dwarf merger (WD-WD), which may be the progenitor of very massive, fast and magnetic white dwarfs. We show that the gravitational wave received in the GW170817 event as a result of a fusion of neutron stars, is not compatible with the observed electromagnetic counterpart, that seems come from a WD-WD merger.

Contents

1	INTRODUCTION	11
2	WHITE DWARFS AND SGRs/AXPs	14
2.1	White dwarfs pulsars	14
2.1.1	AR Scorpii	17
2.1.2	AE Aquarii	18
2.2	Soft Gamma Repeaters (SGRs) and Anomalous X-Ray Pulsars (AXPs)	18
2.2.1	4U 0142+61	20
2.2.2	Radio	20
2.2.3	X-rays	21
2.2.4	γ -rays	23
2.3	SGRs/AXPs - Neutron stars or white dwarfs?	23
2.3.1	Self-consistent mass-radius to SGRs/AXPs as White Dwarfs	25
2.3.2	Particle acceleration	30
2.3.3	High energy cosmic rays from white dwarf pulsars and the Hillas criterion	32
2.3.4	Self-consistent mass-radius to SGRs/AXPs as Neutron Stars	35
2.3.5	Spin-powered pulsar model and magnetic fields	37
2.3.6	Inferred Magnetic fields	38
3	MODELS OF PULSAR ELECTROMAGNETIC EMISSION	41
3.1	Polar Cap Model	42
3.1.1	General Relativity corrections for death lines	45

3.2	Outer Gap Model	46
3.3	Constraining gamma emission	50
3.3.1	Gamma emission of SGRs/AXPs as NSs	53
3.3.2	Gamma emission of SGRs/AXPs as WDs	58
3.4	Constraining radio emission	65
3.4.1	Radio emission of SGRs/AXPs as NSs	65
3.4.2	Radio emission of SGRs/AXPs as WDs	68
4	BINARY COMPACT STAR MERGERS: GAMMA RAY BURSTS, ELECTROMAGNETIC TRANSIENTS AND GRAVITATIONAL WAVES .	70
4.1	Gravitational emission from binary systems	73
4.1.1	Gravitational Radiation Luminosity	74
4.1.2	Strain of Gravitational Radiation	75
4.2	GRB subclasses and observational properties of NS-NS and NS- WD mergers	77
4.3	Gravitational wave emission of NS-NS, NS-WD and WD-WD mergers	79
4.4	Comparison of the prompt, X-rays and optical light-curves of NS-NS and NS-WD mergers	81
4.5	WD-WD mergers as an alternative mildly relativistic uncolli- mated emission for GRB 170817A-AT 2017gfo	84
5	GENERAL CONCLUSIONS	86
	BIBLIOGRAPHY	89
	APPENDIX A – PUBLICATIONS LIST	113
A.1	Published papers	113
A.2	Proceedings	114

1 Introduction

It is generally accepted that stars with masses below ~ 10 solar masses (M_{\odot}) end up their evolution as white dwarfs (WDs). These stars have a typical composition mostly made of carbon, oxygen, or helium, and possess central densities up to $\sim 10^{11}$ g/cm³ (GLENDEENING, 2000). They can be very hot, fast rotating and strongly magnetized. Their internal magnetic fields are not known, but they are expected to be larger than their surface magnetic fields (FRANZON; SCHRAMM, 2015). This is due to the fact that the magnetic field B , in ideal magnetohydrodynamics (MHD), is ‘frozen’ with the fluid and $B \propto \rho$, with ρ being the local mass density. A simple estimate, considering the virial theory, i.e., equating the magnetic field energy with the gravitational binding energy, leads to an upper limit of $\sim 10^{13}$ G on WDs’ surface see e.g., (CHANDRASEKHAR; FERMI, 1953; COELHO *et al.*, 2014). On the other hand, analytic and numeric calculations, in Newtonian theory as well as in General Relativity theory, show that WDs may have internal magnetic fields as large as 10^{12-15} G (CHAMEL; FANTINA; DAVIS, 2013; CHAMEL; FANTINA, 2015; OTONIEL *et al.*, 2016).

Recently, some white dwarfs with high magnetic field (10^{6-9} G) on their surfaces have been observed (KEPLER *et al.*, 2013; KEPLER *et al.*, 2015; FERRARIO; de Martino; GÄNSICKE, 2015). These magnetic fields are higher than normal values for white dwarfs: 10^4 G. Besides their high magnetic fields, most of them have been shown to be massive, and responsible for the high-mass peak at $1 M_{\odot}$. Very recent results from the Sloan Digital Sky Survey (SDSS) have found very massive and magnetized white dwarfs (KEPLER *et al.*, 2017).

Over the last few years this number has grown significantly with new observations. More recently, a white dwarf pulsar known as AR Scorpii has been discovered with few minutes of period, showing radiation in a broad range of frequencies (MARSH *et al.*, 2016; BUCKLEY *et al.*, 2017). Another specific example is the AE Aquarii binary system, formed by a very fast intermediate polar white dwarf with a short period of $P = 33$ s. In addition, Mereghetti *et al.* (MEREGHETTI *et al.*, 2011; MEREGHETTI *et al.*, 2013) showed that the X-ray pulsator RX J0648.04418 is a massive white dwarf with mass $M = 1.28 M_{\odot}$ and radius $R = 3000$ km, with a very fast spin period of $P = 13.2$ s, that belongs to the binary system HD 49798/RX J0648.04418. These observations support the

interest in highly magnetized, massive and rapid rotating WDs.

Apart from the aforesaid interest, the community has given a renewed attention to these objects, motivated by an alternative model to explain Soft Gamma Repeaters (SGRs) and Anomalous X-Ray Pulsars (AXPs) as WD pulsars (MALHEIRO; RUEDA; RUFFINI, 2012).

This alternative model based on white dwarfs pulsars has been proposed to explain a class of pulsars known as SGRs/AXPs (PACZYNSKI, 1990; USOV, 1993; USOV, 1994; MALHEIRO; RUEDA; RUFFINI, 2012; COELHO; MALHEIRO, 2014; LOBATO; COELHO; MALHEIRO, 2015a; LOBATO; COELHO; MALHEIRO, 2015b; LOBATO; MALHEIRO, 2016; LOBATO; MALHEIRO; COELHO, 2016; MUKHOPADHYAY; RAO, 2016; LOBATO; COELHO; MALHEIRO, 2017), usually named as magnetars. In this model, the magnetized white dwarfs can have surface magnetic field $B \sim 10^{7-10}$ G and rotate very fast with angular frequencies $\Omega \sim 1$ rad/s, allowing them to produce large electromagnetic (EM) potentials and generate electron-positron pairs. These EM potentials are comparable with the ones of neutron star pulsars with strong magnetic fields and even larger.

There are two prevalent processes to explain pair production, and consequently, radio emission in neutron stars: the first one considers that pair production happens near of the star polar caps, i.e. inside of the light cylinder, where magnetic field lines are closed (STURROCK, 1971; RUDERMAN; SUTHERLAND, 1975; ARONS; SCHARLEMANN, 1979; DAUGHERTY; HARDING, 1996); the second one considers the pair production in the outer magnetosphere, i.e. far away of the star surface where magnetic field lines are open (CHENG; HO; RUDERMAN, 1986a; CHENG; HO; RUDERMAN, 1986b; ROMANI, 1996; HIROTANI; SHIBATA, 1999a; HIROTANI; SHIBATA, 1999b; TAKATA; WANG; CHENG, 2010; TONG; SONG; XU, 2011; VIGANO *et al.*, 2015a; VIGANO *et al.*, 2015b; VIGANÒ *et al.*, 2015).

The above mentioned physical properties (e.g. mass, rotation period and magnetic field) of the WDs can correspond to the ones described by the remnant of a WD-WD merger i.e. a central massive ($\sim 1.2-1.5 M_{\odot}$), highly magnetized (10^{9-10} G), fast rotating ($P = 1-10$ s) WD, (RUEDA *et al.*, 2013). The WD binary merge puts a new possibility for the origin of the short gamma ray bursts, which have long been expected to be the result of neutron stars mergers (GOODMAN, 1986; NARAYAN; PACZYNSKI; PIRAN, 1992; PIRAN, 2005) and an engine to synthesize neutron-rich heavy elements (LATTIMER; SCHRAMM, 1974; EICHLER *et al.*, 1989). It is believed that SGRBs also can be the product of matter accretion onto a rapidly-spinning black hole or the merger of neutron star and stellar-mass black hole (NS-BH) (NARAYAN; PACZYNSKI; PIRAN, 1992; PIRAN, 2005). The WD binary merge, a novel interpretation (RUEDA *et al.*, 2018; RUEDA *et al.*, 2019), considers a possibility to have a new merger class on this picture.

In chapter 2, we present a short review of magnetic white dwarfs and WDs pulsars, and we highlight in special the sources AR Scorpii and AE Aquarii. We discuss the possibility of highly magnetized white dwarfs to be sources to the of Ultra High Energy Cosmic Rays (UHECR), analysing the particle acceleration mechanism. The properties of SGRs and AXPs, known as magnetars, are also pointed out in this chapter. We also discuss the possible nature of these sources, in the context of WDs and NSs. The models of electromagnetic emission mechanisms are presented in chapter 3, and applied to SGRs and AXPs considering a self-consistent calculation taking in account the mass, star radius and momentum of inertia (for WDs and NSs), using realistic equations of state (EoSs) and the specific rotational period of each source. Respective death lines for the electromagnetic emission are obtained for each model. These lines are presented for SGRs/AXPs described as white dwarf or neutron star pulsars and are compared with the observations. The surface magnetic field is also showed considering both cases. Using these realistic parameters, we have constrained the hard X, gamma rays and the possibility of radio emission. In chapter 4 we discuss the gravitational wave event GW170817. The electromagnetic transient generated by the system is described and the discrepancies between this counterpart and the gravitational one is analysed. The gravitational signal is studied within the context of two point particles and the properties of the binaries are computed for NS-NS, WD-NS and WD-WD. This is compared with the emissions observed. Finally, in chapter 5 we present the general conclusions of the thesis.

2 White dwarfs and SGRs/AXPs

2.1 White dwarfs pulsars

White dwarfs are the final evolution state of main sequence stars with initial masses up to $8.5 - 10.6M_{\odot}$. They correspond to 95–97% of all observed stars in the Universe (KEPLER *et al.*, 2017). The main sequence progenitors can reach sufficiently high core temperatures ($8 - 12 \times 10^8$ K), to proceed to carbon burning and produce either oxygen-neon (ONe) core WDs or undergo a core-collapse supernova (SNII) via electron capture on the products of carbon burning (KIPPENHAHN; WEIGERT; WEISS, 2012). Chandrasekhar has shown that a WD cannot sustain a mass over $1.4M_{\odot}$, establishing the so-called Chandrasekhar mass limit (CHANDRASEKHAR, 1931). If a WD grows over this limit, as in binary systems in which a WD is receiving mass from a nearby star, the white dwarf can collapse to form a neutron star.

White dwarfs near to the Chandrasekhar limit, i.e. very dense WDs, can have conditions of unstable nuclear burning that lead to a type Ia supernova (SNIa) explosion, which happens when the fusion timescale is faster than the process of cooling for example; the time to reach explosive conditions is shorter than that needed to have inverse beta-decay instability or the secular instability, which leads to gravitational collapse (BECERRA *et al.*, 2018). SNIa progenitors are expected to be similar, with nearly equal luminosity, therefore being considered standard candles (WEINBERG, 2008; BECERRA *et al.*, 2018). In fact, in the late 1990s, the use of SNIa led to the discovery that the expansion of the Universe is accelerating (RIESS *et al.*, 1998; PERLMUTTER *et al.*, 1998).

Nevertheless, some super luminous SNIas were found recently (HOWELL *et al.*, 2006; SCALZO *et al.*, 2010). It has been suggested that their progenitors are WDs that exceed the Chandrasekhar mass limit (HOWELL *et al.*, 2006; HICKEN *et al.*, 2007; YAMANAKA *et al.*, 2009; SCALZO *et al.*, 2010; TAUBENBERGER *et al.*, 2011; SILVERMAN *et al.*, 2011), being termed “super-Chandrasekhar WDs” (DAS; MUKHOPADHYAY, 2012; DAS; MUKHOPADHYAY, 2013; DAS; MUKHOPADHYAY, 2014).

To bypass $1.4M_{\odot}$, some studies evoke different physical scenarios, as follows: Mergers of WDs emerge as an option to possible progenitors (MOLL *et al.*, 2014; RASKIN *et al.*,

2014). A recent letter (GVARAMADZE *et al.*, 2019) presented a hot star with a spectrum dominated by emission lines, which is located at the centre of a circular mid-infrared nebula. The properties of the star and nebula agree with models of the post-merger evolution of super-Chandrasekhar-mass white dwarfs (SCHWAB; QUATAERT; KASEN, 2016). Numerical models suggest that a detonation might occur before the coalescence (JI *et al.*, 2013). Additionally, a theoretical work suggests that mergers which fail to detonate can produce magnetized rapidly rotating WDs (ROSSUM *et al.*, 2016).

Along this line of magnetized white dwarfs, Das & Mukhopadhyay (D&M) (DAS; MUKHOPADHYAY, 2012; DAS; MUKHOPADHYAY, 2012; DAS; MUKHOPADHYAY, 2013) proposed that super-Chandrasekhar WDs are generated by the existence of super-strong uniform magnetic fields inside WDs. Although this description can uplift the mass of WDs, it suffers from severe stability issues (CHAMEL; FANTINA; DAVIS, 2013; DONG *et al.*, 2014; COELHO *et al.*, 2014; NITYANANDA; KONAR, 2015). D&M refined their work (DAS; MUKHOPADHYAY, 2014; DAS; MUKHOPADHYAY, 2014) considering effects of a magnetic field and showed that super-Chandrasekhar WDs can reach $3.33M_{\odot}$. In addition, the authors of Refs. (LIU; ZHANG; WEN, 2014; CARVALHO *et al.*, 2018) obtained super-Chandrasekhar WDs for charged stars.

Studies with rotation and different topology for magnetic field configurations have been performed in References (BOSHKAYEV *et al.*, 2013; FRANZON; SCHRAMM, 2015; SUBRAMANIAN; MUKHOPADHYAY, 2015; CARVALHO; MARINHO; MALHEIRO, 2015; CARVALHO; JR; MALHEIRO, 2015; BERA; BHATTACHARYA, 2016; OTONIEL *et al.*, 2016; BECERRA *et al.*, 2019), resulting in very massive white dwarfs.

The chance of rapidly rotating and massive white dwarfs was shown to be possible some decades ago by Ostriker's group (Lynden-Bell; OSTRIKER, 1967; OSTRIKER; HARTWICK, 1968; OSTRIKER; BODENHEIMER, 1968; OSTRIKER; MARK, 1968; OSTRIKER, 1968; OSTRIKER; TASSOUL, 1969). To explain a peculiar rapid pulsating radio signal observed by the Cambridge radio astronomy group, they have done a model considering rotating white dwarfs as the source. On that case the source would be fast and compact, requiring a more realistic equation of state, which already have been derived by Hamada and Salpeter (HAMADA; SALPETER, 1961; SALPETER, 1961). Later Usov (USOV, 1988; USOV, 1993), has shown that WD can produce pairs of electron-positron e^{\pm} in its magnetosphere like a neutron star pulsar.

Zhang and Gil (ZHANG; GIL, 2005) interpret the transient radio source, GCRT J1745-3009, as a white dwarf pulsar with a period of 77.13 minutes.

These works always have explored the possibility of white dwarf pulsar, essentially, from the theoretical point of view. The confirmation of this hypothesis happened in a very recent discovery with the source AR Scorpii (AR Sco's), see section 2.1.1, which is

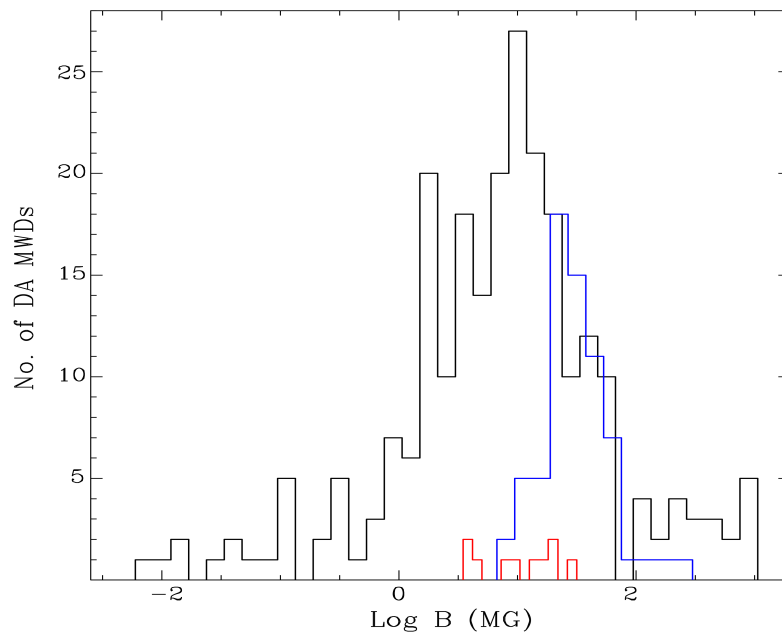


FIGURE 2.1 – Distribution of magnetic field strength in polars (blue lines) and IPs (red lines) in comparison with single magnetic WDs (black lines). Figure from (FERRARIO; de Martino; GÄNSICKE, 2015).

a binary system with a pulsating white dwarf (MARSH *et al.*, 2016; BUCKLEY *et al.*, 2017), and AE Aquarii, see section 2.1.2, the first white dwarf pulsar (an intermediate polar WD) (TERADA *et al.*, 2008; ORURU; MEINTJES, 2012).

Magnetic WDs observed in binary system are known as cataclysmic variable (CV), and usually accrete matter from a main-sequence star (e.g. AE Aquarii) companion through Roche lobe. CVs are mainly divided in polar and intermediate polar (IP). The WD in polar has magnetic field $B_s > 10$ MG which lock the two stars in synchronous rotation. The dipole moment is the order of $\sim 10^{33}$ G cm². For IP the magnetic field is $B_s \sim 0.1$ -10 MG, not enough to lock the system. In general the magnetic fields in WDs are between the values 10^3 - 10^9 G, having a distribution according the Figure (2.1).

A synchronous rotation in Polars prevents a formation of an accretion disk (there is no angular momentum of the accreting matter relative to the WD) while in an IP, the accretion disk forms around the WD. The number of CVs has increased. Today, they are approximately 170 and one half of them have magnetic fields in the range $7 \times 10^6 - 2.3 \times 10^9$ G (FERRARIO; de Martino; GÄNSICKE, 2015). The two systems, AR Scorpii and AE Aquarii are examples of a polar and an intermediate polar.

2.1.1 AR Scorpii

AR Scorpii is a white dwarf/cool star binary system that emits from X-ray to radio wavelengths. The system has a 3.56 hour orbital period. The WD in AR Sco's has a mass range of $0.81M_{\odot} < M_1 < 1.29M_{\odot}$ and pulses with the quite short period of 1.97 minutes ~ 118.2 s. The spin-down power is an order of magnitude larger than the observed luminosity (dominated by the X-rays), which, together with an absence of obvious signs of accretion, suggests that AR Sco is primarily rotation-powered. Then, these pulses reflect the spin of the WD, slowing down on a timescale $\tau = P/2\dot{P} \cong 10^7$ years (MARSH *et al.*, 2016).

The white dwarf pulsar broadband spectrum is characteristic of synchrotron radiation (KATZ, 2017), requiring relativistic electrons what must be generated near of the WD or at the cool star (MARSH *et al.*, 2016; TAKATA; YANG; CHENG, 2017). This type of radiation typically happens in neutron star pulsars. Thus, this rapidly rotating magnetized WD mimics the neutron star pulsars, being the first WD radio-pulsating source where there is no evidence of radio outflow or jets as principal source of radio emission (MARCOTE *et al.*, 2017). Instead, it consists of synchrotron radiation powered by rotational energy. The efficiency to convert rotational energy into EM power was calculated to be $\sim 4\%$ (STILLER *et al.*, 2018), considering spin-down measurements of two years. The system has a low X-luminosity, being the accretion onto the WD insignificantly.

Propertires of AR Scorpii (MARSH *et al.*, 2016; BUCKLEY *et al.*, 2017):

- Period: $P = 118.2$ s,
- Spin-down rate: $dP/dt \approx 3.99 \times 10^{-13}$ s/s,
- Luminosity: $L_X = 10^{32}$ erg/s,
- Light cylinder: $R_{lc} = cP/(2\pi) \approx 5.64 \times 10^{11}$ cm,

where c is the speed of light. The white dwarf radius assumed is $R \approx 7 \times 10^8$ cm (MARSH *et al.*, 2016; GENG; ZHANG; HUANG, 2016). The companion red star has a mass range 0.28 - 0.45 M_{\odot} and radius $R \approx 2.5 \times 10^{10}$ cm.

The age determined by cooling differs from the one inferred by spin-down. Cooling time of the WD with temperature of $T_{WD} \sim 10^4$ K is 10^9 yr (BESKROVNAYA; IKHSANOV, 2017). Considering this, one can conclude that the fast rotation of the white dwarf is due to its evolution i.e., an accretion disk has spun-up the WD. A significant accretion can happen under the condition $\dot{M}_{ac} > \dot{M}_{cr}$, being $\dot{M}_{cr} \simeq 10^{-7} M_{\odot}/\text{yr}$ (BESKROVNAYA; IKHSANOV, 2017). The WD in AR Scorpii, besides the ejector state, shares other properties with another white dwarf pulsar, the AE Aquarii.

2.1.2 AE Aquarii

AE Aquarii was the first white dwarf pulsar (an intermediate polar WD), very fast with a short period $P \approx 33$ s, and spinning down at a rate $\dot{P} = 5.64 \times 10^{-14}$ s/s (de Jager *et al.*, 1994). The luminosity of this source and the nature of pulse hard X-ray emission detected with SUZAKU space telescope (TERADA *et al.*, 2008; ORURU; MEINTJES, 2012) can be explained in terms of spin-powered pulsar mechanism (IKHSANOV, 1998; ORURU; MEINTJES, 2014) and emit detectable high-energy radiation (CACERES *et al.*, 2017; LOBATO; COELHO; MALHEIRO, 2015a; LOBATO; COELHO; MALHEIRO, 2015b). The magnetic field prevents influx of the material around the WD. According Beskrovnaya and Ikhasanov (BESKROVNAYA; IKHSANOV, 2015), an accretion onto the surface of the white dwarf have resulted in a temporary screening of its magnetic field. This had allowed the WD to reach its present spin period and turned into the ejector state after its magnetic field had emerged from the material deposited, due to diffusion. This system, as AR Scorpii, shows a discrepancy between the age estimated by cooling and spin-down, being the difference more than one order of magnitude. The accretion rate in AE Aquarii was estimated to be $\sim 10^{-7} - 10^{-6} M_{\odot}/\text{yr}$ (MEINTJES, 2002).

2.2 Soft Gamma Repeaters (SGRs) and Anomalous X-Ray Pulsars (AXPs)

Soft Gamma Repeaters (SGRs) and Anomalous X-Ray Pulsars (AXPs) are a new class of pulsars in comparison with the rotation-powered pulsars (RPPs). They are normally understood as neutron stars (magnetars) with magnetic fields larger than the quantum magnetic critical field, $B_c = m^2 c^3 / e \hbar$. They have huge magnetic fields (100-1000) times larger than typical radio pulsars of neutron stars $B \sim 10^{12}$ G. They present long period $P \sim 2 - 12$ s and also have spin-down rates $\dot{P} \sim (10^{-13} - 10^{-10})$ s/s, larger than normal pulsars $\dot{P} \sim (10^{-15} - 10^{-14})$ s/s (MEREGHETTI, 2013; TUROLLA; ZANE; WATTS, 2015). Magnetars have been center of some discussion in the last years, some questions are not understood very well, and even their nature are still in debate. Several models were proposal to explain their origin (WOOSLEY; WALLACE, 1982; LIVIO; TAAM, 1987; BLAES *et al.*, 1989; KATZ; TOOLE; UNRUH, 1994).

In beginning, the efforts to understand the nature of these sources were not compensated due the lack of information. But now this scenario is changing with the new observations from several telescopes (Fermi, Chandra, Integral, XMM).

According the magnetar model, the high X-ray luminosity from these sources is powered by the energy stored in their strong magnetic fields (DUNCAN; THOMPSON, 1992;

THOMPSON; DUNCAN, 1993; THOMPSON; DUNCAN, 1995; THOMPSON; DUNCAN, 1996; DUNCAN, 2001; THOMPSON; LYUTIKOV; KULKARNI, 2002; THOMPSON, 2002; THOMPSON, 2008a; THOMPSON, 2008b; MEREGHETTI, 2013; TUR-OLLA; ZANE; WATTS, 2015; KASPI; BELOBORODOV, 2017). Although the interpretation as neutron stars is the one most accepted, exist some features about SGRs/AXPs not very well understood in the magnetar model (COELHO; MALHEIRO, 2014):

- RPPs are assumed born with a short period ~ 1 ms resulting in large magnetic fields by dynamo process (TONG; SONG; XU, 2011). SGRs/AXPs present long periods, such that generation of high magnetic fields by this mechanism does not make sense in this class.
- the large spin-down rates in comparison with the typical pulsars, for example the source SGR 0418+5729 has a characteristic age $\tau = P/2\dot{P} = 2.4 \times 10^7$ years, this means, even being older than ordinary pulsars, it has a major slowdown.

Some SGRs/AXPs with low magnetic fields and smaller spin-down rates were observed (REA *et al.*, 2010). Within of these observations, we highlight SGR 0418+5729, with period $P = 9.08$ s, spin-down $\dot{P} < 6.0 \times 10^{-15}$ s/s and X-ray luminosity $L_X < 6.2 \times 10^{31}$ erg/s. Considering this source as a neutron star, the loss of energy associated with injection of rotational energy in the pulsars' magnetosphere does not explain the luminosity of this star, i.e., $\dot{E}_{\text{rot}}^{\text{NS}} < L_X$, excluding the possibility to be an RPP, where $\dot{E}_{\text{rot}}^{\text{NS}} > L_X$. Recent observations of Fermi satellite (ABDO *et al.*, 2010; TONG; SONG; XU, 2010; TONG; SONG; XU, 2011) do not find evidences of γ radiation. In addition, 4 SGRs/AXPs were observed to emit in radio wavelenght, while the others do not. These observations carried some uncertainties about the nature of SGRs/AXPs. There are some extensions in the magnetar model (TONG; SONG; XU, 2011), always describing them as neutron star or hybrid stars.

A model proposed by Malheiro, Rueda and Ruffini (MALHEIRO; RUEDA; RUFFINI, 2012) following the work of Morini *et al.* (MORINI *et al.*, 1988) and Paczynski (PACZYNSKI, 1990) suggested an alternative model, which consider SGRs/AXPs as very massive, rapidly rotating magnetic white dwarfs. There are some features to fit in order to explain SGRs/AXPs as WDs. The masses need to be $M > 1.2 M_{\odot}$, the magnetic field $\approx 10^7$ G and rotation < 12 s. All these characteristics were already found by observations or simulations (KÜLEBI *et al.*, 2009; BOSHKAYEV *et al.*, 2013; LOBATO; MALHEIRO; COELHO, 2016). As we will discuss in section 2.3.1, the SGRs/AXPs can be understood in the context of WD with self-consistent models, being very massive and having high magnetic fields.

Discovered in X and soft gamma-rays, the SGRs/AXPs have been detected in a broad

wavelength spectrum: they emit in optical/near infrared, radio, soft and hard X-ray (TUROLLA; ZANE; WATTS, 2015).

2.2.1 4U 0142+61

Among the SGRs/AXPs there is one source best observed in infrared, optical and ultraviolet (WANG; CHAKRABARTY; KAPLAN, 2006; KUIPER *et al.*, 2006). The source was modeled as being a central WD resulting from a merger of two others stars (RUEDA *et al.*, 2013). From observations, we can have the properties of this source:

- Period: $P \approx 8.69$ s,
- Spin-down rate: $dP/dt \approx 2 \times 10^{-12}$ s/s,
- Luminosity: $L_X \approx 10^{35}$ erg/s,
- Light cylinder: $R_{lc} \approx 4.15 \times 10^{10}$ cm.

According to the model of Rueda *et al.* (RUEDA *et al.*, 2013), the resulting WD would have a mass of $1.1 M_\odot$, period of 15.7 s and a surrounding disk which may reflect the infrared excess. The system is in an ejector state, inhibiting accretion onto the WD. The time-integrated X-ray spectrum is well described by an absorbed blackbody ($kT \sim 0.4$ keV) and a power-law model with index $\Gamma = 3.6$. In this system, the mechanism to produce non-thermal radiation is the *polar cap*¹, considering a particle flux onto the WD by magnetic field. The estimated 4U 0142+61 radius, which is in agreement with photometric value is $R_{WD} \approx 4.17 \times 10^8$ cm.

The source 4U 0142+61 is the most known source in the X-ray wavelength being at the distance of ~ 3.6 kpc, as neutron star, the magnetic field estimated is very strong $\sim 1.3 \times 10^{14}$ G (OLAUSEN; KASPI, 2014)². Brighter, 1-10 keV, emission coming from this source has been observed by many X-ray satellites (ALEKSIĆ *et al.*, 2013). As shown by (KUIPER *et al.*, 2006) a strong hard X-ray flux was reported by INTEGRAL.

2.2.2 Radio

The most common feature of a neutron star is the detection of very regular pulses in radio, in fact it was a serendipitous discovery of this kind of electromagnetic pulse in 60s (HEWISH *et al.*, 1968) which led us to NSs confirmation. Currently, there are known around 2500 radio pulsars (MANCHESTER *et al.*, 2005; KRISHNAN *et al.*,

¹Will be described in section 3.1

²<<http://www.physics.mcgill.ca/~pulsar/magnetar/main.html>>

2019), including 4 radio loud SGRs/AXPs (CAMILO *et al.*, 2006; CAMILO *et al.*, 2007a; CAMILO *et al.*, 2007b; LEVIN *et al.*, 2010; SHANNON; JOHNSTON, 2013). However, the radio properties of these four sources are somehow different from NS radio pulsars (including high B pulsars). The flux is highly variable in a timescale of days, the spectrum is very flat, there are changes in the pulses profile, there is an association with the X-ray bursts and decays the same way as it (MEREGETTI, 2008; TUROLLA; ZANE; WATTS, 2015; REA *et al.*, 2012). One can conclude that the regions (the topology) in the SGRs/AXPs where the radiation is produced is quite complex, and the mechanism may differ from the usual.

Initially, SGRs/AXPs were thought to be radio quiet. It was suggested that due to the high magnetic field in the magnetosphere, the pair production and consequently the pair cascade is suppressed by photon splitting, a third-order QED process that may become important in strong magnetic fields above the B_c (BARING; HARDING, 1998; BARING; HARDING, 2001), but this was demonstrated to be wrong (MEREGETTI, 2008; MEREGETTI, 2013). Transient radio emission were discovered from SGRs associated with giant flares (REA; TORRES, 2011), furthermore, pulsed emission were also discovered. The first detection of pulsed radio in SGRs/AXPs was from the source XTE J1810-197 (IBRAHIM *et al.*, 2004; CAMILO *et al.*, 2006) as a continuous source, then from the source AXP 1E 1547-5408 (CAMILO *et al.*, 2007a), similar to the first one. After these two, a third one was found, the source PSR 1622-4950, this was discovered thanks the observations of the radio band (TUROLLA; ZANE; WATTS, 2015). The last source detected, so far, was the source SGR J1745-2900 (REA *et al.*, 2013; KASPI *et al.*, 2014). All four are transient magnetars and transient radio emitters, for the persistent ones, have been a search for radio pulsation, but without success (TONG; YUAN; LIU, 2013).

As pointed by the review of Turolla *et al.* (TUROLLA; ZANE; WATTS, 2015) and showed by Rea *et al.* (REA *et al.*, 2013) and Ho (HO, 2013), the radio-loud magnetars are characterized by $L_X < \dot{E}$ in quiescence state and X-ray luminosity exceeds the rotational energy as in some NS. This suggests that in magnetars the particle acceleration and the cascade process could happen as in normal pulsars, leading to radio emission.

2.2.3 X-rays

The X-ray emission is generally separated as low (<10 keV) and high-energy (>20 keV) and seems that different mechanism are responsible for the two (REA; TORRES, 2011; TUROLLA; ZANE; WATTS, 2015). The low energy component is fitted with a blackbody with temperature $kT \sim 0.3 - 0.6$ keV and a power-law with photon index $\Gamma \sim 3 - 4$ (MEREGETTI *et al.*, 2002) or two blackbodies (REA; TORRES, 2011).

An example from Kaspi and Beloborodov (KASPI; BELOBORODOV, 2017) of such a spectrum is shown in fig. 2.2. The nonthermal component begins to dominate above 10 keV. The soft X-ray emission is predominantly of thermal origin (MEREGHETTI, 2008) and is complex, i.e., the emission from the surface can get distorted by resonant cyclotron scattering. The thermal component which dominates the lowest energy band is from a region much smaller than the whole surface of the star (TUROLLA; ZANE; WATTS, 2015) and the tail of the power-law likely arises from magnetospheric effects. Although this picture is broadly accepted, there are still some open problems, either because a reprocessing by return currents or because the surface itself may be sort of condensed state, being a self-consistent model needed. For more details in attempts to do that with state-of-the art numerical codes, see the review of Turolla et al. (TUROLLA; ZANE; WATTS, 2015)

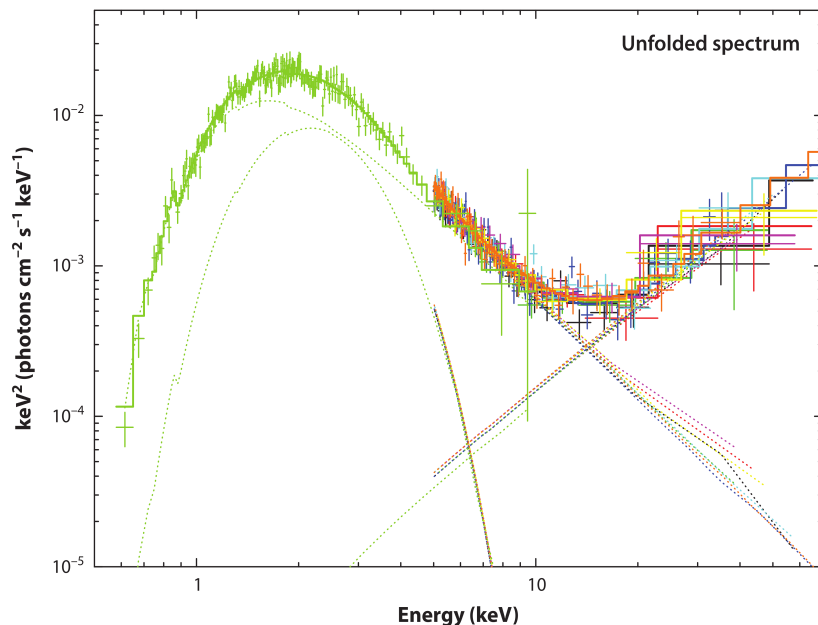


FIGURE 2.2 – Broadband in X-ray spectrum from swift/XRT (green) and NusTAR of 1E 2259+586. The fitted model of a blackbody and two power laws is shown. Figure from Kaspi and Beloborodov (KASPI; BELOBORODOV, 2017).

An important point to highlight is the average temperature of the thermal component which for the magnetars is more luminous than rotation-powered pulsars of comparable age (MEREGHETTI, 2008; TUROLLA; ZANE; WATTS, 2015).

The persistent hard X-ray emission extends to ~ 150 keV. This radiation has a nonthermal characteristic and some studies considering spectroscopy suggest that a considerable fraction of the luminosity comes from the hard band instead of the soft one (KUIPER; HERMSEN; MENDEZ, 2004; MEREGHETTI *et al.*, 2005; MOLKOV *et al.*, 2005; GÖTZ *et al.*, 2006; KUIPER *et al.*, 2006; MEREGHETTI, 2008; ENOTO *et al.*, 2011), i.e., the energy released in this range is a large fraction of the total energy released in these

sources. There are some attempts to study the spectral location of the soft-hard X-ray turnover (KASPI; BOYDSTUN, 2010), which in general is believed to be correlated with the magnetic field on the surface (TUROLLA; ZANE; WATTS, 2015). For higher energy observations, Fermi LAT failed to detect emission, implying in a spectral break above a few hundred keV (KUIPER *et al.*, 2006; HARTOG *et al.*, 2006), the source AXP 1E 2259+586 seemed to show γ -ray pulsation above 200 MeV (WU *et al.*, 2013), however this is not confirmed yet.

The mechanism for hard X-ray is not well understood, ones can suggest that the these X-rays can be generated by thermal bresstrahlung in the surface, heated by returning current or by synchrotron emission from pairs on the magnetosphere (THOMPSON; BELOBORODOV, 2005) or even by resonat up-scattering of seed photons (BARING; GONTHIER; HARDING, 2005; BARING; HARDING, 2008). Nevertheless, this still is an open question due the dramatically number of degrees of freedom for the magnetosphere.

2.2.4 γ -rays

The SGRs/AXPs are characterized by the short and intense burst in the hard X/soft gamma-ray band (few keV to few hundreds keV) (MEREGHETTI, 2008; MEREGHETTI *et al.*, 2013; TUROLLA; ZANE; WATTS, 2015) raging from few seconds to several seconds. There three kinds of bursts events (TUROLLA; ZANE; WATTS, 2015):

- short burst: most common and with duration of $\sim 0.1-1$ s, peak luminosity $\sim 10^{39-41}$ erg/s and soft thermal spectra (10 keV).
- intermediate bursts: duration of $\sim 1 - 40$ s, peak luminosity of $\sim 10^{41-43}$ erg/s with thermal spectra.
- giant flares: rare events, peak luminosity of $\sim 10^{44-47}$ erg/s.

The burst activity is very variable and often are enhanced by the persistent emission (MEREGHETTI *et al.*, 2013). It seems that there is no dependence of short/intermediate burst activity on the magnetic field strength of sources (TUROLLA; ZANE; WATTS, 2015).

2.3 SGRs/AXPs - Neutron stars or white dwarfs?

Despite the interpretation of all SGRs/AXPs as WDs, there is a recent work (COELHO *et al.*, 2017), which considers the possibility of some of them to be rotation-powered NSs,

TABLE 2.1 – Nine sources which are considered as rotation powered NS (COELHO *et al.*, 2017). Within the magnetar group these are the rapidly sources.

Source	P (s)
PSR J1846-0258	0.32657128834
1E 1547.0-5408	2.0721255
SWIFT J1834.9-0846	2.4823018
SGR 1627-41	2.594578
SGR J1745-2900	3.76363824
CXOU J171405.7-381031	3.825352
PSR J1622-4950	4.3261
XTE J1810-197	5.5403537
SGR 0501+4516	5.7620695

i.e., the rotation powers the sources, instead of the huge magnetic field as in the magnetar case. This conclusion relies on the efficiency of these sources and on the magnetic field value. Using realistic parameters Coelho *et al.* (COELHO *et al.*, 2017) have shown that these two quantities are lowered, being close to canonical rotation-powered pulsars (where $\dot{E}_{\text{rot}} \geq L_X$ and $B_p < B_c$). So in this view, we have the possibility that nine (table 2.1) SGRs/AXPs being power rotating neutron stars and the remaining being white dwarfs; we highlight that the classification follows the period of the sources, being the rapidly source PSR J1846-0258 with period of 0.32 s and the slowest, the source SGR 0501+4516 with period of 5.76 s. The source PSR J1846-0258 is classified as a young rotation-powered pulsar, but it was seen to undergo a magnetar-like outburst in 2006 (GAVRIIL *et al.*, 2008), being added recently in the McGill catalog (OLAUSEN; KASPI, 2014). It does not have a magnetic field higher than the critical value and its efficiency is lower than 1, i.e., $L_X < \dot{E}_{\text{rot}}$.

Within the nine sources presented above there are four³ where emission in radio wavelength was observed. It was recently reported the radio disappearance of two of these sources. The first one was XTE J1810-197 (CAMILO *et al.*, 2016) and the second PSR J1622-4950 (SCHOLZ *et al.*, 2017) around 2015: these two pulsars are the slowest in the radio group. But interestingly, the magnetar PSR J1622-4950 reappeared as a radio pulsar in 2017 (KRISHNAN *et al.*, 2019).

Apart from the period, there is no intrinsic characteristic to distinguish between these nine and the remaining ones or a conclusive definition of the sources' nature, being the

3

- 1E 1547.0-5408
- SGR J1745-2900
- PSR J1622-4950
- XTE J1810-197

TABLE 2.2 – Ten sources which present soft γ -rays/hard X-rays (OLAUSEN; KASPI, 2014) (>10 keV). The blue ones are considered as rotating powered NS pulsars according (COELHO *et al.*, 2017)

Source	P (s)
PSR J1846-0258	0.32657128834
1E 1547.0-5408	2.0721255
SGR J1745-2900	3.76363824
SGR 1900+14	5.19987
SGR 0501+4516	5.7620695
1E 1048.1-5937	6.457875
SGR 1806-20	7.54773
4U 0142+61	8.68869249
1RXS J170849.0-400910	11.00502461
1E 1841-045	11.788978

puzzle still open, since these two possible group share a common feature, which is the persistent emission in soft γ -rays/hard X-rays (>10 keV). This waveband brings them all into one group again, as we will see in section 3.2.

In the next subsections, using self-consistent calculations for white dwarfs, section 2.3.1, and reviewing Coelho *et. al.* (COELHO *et al.*, 2017), section 2.3.4, we will analyse the SGRs/AXPs within the context of WD and NS with realist moment of inertia/mass-radius, studying the electromagnetic radiation, i.e., the radio and soft γ /hard X-rays (which are directly attached to the magnetic field of the stars), in order to see if it is possible to find an answer concerning their nature.

2.3.1 Self-consistent mass-radius to SGRs/AXPs as White Dwarfs

Here we present the general formalism for rotating stars, the so-called Hartle’s formalism, which will be applied to SGRs/AXPs as WDs and NSs, in order to obtain mass-radius and moment of inertia to compute the magnetic fields for the sources. In section 2.3.1.3 we will present the mass-radius and the moment of inertia for the SGRs/AXPs as WDs. It was taken into account the period observed (OLAUSEN; KASPI, 2014) i.e., it was considered the rotation of each star. It was also used a more modern EoS, section 2.3.1.2, which considers not only the electron pressure but a crystal lattice pressure as well. In order to construct the equilibrium configurations of a uniformly rotating the Hartle’s formalism was used.

2.3.1.1 White dwarf structure

The structure of white dwarfs is governed by the equations of hydrostatic equilibrium, where the gravitational force pulling the star's matter toward the center is balanced by the pressure force generated by the degenerate electrons (SHAPIRO; TEUKOLSKY, 2008). Recently it has been noted that contributions emerging from general relativity (GR) ought to be taken into account when modelling the structure of white dwarfs (ROTONDO *et al.*, 2011; BOSHKAYEV *et al.*, 2013; CARVALHO; JR; MALHEIRO, 2015; CARVALHO; MARINHO; MALHEIRO, 2015; CARVALHO; MARINHO; MALHEIRO, 2018). This is accomplished by using the Tolman-Oppenheimer-Volkoff (TOV) equation (TOLMAN, 1939; OPPENHEIMER; VOLKOFF, 1939) for the calculation of the properties of non-rotating white dwarfs. Adopting the geometrized unit system ($G = c = 1$), this equation is

$$\frac{d\mathbf{p}(r)}{dr} = -\frac{(\varepsilon(r) + \mathbf{p}(r))(M(r) + 4\pi\mathbf{p}(r)r^3)}{r^2(1 - 2M(r)/r)}, \quad (2.1)$$

where $M(r)$ denotes the gravitational mass of a white dwarf contained inside of a sphere with radius r , ε the energy density and \mathbf{p} the pressure. The mass is computed from

$$\frac{dM(r)}{dr} = 4\pi\varepsilon(r)r^2. \quad (2.2)$$

Modeling the properties of rotating white dwarfs is considerably more complicated than modeling the properties of non-rotating white dwarfs. The exterior metric of a rapidly white dwarfs can be modeled using the Hartle's method (HARTLE, 1967), which computes rotating stars in the slow rotation approximation.

In the Hartle's formalism, a perturbation solution based on the Schwarzschild metric

$$ds^2 = -e^{2\check{\nu}} dt^2 + e^{2\check{\lambda}} dr^2 + r^2 (d\theta^2 + \sin^2 \theta d\phi^2) \quad (2.3)$$

is developed. The metric is expanded through second order in the star's rotational frequency Ω , having the form

$$ds^2 = -e^{2\check{\nu}} dt^2 + e^{2\check{\psi}} (d\phi - \bar{\omega} dt)^2 + e^{2\check{\mu}} d\theta^2 + e^{2\check{\lambda}} dr^2 + O(\Omega^3). \quad (2.4)$$

The metric functions are written as:

$$e^{2\check{\nu}(\Omega)} = e^{2\Phi} \{1 + 2 [h_0 + h_2 P_2(\cos \theta)]\}, \quad (2.5)$$

$$e^{2\check{\psi}(\Omega)} = r^2 \sin^2 \theta [1 + 2 (v_2 - h_2) P_2(\cos \theta)], \quad (2.6)$$

$$e^{2\check{\mu}(\Omega)} = r^2 [1 + 2 (v_2 - h_2) P_2(\cos \theta)], \quad (2.7)$$

$$e^{2\check{\lambda}(\Omega)} = \left[1 + \frac{2 m_0 G + m_2 P_2}{r [1 - (2MG/r)]} \right] \left(1 - \frac{2MG}{r} \right)^{-1}. \quad (2.8)$$

The quantity Φ denotes the metric function of a spherically symmetric object and m the mass within r . P_2 are the Legendre polynomials of order 2 and m_0, m_2, h_0, h_2, v_2 functions of r and Ω (the frequency seen by a distant observer, which is constant i.e., uniform rotation) calculated from Einstein equations (for details, see Refs. (WEBER, 2005; WEBER, 2017)). In the metric element, $\bar{\omega}$ is the angular velocity of the star's fluid in a local frame and depends on the radial coordinate r . It is related to Ω , which must be in the range $0 \leq \Omega \leq \Omega_K$, with Ω_K denoting the Kepler (mass shedding) frequency, which sets an absolute upper limit on stable rotation (WEBER; GLENDENNING; WEIGEL, 1991; WEBER; GLENDENNING, 1992; GLENDENNING; WEBER, 1994). It is given by

$$\Omega_K = \bar{\omega} + \frac{\bar{\omega}'}{2\check{\psi}'} + e^{\check{\nu}-\check{\psi}} \sqrt{\frac{\check{\nu}'}{\check{\psi}'} + \left(\frac{\bar{\omega}'}{2\check{\psi}'} e^{\check{\psi}-\check{\nu}} \right)^2}, \quad (2.9)$$

where the primes refer to partial derivatives with respect to the radial coordinate (WEBER, 2017).

The Kepler period P_K follows from Eq. (2.9) as

$$P_K \equiv \frac{2\pi}{\Omega_K}. \quad (2.10)$$

The Hartle's formalism was improved by Weber and Glendenning (WEBER; GLENDENNING, 1992), to obtain a more accurate estimate of the angular velocity at the mass shedding. Therefore, a self-consistent problem is solved, in order to find the Kepler frequency in (2.9).

The self-consistency relies in the dependence of Ω_K on the metric functions at the equator.

The angular momentum J of the star is defined by (WEBER, 2017)

$$J(\Omega) = I(\Omega)\Omega \equiv \frac{1}{6} R^4 \left(\frac{d\bar{\omega}}{dr} \right)_{r=R}, \quad (2.11)$$

and the angular velocity Ω is related to it by

$$\Omega(\bar{\omega}) = \bar{\omega}(R) + \frac{2J}{R^3}, \quad (2.12)$$

where R is the radius of the non-rotating star with the same central density as the rotating one, $\bar{\omega} = \Omega - \omega(r)$ is the angular velocity of the fluid relative to the local inertial frame, and ω is the angular velocity of the local frame.

The moment of inertia, given by,

$$I = \frac{J}{\Omega}, \quad (2.13)$$

which within of the Hartle formalism does not account for deviations from spherical symmetry (BELVEDERE; RUEDA; RUFFINI, 2015).

A complet explanation of this method step by step can be found in Chapter 15 of the book "Pulsars as Astrophysical Laboratories for Nuclear and Particle Physics" (WEBER, 2017).

With this formalism, we can model the rotating white dwarfs in this rotation approximation self-consistently. The equilibrium equations become a set of coupled ordinary differential equations to be solved. In order to solve this system of equations numerically, it is needed to provide a EoS for the system. We have considered an EoSs for strongly magnetized white dwarfs considering effects of ions energy and pressure.

2.3.1.2 Equation of state (EoS) of strongly magnetized white dwarfs

The first attempt to have a realistic equation of state, was that one derived by Hamada and Salpeter (HAMADA; SALPETER, 1961; SALPETER, 1961) which considered corrections to the Chandrasekhar's EoS (CHANDRASEKHAR, 1931) where the mean molecular weight μ , i.e., the ratio of the number of nucleons to the number of electrons is fixed and the electrons are non-interacting. These seminal works have taken in account the Coulomb effects and inverse beta decays.

In more modern treatment derived from neutron star crusts (LAI; SHAPIRO, 1991; CHAMEL *et al.*, 2012), it is considered that in the center of a white dwarf the pressure is given by the sum of the degenerate electron pressure p_e and the lattice pressure p_L (the stellar interior is composed of a regular crystal lattice made of carbon ions immersed in a degenerate relativistic electron gas), and the energy density by the sum of the ions' energy density, degenerate electron energy e_e , and energy density of the ionic lattice e_L

(CHAMEL *et al.*, 2014)

$$\mathbf{p} = \mathbf{p}_e + \mathbf{p}_L(Z), \quad (2.14)$$

$$\mathbf{e} = n_x \mathbf{M}(Z, A)c^2 + \mathbf{e}_e + \mathbf{e}_L - n_e mc^2, \quad (2.15)$$

where Z is the average proton numbers, n_x the number densities of nuclei, and $\mathbf{M}(Z, A)$ the experimental nuclear masses (CHAMEL; FANTINA; DAVIS, 2013), n_e the electron number density, m the electron mass. The pressure of the ionic lattice is given by (CHAMEL *et al.*, 2014)

$$\mathbf{p}_L = \frac{\mathbf{e}_L}{3}, \quad (2.16)$$

where the ionic energy density is

$$\mathbf{e}_L = Ce^2 n_e^{4/3} Z^{2/3}. \quad (2.17)$$

where e is the electron charge and C the lattice constant of a regular crystal structure of the type body-centered-cubic (bcc), being its value = -1.444231 .

2.3.1.3 Mass-radius relation and moment of inertia

Considering the source's frequency from (OLAUSEN; KASPI, 2014), the EoS (degenerate electrons and ionic lattice) and using Hartle's formalism (HARTLE, 1967; HARTLE; THORNE, 1968; HARTLE; THORNE, 1969; HARTLE, 1970; HARTLE; THORNE; CHITRE, 1972; HARTLE, 1975; HARTLE; MUNN, 1975; HARTLE; FRIEDMAN, 1975) for the stellar structure, one can compute the mass-radius diagram fig. 2.3 and obtain the maximum mass with its respective radius for white dwarfs.

The maximum masses are around $1.39M_\odot$ and the respective radius around 1150 km. The central stellar densities used are around $9 \times 10^9 \text{ g/cm}^3$. As we can observe from fig. 2.3, the effects of the sources' rotation is only important for non-massive WD (SGRs/AXPs) and larger radius. The obtained maximum radius (in average) is around 3000 km, corresponding to a mass more than $1.2M_\odot$. As one can see, this mass-radius range are plausible to explain the SGRs/AXPs. If we compare the mass range for the WD AR Scorpii, $0.8\text{-}1.29M_\odot$, having an estimated radius of $7 \times 10^8 \text{ cm}$ (GENG; ZHANG; HUANG, 2016), the values in fig. 2.3 are in this range. We note that the rotation frequency of SGRs/AXPs as WDs are near of the Kepler frequency. Given the centrifugal and gravitational forces, the ratio between these two is around 3%. For typical compact stars in ms^{-1} regime, i.e., for some NS pulsars observed the rotation frequency are not too far from that limit. Below the Kepler limit, the stars can suffer from other rotational instabilities, such as r-mode instability.

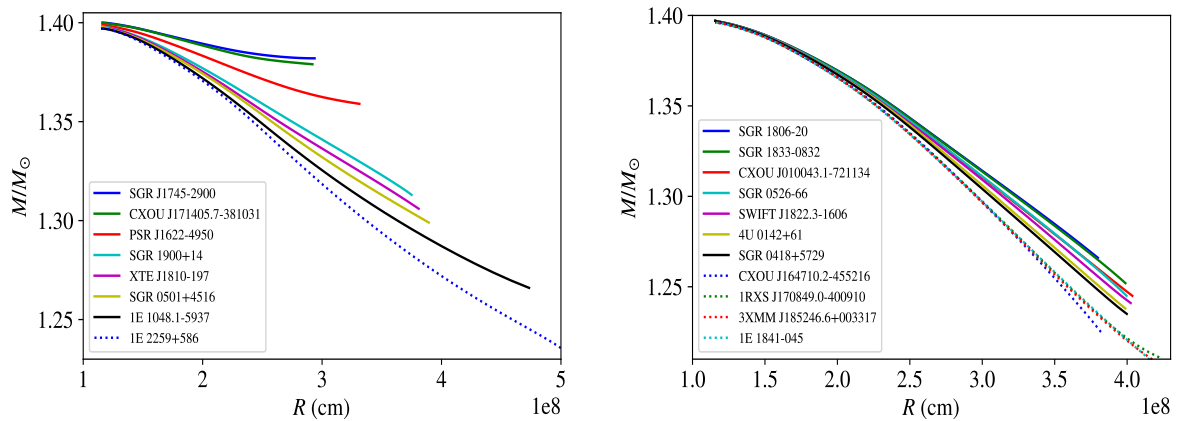


FIGURE 2.3 – Mass-Radius relation using the Hartle’s formalism for the SGRs/AXPs as WDs using the lattice EoS and the observed periods from Olausen et al. (OLAUSEN; KASPI, 2014). In the left panel we have the rapidly sources and in the right panel the slowest.

Using rotation and a realistic EoS, it not possible to have super-chandrasekhar white dwarfs. The EoS effect reduces the maximum mass due the ion interaction.

The relation between moment of inertia and radius is also obtained numerically self-consistently [see fig. 2.4] from the formalism. A maximum value for the moment of inertia is around 1.5×10^{50} g cm². Using the moment of inertia for a sphere $2/5MR^2$ for AR Scorpii with the mass of $1.29M_{\odot}$ and the radius 7×10^8 , the moment of inertia for this source is $\approx 5 \times 10^{50}$ g cm²

Having the radius and moment of inertia calculated self-consistently for each source, is possible to obtain the magnetic field associated, as we will see in section 2.3.6.1

2.3.2 Particle acceleration

As we have already discussed, there is a great number of magnetic white dwarfs and according to Usov (USOV, 1988; USOV, 1993), if the surface temperature is less than 10^6 K [see (CACERES *et al.*, 2017), for the thermal emission in fast rotating, highly magnetized white dwarfs], a scale height of its atmosphere is essentially smaller than the radius of white dwarf R and the WD will have a strong electric field \mathbf{E} in its magnetosphere,

$$\mathbf{E}_{\parallel} = \vec{\mathbf{E}} \cdot \vec{\mathbf{B}} / |\vec{\mathbf{B}}| \neq 0. \quad (2.18)$$

This parallel electric field determines a charge distribution, known as Goldreich-Julian charge density (GOLDREICH; JULIAN, 1969),

$$\rho_{\text{GJ}} = \frac{1}{4\pi} \vec{\nabla} \cdot \vec{\mathbf{E}} = -\frac{1}{2\pi c} \vec{\Omega} \cdot \vec{\mathbf{B}}. \quad (2.19)$$

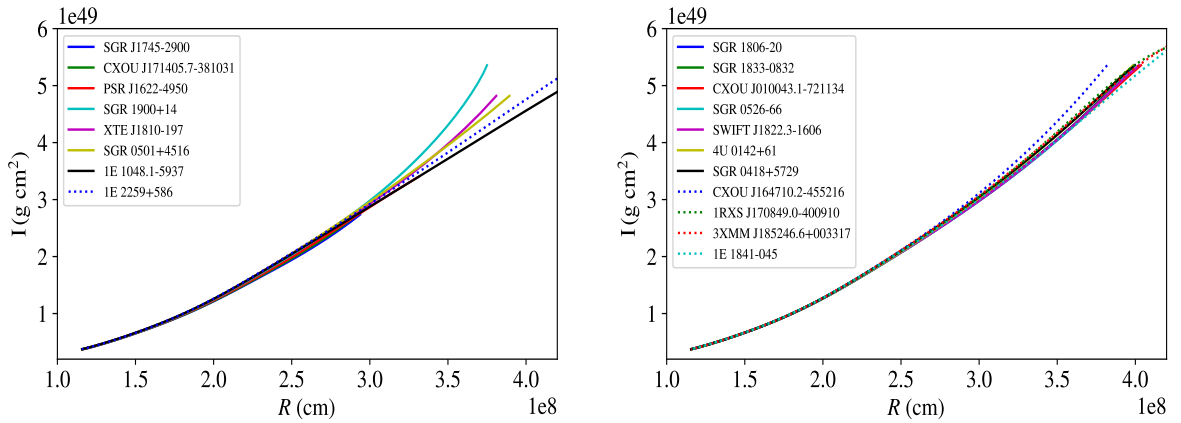


FIGURE 2.4 – Moment of inertia-radius relationship using the Hartle’s formalism for the SGRs/AXPs as WDs using the lattice EoS and the observed periods from Olausen et al. (OLAUSEN; KASPI, 2014). In the left panel we have the rapidly sources and in the right panel the slowest.

Near the surface of the star, the intense electric field tears away particles. Ultra relativistic particles flowing out, move along the open magnetic field lines producing curvature radiation (JACKSON, 1975) with characteristic energy,

$$E_\gamma = \frac{3 \hbar \gamma^3 c}{2 r_c}, \quad (2.20)$$

where

$$r_c \sim (Rc/\Omega)^{1/2} \quad (2.21)$$

is the curvature radius of the field lines. The perpendicular energy of the particle is rapidly dissipated by synchrotron radiation. This curvature radiation interact with the magnetic field and produce secondary e^\pm pairs, $\gamma + B \rightarrow e^- + e^+$, leading to a pair creation avalanche. The value of the Lorentz γ factor of the e^\pm pairs produced is given by the potential difference in the polar cap region,

$$\gamma = \frac{e\Delta V}{mc^2}. \quad (2.22)$$

Neutron star pulsars are able to produce electrons with Lorentz factors $\gamma \gtrsim 10^7$. There is a gap h above the polar region, and the potential difference becomes (RUDERMAN; SUTHERLAND, 1975)

$$\Delta V = \frac{B_p \Omega h^2}{2c}, \quad (2.23)$$

where h is given by

$$h \approx \left(\frac{R^3 \Omega}{c} \right)^{1/2}. \quad (2.24)$$

2.3.3 High energy cosmic rays from white dwarf pulsars and the Hillas criterion

Highly magnetized white dwarfs are able to have a large electric field on their surface, and can be a potential source for ultra-high-energy-cosmic rays (UHECR).

2.3.3.1 General constrains from geometry and radiation to UHECR

There are some constrains that UHECR particles should satisfy, as shown by (PTIT-SYNA; TROITSKY, 2010):

- geometry - the accelerated particle should need to be kept inside the source while being accelerated;
- power - the source should posses the required amount of energy to give it to accelerated particles;
- radiation losses - the energy lost by a particle for radiation in the accelerating field should not exceed the energy gain;
- interaction losses - the energy lost by a particle in interactions with other particles should not exceed the energy gain;
- emissivity - the total number (density) and power of sources should be able to provide the observed UHECR flux;
- accompanying radiation of photons, neutrinos and low-energy cosmic rays should not exceed the observed fluxes, both for a given source and for the diffuse background.

2.3.3.2 Hillas criterion

If a particle escapes from the region where it was being accelerated, it will not be able to gain more energy. This establishes a limit on the maximum energy E_{\max} acquired by a particle passing in a medium with magnetic field B ,

$$E_{\max} = ZqBR_s, \quad (2.25)$$

where q is the electric charge of the particle, B is the magnetic field, R_s is the size of the accelerator and Z the atomic number of the particle (for the case of iron, $Z = 26$). This equation considers the Larmour radius of the particle, $R_L = E_{\max}/(ZqB) \leq R_s$. This is a general geometrical criterion known as the *Hillas criterion* for all types of cosmic ray sources (HILLAS, 1984; HILLAS, 2004). Neglecting energy losses, i.e., the accelerator is

100% efficient, we see that only the parameters R_s and B can describe the source, showing a relationship between the sources' magnetic field strength and its size.

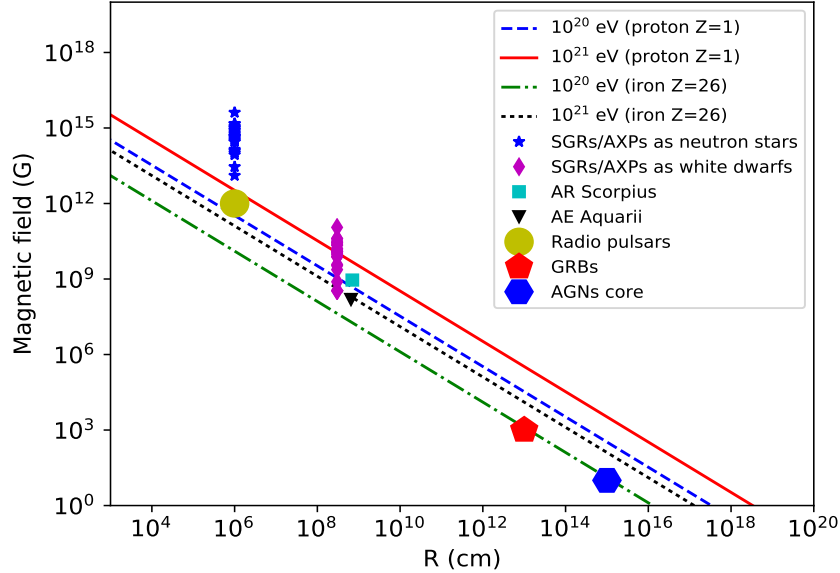


FIGURE 2.5 – Hillas plot showing the magnetic field strength versus size of SGRs/AXPs as NSs (magnetic field $\sim 10^{13-15}$ G and radius of 10^6 cm) and WDs (magnetic field $\sim 10^{8-10}$ G and radius of 3×10^8 cm). The blue-stars and magenta-diamonds describe the SGRs/AXPs as neutron stars and white dwarfs, respectively. Here, we are considering these cosmic ray sources for a maximum energy of $E_{\max} = 10^{20-21}$ eV for protons (blue and orange lines) and $E_{\max} = 10^{20-21}$ eV for iron (green and black lines). The cyan-square and black-triangles represent AR Scorpius with magnetic field of $\approx 9 \times 10^8$ G and radius of 7×10^8 cm, and AE Aquarii with magnetic field of $\approx 1.5 \times 10^8$ G and radius of 6.5×10^8 cm, respectively. As we can see these two sources are able to accelerate ultra-high energy cosmic rays. It's worth mentioning other possible sources of cosmic rays pointed in the literature: the yellow-circle, red-pentagon and blue-hexagon are the known radio pulsars, gamma rays-bursts (GRBs) and active Galaxy nuclei (AGNs), respectively.

Figure 2.5 show the Hillas plot for a maximum energy of $E_{\max} = 10^{20-21}$ eV for protons and for iron. The sources above the green and black lines are able to accelerate atoms of iron up to 10^{20} eV and 10^{21} eV, respectively. Similarly, the sources above the blue and orange lines are able to accelerate protons up to 10^{20} eV and 10^{21} eV, respectively. This figure shows that SGRs/AXPs described as WDs and the two known white dwarf pulsars are all on the line of the Hillas plot obtained by Hillas criterion, and consistent with all the others cosmic ray sources known in the universe. Moreover, SGRs/AXPs as magnetars (neutron star pulsars) are out and much above this line, which is not the case for ordinary neutron star pulsars as we also show in fig. 2.5. Thus, it is quite important to obtain precision measurements of the radius and surface magnetic field of SGRs/AXPs with the new telescopes.

Using the dipole formula (FERRARI; RUFFINI, 1969) to calculate the magnetic

field, we have shown that the magnetic fields for SGRs/AXPs as highly magnetized white dwarf are at the order of (COELHO; MALHEIRO, 2012; COELHO; MALHEIRO, 2013; LOBATO; COELHO; MALHEIRO, 2015a; LOBATO; COELHO; MALHEIRO, 2015b; LOBATO; MALHEIRO, 2016; LOBATO; MALHEIRO; COELHO, 2016; LOBATO; COELHO; MALHEIRO, 2017; LOBATO; MALHEIRO; COELHO, 2017),

$$B_p^{\text{WD}} \sim 10^9 \text{G}. \quad (2.26)$$

This allows us to estimate the charge density in the magnetosphere, i.e., the Goldreich-Julian density given by eq. (2.19),

$$\rho_{\text{GJ}}^{\text{WD}} \sim 10^{-2} \text{cm}^{-3}, \quad (2.27)$$

this value is 10^5 smaller than the ones when SGRs/AXPs are considered as neutron stars, which have a magnetic field $B \sim 10^{14-15}$ G. Thus, in the magnetosphere of SGRs/AXPs being white dwarfs, there are less charged particles than the neutron stars ones.

From eq. (2.23), we can calculate the maximum potential difference achieved on the surface of SGRs/AXPs as white dwarfs, using $\Omega \sim 1$ Hz, $R \sim 3 \times 10^3$ km,

$$\Delta V \sim 10^{16} \text{V}. \quad (2.28)$$

This difference is achieved in a length of $h \sim 10^3$ cm, and allows the particles accelerated to reach ultra relativistic energies, larger than that of neutron star pulsars. Therefore, white dwarfs can accelerate electrons with Lorentz factors at least $\gamma \sim 10^{10}$, one thousand times larger than those accelerated by neutron star pulsars, being capable to produce curvature photons with an energy up to $\sim 10^{21}$ eV.

The interaction losses are minimum in the stars' magnetosphere, considering the photon is emitted in a cone with an angular aperture $1/\gamma$ and there is a low charged particle density. Among all SGRs/AXPs, CXOU J010043.1 is the most distant source, located ~ 62.4 kpc, thus all sources are within the GZK limit, which is a theoretical upper limit on the energy of cosmic rays coming from outside of our Galaxy (≈ 10 Mpc for protons with energy of 10^{19} eV) (ZATSEPIN; KUZ'MIN, 1966; GREISEN, 1966). Particles accelerated in these sources could be a fraction of ultra-high cosmic ray observed in our planet. All these findings support the plausibility of ultra-high energy cosmic rays from SGRs/AXPs (fast and magnetic massive white dwarfs), in line with important and recent astronomical observations of white dwarf pulsars.

2.3.4 Self-consistent mass-radius to SGRs/AXPs as Neutron Stars

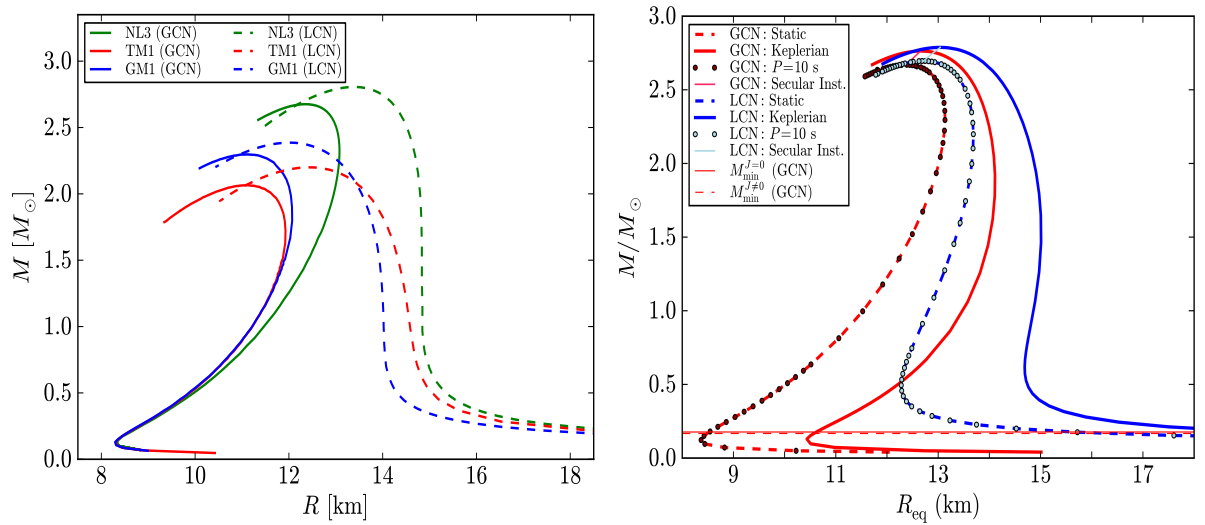
Here we review the Belvedere et al. (BELVEDERE *et al.*, 2014) and Coelho et al.'s (COELHO *et al.*, 2017) works, who have studied the SGRs/AXPs as NS self-consistently, using the Hartle's formalism and a modern nuclear EoS.

2.3.4.1 Neutron star structure

In order to compute the rotational energy loss of a NS as a function of its structure parameters, e.g. mass and radius, is necessary to construct the equilibrium configurations of a uniformly rotating NS in the range of the observed periods. Recently was shown by ICRANet group in (ROTONDO *et al.*, 2011; RUEDA; RUFFINI; XUE, 2011; BELVEDERE *et al.*, 2012; BELVEDERE *et al.*, 2014) that in the case of both static and rotating NSs, the Tolman-Oppenheimer-Volkoff (TOV) system of equations (OPPENHEIMER; VOLKOFF, 1939; TOLMAN, 1939) is superseded by the Einstein-Maxwell system of equations coupled to the general relativistic Thomas-Fermi equations of equilibrium, giving rise to what is called the Einstein-Maxwell-Thomas-Fermi (EMTF) equations. In the TOV-like approach, the condition of local charge neutrality is applied to each point of the configuration, while in the EMTF equations the condition of global charge neutrality is imposed. The EMTF equations account for the weak, strong, gravitational and electromagnetic interactions within the framework of general relativity and relativistic nuclear mean field theory.

2.3.4.2 Nuclear EoS

The NS interior is made up of a core and a crust. Its core has densities higher than the nuclear one, $\rho_{\text{nuc}} \approx 3 \times 10^{14} \text{ g/cm}^3$, and it is composed of a degenerate gas of baryons (e.g. neutrons, protons, hyperons) and leptons (e.g. electrons and muons). The crust, in its outer region ($\rho \leq \rho_{\text{drip}} \approx 4.3 \times 10^{11} \text{ g/cm}^3$), is composed of ions and electrons, and in the so-called inner crust ($\rho_{\text{drip}} < \rho < \rho_{\text{nuc}}$), there are also free neutrons that drip out from the nuclei. For the crust, is possible to adopt the Baym-Pethick-Sutherland (BPS) EOS (BAYM; PETHICK; SUTHERLAND, 1971), which is based on the (BAYM; BETHE; PETHICK, 1971) work. For the core, modern models based on relativistic mean-field (RMF) theory can be used. Belvedere et al. (BELVEDERE *et al.*, 2014) have used an extension of the formulation of Boguta and Bodmer (BOGUTA; BODMER, 1977) with a massive scalar meson (σ) and two vector mesons (ω and ρ) mediators, and possible interactions between them. There are three sets of parameterizations for these models: the NL3 (LALAZISSIS; KÖNIG; RING, 1997), TM1 (SUGAHARA; TOKI, 1994), and



(a) Total mass vs radius for static stars, considering local and global charge neutrality. (b) Total mass vs equatorial radius for static and rotating stars.

FIGURE 2.6 – Left panel: Mass-Radius relation for the NL3, TM1, and GM1 EOS in the cases of global (solid curves) and local (dashed curves) charge neutrality for non-rotating stars. Figure from (COELHO *et al.*, 2017). Right panel: Total mass vs equatorial radius for global (red) and local (blue) charge neutrality. The dashed lines represent the static configurations and the solid ones are for rotating stars. The dots represent a sequence of constant period $P = 10$ s. Figure from (BELVEDERE; RUEDA; RUFFINI, 2015).

GM1 (GLENDEENING; MOSZKOWSKI, 1991) EOS.

2.3.4.3 Mass-radius relation and moment of inertia

For the rotational periods as the ones observed in SGR/AXPs ($P \sim 2\text{--}12$ s), the structure of the rotating NS can be accurately described by small departures from the spherically symmetric case, see e.g., (BELVEDERE *et al.*, 2014; BELVEDERE; RUEDA; RUFFINI, 2015), using Hartle’s formalism. The mass-radius relation for non-rotating configurations in the cases of global and local charge neutrality are shown in fig. 2.6 from Coelho et al. (COELHO *et al.*, 2017). For the rotation periods of interest here, the mass-equatorial radius relation of the uniformly rotating NSs practically overlaps the one given by the static sequence (see fig. 2.6b from Belvedere et al. (BELVEDERE; RUEDA; RUFFINI, 2015)). Thus, is possible to use the masses and radius of the non-rotating NSs.

Figure 2.7 shows the moment of inertia vs the mass for NS for the tree EoS NL3, TM1 and GM1 for global fig. 2.7a and local neutrality fig. 2.7b.

With these two quantities is possible to infer the magnetic field of the SGRs/AXPs as NS, section 2.3.6.2.

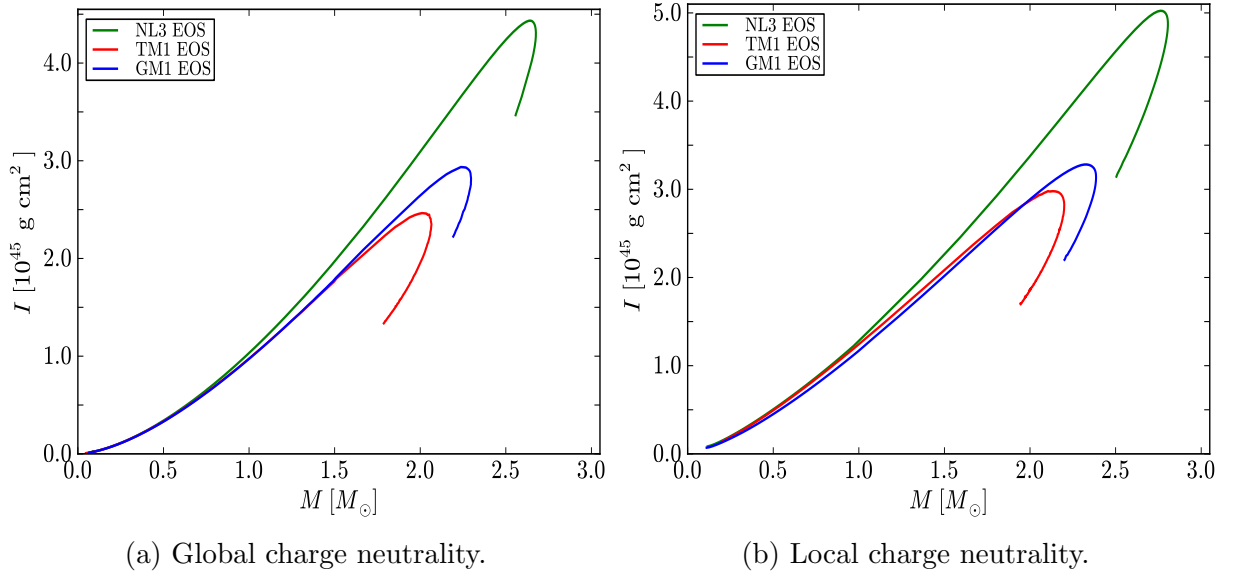


FIGURE 2.7 – Moment of inertia and radius for the NL3, TM1, and GM1 EOS in the cases of global (left panel) and local (right panel) charge neutrality. Figure from (COELHO *et al.*, 2017; MALHEIRO *et al.*, 2017).

2.3.5 Spin-powered pulsar model and magnetic fields

In the framework of pulsars there is one class known as rotation-powered pulsars (RPPs), that are neutron stars rotating uniformly with a frequency Ω , where the conversion of rotational energy into electromagnetic energy occurs, i.e, the loss of rotational energy of the star provides the power (HARDING, 2013). If the magnetic dipole μ is inclined by some angle α from the rotation axis, it emits electromagnetic radiation. On the surface of the star the magnetic field at the equator is $B_e \sim \mu/R^3$ and at the poles $B_p = 2\mu/R^3$, where R is the radius of the star. The rotational energy is given by (SHAPIRO; TEUKOLSKY, 2008),

$$E_{\text{rot}} = \frac{1}{2}I\Omega^2, \quad (2.29)$$

where I is the moment of inertia, and the loss of rotational energy of the pulsar is,

$$\dot{E}_{\text{rot}} = I\Omega\dot{\Omega} + \frac{1}{2}\dot{I}\Omega^2 \approx I\Omega\dot{\Omega}. \quad (2.30)$$

Such configuration has time-varying dipole moment, and radiates energy with a rate given by (JACKSON, 1975)

$$\dot{E}_{\text{dip}} = \frac{2\mu^2\Omega^4 \sin^2 \alpha}{3c^3}. \quad (2.31)$$

2.3.6 Inferred Magnetic fields

Combining eq. (2.30) and eq. (2.31) we obtain the surface magnetic field at the equator as (FERRARI; RUFFINI, 1969),

$$B_e = B_p/2 = \left(\frac{3c^3 I}{8\pi^2 R^6} P \dot{P} \right)^{1/2}, \quad (2.32)$$

with period $P = 2\pi/\Omega$, and $\dot{P} = dP/dt$. We see that the value of the magnetic field is inferred from $\sqrt{P\dot{P}}$ that are values obtained by astronomical observations, and two physical quantities, the moment of inertia I and the star radius R that depend on how the mass-energy density is distributed inside the star. These quantities are obtained solving self-consistent models as that ones we have used for WD and NS in section 2.3.1.3 and in section 2.3.4.3. So it is possible to obtain the magnetic field in the dipole formula, realistic as possible.

Considering that star has spherical symmetry, we can solve the Tolman-Oppenheimer-Volkoff equation for specific equations of states that are quite different for neutron stars or white dwarfs. However, for high magnetic fields, as was shown by Coelho et al. (COELHO *et al.*, 2014), they induce a breaking of spherical symmetry. The intrinsic geometry of this system is axisymmetric rather than spherical. Some recent works assumed a cylindrical metric and an anisotropic energy-momentum tensor for the source in a first approximation (PARET; HORVATH; MARTINEZ, 2014).

Depending on the stellar compactness

$$\epsilon = 2GM/Rc^2 \quad (2.33)$$

is necessary introduce corrections from general relativity for the radiation power of the dipole, see Refs. (REZZOLLA; AHMEDOV, 2004; BELVEDERE; RUEDA; RUFFINI, 2015; COELHO *et al.*, 2017) for details,

$$\dot{E}_{\text{dip}} = \frac{2\mu^2 \Omega^4 \sin^2 \alpha}{3c^3} \left(\frac{\mathbf{f}}{1 - \epsilon} \right), \quad (2.34)$$

where

$$\mathbf{f} = -3 \left(\frac{1}{\epsilon} \right)^3 \left[\ln(1 - \epsilon) + \epsilon \left(1 + \frac{\epsilon}{2} \right) \right]. \quad (2.35)$$

Combining eq. (2.30) and eq. (2.34), ones can obtain

$$B_e = B_p/2 = \frac{1 - \epsilon}{\mathbf{f}} \left(\frac{3c^3 I}{8\pi^2 R^6} P \dot{P} \right)^{1/2}. \quad (2.36)$$

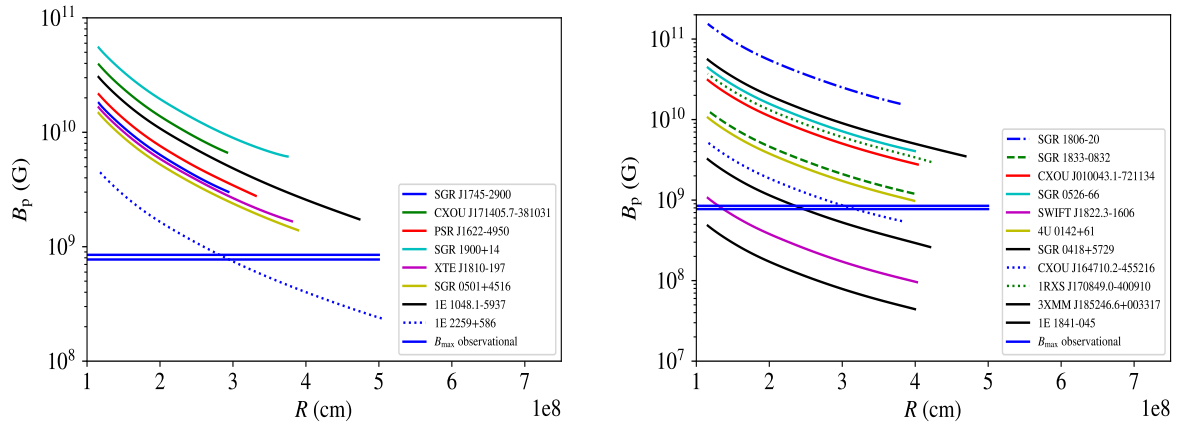


FIGURE 2.8 – Newtonian magnetic fields for the SGRs/AXPs that we consider as WDs. Two observed magnetic white are also shown (J033320.36+000720.6 (KÜLEBI *et al.*, 2009) and 135141.13+541947.35 (KEPLER *et al.*, 2013)), they are the WDs with the highest magnetic field detected so far.

2.3.6.1 Surface Magnetic Field of SGRs/AXPs as White Dwarfs

Using Newtonian dipole formula eq. (2.32), the mass-radius and moment of inertia from section 2.3.1.3 we can infer the value of magnetic field for SGRs/AXPs as WDs using realistic configurations.

Figure 2.8 shows the theoretical prediction for the surface magnetic fields of the WD as a function of the moment of inertia and radius, using the general Newtonian formula eq. (2.32). As we can see, for the small radius $< 4 \times 10^8$ cm, the values of magnetic field start to be more than $\sim 10^9$ G, for these sources. These values are in agreement with the observations of two WDs, J033320.36+000720.6 (KÜLEBI *et al.*, 2009) and 135141.13+541947.35 (KEPLER *et al.*, 2013)). They are the WDs with the highest magnetic field detected so far. Therefore, SGRs/AXPs as WDs more massive than $1.2M_{\odot}$ and radius less than 4000 km, can produce highly magnetic field on the surface.

The strength of the magnetic field is also associated with the period of the sources, being the ones with higher magnetic field the ones with the lowest period.

As we already mentioned in section 2.3.3, these magnetic field are enough to produce difference of potential around $\sim 10^{16}$ V, being able to accelerate particles to high energy.

If we consider the WD AE Scorpii, using the inferred radius of $\approx 7 \times 10^8$ cm and the maximum mass of $1.23M_{\odot}$ the estimated dipolar magnetic field is $\approx 9 \times 10^8$ G.

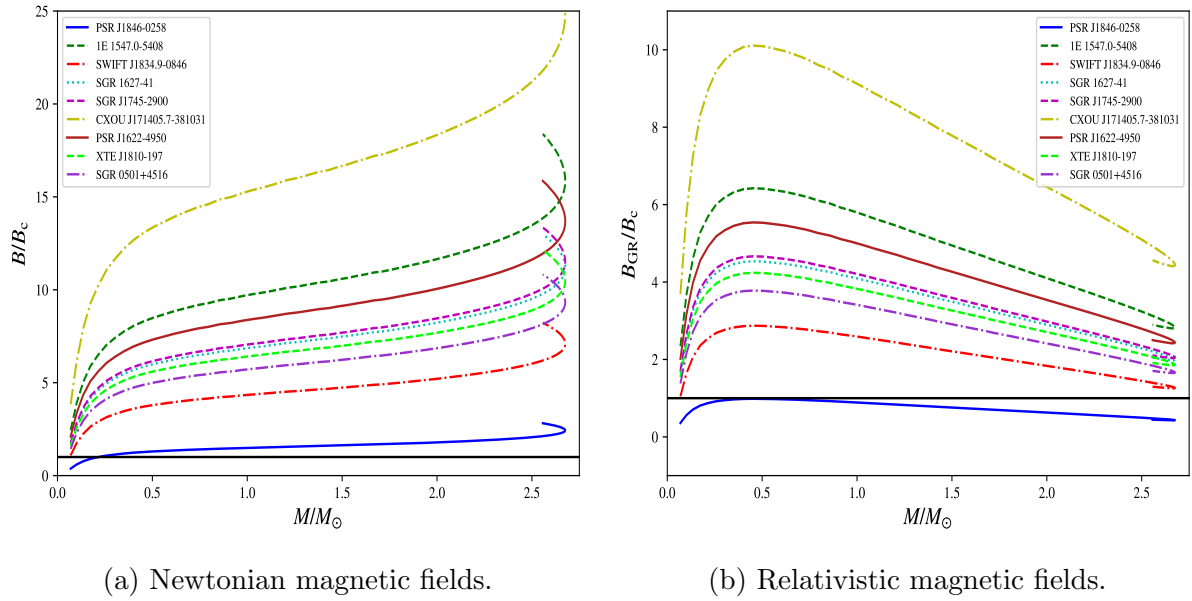


FIGURE 2.9 – Left panel: Newtonian magnetic fields for the GM1 equation of state for nine SGRs/AXPs that we consider as NS. Right panel: Relativistic magnetic fields for the GM1 equation of state for nine SGRs/AXPs that we consider as NS. Reproduced from (COELHO *et al.*, 2017; MALHEIRO *et al.*, 2017).

2.3.6.2 Surface Magnetic Field of SGRs/AXPs as Neutrons Stars

Figure 2.9a shows the theoretical prediction for the surface magnetic fields of the NS as a function of the mass, using the general Newtonian formula eq. (2.32). Figure 2.9b shows the theoretical prediction for the surface magnetic fields using the relativistic formula eq. (2.36). The two figure have considered the GM1 parametrization.

The nine sources highlighted are pointed by Coelho *et al.* (COELHO *et al.*, 2017) as potential rotation-powered neutron stars, since their steady luminosity can be explained by loss of rotational energy. If we use the general Newtonian formula eq. (2.32), the value of magnetic field is very high, i.e., larger than B_c , for high values of NS masses. Nevertheless, the relativistic formula decrease the value of magnetic field at least one order of magnitude in comparison with the Newtonian case as we can see in fig. 2.9b.

3 Models of pulsar electromagnetic emission

Although pulsars were discovered more one half-century, their mechanics of electromagnetic emission are still not well understood. There is a challenge to find the correctly coherent mechanism that supports the radio emission (MELROSE, 2006).

There are three aspects about this: the first is associated with the structure of magnetosphere, we not know the particles and fields distributions, so it's impossible to use first principles in our calculations. A second aspect is due to phenomenological interpretation of data, which means that is difficult from the data to identify the place where the emission occurs. The third concerns to the processes involved in coherent emission (MELROSE, 1995).

Initial models considered the acceleration of electrons/positrons (e^\pm) to extremes energies. The radiation originated by these particles via synchrocurvature or inverse-Compton process, creates news pairs e^\pm and a cascade, and this avalanche hold a coherent flux of radio. This mechanism is considered as essential to produce radio emission in pulsars.

Following this main idea, models were developed to explain the e^\pm pair production and emission of radiation on pulsars. Their differences depend on some assumptions regard to location, magnetic field and its geometry, the sources of photons and the dynamic of the pairs.

In the first, the region where pairs are created begins immediately above the polar cap, the *polar cap* model (STURROCK, 1971; RUDERMAN; SUTHERLAND, 1975; ARONS; SCHARLEMANN, 1979; DAUGHERTY; HARDING, 1996) hereafter PC. The second considers the production far away of the star, the *outer gap* model (CHENG; HO; RUDERMAN, 1986a; CHENG; HO; RUDERMAN, 1986b; ROMANI, 1996; HIROTANI; SHIBATA, 1999a; HIROTANI; SHIBATA, 1999b; TAKATA; WANG; CHENG, 2010; TONG; SONG; XU, 2011; VIGANO *et al.*, 2015a; VIGANO *et al.*, 2015b; VIGANÒ *et al.*, 2015) hereafter OG.

In polar cap models, γ -rays and radio photons are generated in the same region, near

the star surface, while in the outer gap model we have a large region, far from the star, where the radio and gamma emission is produced. Moreover, the polar cap model predicts a super-exponential cut-off in γ -ray spectra by magnetic absorption on the surface. The lack of observation of this behaviour lead to the conclusion that outer magnetosphere models are in better agreement with the data (RUBTSOV; SOKOLOVA, 2015). When compared with the observed pulse profiles, outer magnetospheric models are favoured, because radio and γ -ray pulse profiles are usually not coincident. The GeV spectrum observed by *Fermi* shows that the cutoffs are in fact soft and not sharp as expected by the polar cap model (ABDO *et al.*, 2009; ABDO *et al.*, 2013). The emission mechanism in outer region is due to the curvature radiation in the primary particles.

3.1 Polar Cap Model

The first model is the polar-cap, where electrons are accelerated on the stellar surface emitting γ -rays by curvature radiation [see Ref. (GHOSH, 2007), and references therein]. It is an extension of the canonical model made by Sturrock (STURROCK, 1971) who investigate the flux of particle over open magnetic field lines. In this model one considers a polar cap region, which has an electric field component parallel to \vec{B} , this electric field is given

$$\mathbf{E}_{\parallel} \simeq \frac{\Omega R}{c} B_p, \quad (3.1)$$

and could pull out particles from star's surface. The magnetosphere is not empty, but have a plasma distribution that is governed by electric forces and flowed. If we assume the electric conductivity as infinity, the version of Ohm's law $J = \sigma(\mathbf{E} + v\mathbf{B}/c)$ implies (KRALL; TRIVELPIECE, 1973),

$$\vec{\mathbf{E}} + \frac{1}{c}(\vec{\Omega} \times \vec{r}) \times \vec{B} = 0. \quad (3.2)$$

The plasma distribution is the Goldreich-Julian charge density (GOLDREICH; JULIAN, 1969)

$$\rho_{\text{GJ}} = -\frac{1}{2\pi c} \vec{\Omega} \cdot \vec{B}. \quad (3.3)$$

This density is composed of particles arrived from the surface of the star and the equation (3.3) implies that these charges are co-rotating with the star. Since the co-rotating speed field lines cannot exceed the speed of light in some region, there is a surface between the lines closed and open, known as light cylinder

$$R_{\text{lc}} = c/\Omega. \quad (3.4)$$

This fact leads to the open magnetic field lines are in the polar region which, since the lines' equation is defined as $R = R_{lc} \sin^2 \theta$ and the open angle of the polar cap $\theta_p \approx \theta_p = \sqrt{R/R_{cl}}$, has a radius given by

$$R_p \simeq R \sin \theta_p = R(\Omega R/c)^{1/2}. \quad (3.5)$$

Current of charged particles along open lines becomes relativistic when approximates to the light cylinder and reach regions far away of the star. The potential difference along an open magnetic line is given by (RUDERMAN; SUTHERLAND, 1975):

$$\Delta V_{\max} = \frac{B_p \Omega^2 R^3}{2c^2}. \quad (3.6)$$

This potential is able to accelerates particles e^\pm with Lorentz factors

$$\gamma = e\Delta V/mc^2 \gtrsim 10^7, \quad (3.7)$$

for ordinary pulsars. Electrons and ions emerging with this ultra-relativistic energies, moving along the magnetic field lines, have the perpendicular energy rapidly dissipated by synchrotron radiation, but the longitudinal energy acquired could radiate far way of the star by curvature radiation.

Considering the potential difference, the curvature radius and the magnetic field, Cheng and Ruderman (CHEN; RUDERMAN, 1993) determined the condition for pair production in the polar cap regions of pulsars as

$$\left(\frac{e\Delta V}{mc^2} \right) \frac{\hbar}{2mcr_c} \frac{h B_s}{r_c B_c} \approx \frac{1}{15}, \quad (3.8)$$

where h is the distance (gap) above the pulsar surface, r_c is the curvature radius of the magnetic field lines, $B_c = m^2 c^3 / e \hbar = 4.4 \times 10^{13}$ G and B_s the magnetic field on the surface. The surface magnetic field B_s in Eq. (3.8) may have a complicated structure, with a dependence on the geometry of magnetic field lines,

If ones consider the magnetic field of the star as a pure dipole $B_s = B_p$, so the theoretical (Newtonian) polar cap death line from Eq. (3.8) can be written as,

$$B_p = \left(\frac{m^4 2^4 c^{29/2} B_c R^{-19/2} P^{15/2}}{15 e^3 \hbar (2\pi)^{15/2}} \right)^{1/4}. \quad (3.9)$$

If ones consider the magnetic field of the star very curved, the theoretical polar cap

death line from Eq. (3.8) can be written as,

$$B_p = \left(\frac{m^4 2^4 c^{27/2} B_c R^{-21/2} P^{13/2}}{15 e^3 \hbar (2\pi)^{13/2}} \right)^{1/4}. \quad (3.10)$$

Now, if is considered a very curved magnetic field with a decreased polar cap area, the Eq. (3.8) becomes

$$B_p = \left(\frac{m^8 2^8 c^{27} B_c^2 R^{-21} P^{13}}{15^2 e^6 \hbar^2 (2\pi)^{13} B_s} \right)^{1/7}. \quad (3.11)$$

These lines are known as death line, being a lower limit for the pair production.

As explained by Zhang (ZHANG, 2003) the pair production for radio emission is mandatory. A pair plasma is required as the source for the coherent mechanism, i.e., the emission is likely generated by plasma instabilities. Although the pair condition is mandatory, it is not a sufficient condition, being poorly known (ZHANG, 2003). However, it is the best we have to obtain the radio pulsar death lines (ZHANG; HARDING; MUSLIMOV, 2000). The above lines are conditions for the pair creation and are intrinsically linked to the two quantities P and \dot{P} . This can be understood since $B \propto \sqrt{P\dot{P}}$, and $\Delta V \propto B$. Thus, if the unipolar potential is not enough because the magnetic field is not large, the accelerated particles cannot achieve high energies generating photons and no longer produces the pairs. These lines are represented as $P - \dot{P}$ or $B - P$ diagram, where the sources above/below are able/unable to produce pairs. In general the power law dependence of magnetic field with the period, as we see in eqs. (3.9) to (3.11), determine the position and the slope of the lines in the $B - P$ plane. The specific power law dependence discussed above is very sensitive to several assumptions and definitions:

- the first element is the h mean free path of the charges, which is the distance that the particles travel before radiates
- a second element can be the potential difference: there are some different models to explain the ΔV of the gap (ZHANG; HARDING; MUSLIMOV, 2000; ZHANG; HARDING, 2000)
- the third relies on the equation of state, the EoS influences the strength of the magnetic field on the surface through the momentum of inertia I and the star radius R by eqs. (2.32) and (2.36).
- the last one concerns to the geometry of the magnetic field, i.e., if it is bipolar or multipolar (CHEN; RUDERMAN, 1993).

As pointed by Zhang (ZHANG, 2003) it is not easy to draw the lines since there are many factors involved and affecting the position of the deathline, eq. (3.8).

3.1.1 General Relativity corrections for death lines

Considering SGRs/AXPs as NSs we will have a very massive star and the effects of General Relativity needs to be take account in the death lines. Beskin (BESKIN, 1990), Muslimov and Tsygan (MUSLIMOV; TSYGAN, 1990) were the first to show that general relativistic effects provide a source of additional electric field, contributing to particle acceleration in the polar cap region. As showed later by several authors (see (MOROZOVA; AHMEDOV; ZANOTTI, 2010) and references therein) the corrections in the magnetospheric plasma are first-order in the angular velocity and should be considered in a self-consistent model for the magnetosphere. The electrodynamics of a rotating, magnetic neutron star in the general relativistic framework produces a scalar potential in the vicinity of the polar cap, and can be written as (MUSLIMOV; TSYGAN, 1992; MOROZOVA; AHMEDOV; ZANOTTI, 2012)

$$\begin{aligned} \Phi &= \frac{1}{2}\Phi_0\mathcal{K}\Theta_0^2\left(1 - \frac{1}{\mathcal{N}^3}\right)(1 - \xi^2)\cos\alpha \\ &+ \frac{3}{8}\Phi_0\Theta_0^3H(1)\left(\frac{\Theta(\mathcal{N})H(\mathcal{N})}{\Theta_0H(1)} - 1\right)\xi(1 - \xi^2)\sin\alpha\cos\phi, \end{aligned} \quad (3.12)$$

where

$$\begin{aligned} H(\mathcal{N}) &= \frac{1}{\mathcal{N}}\left(\varepsilon - \frac{\mathcal{K}}{\mathcal{N}^2}\right) + \left(1 - \frac{3}{2}\frac{\varepsilon}{\mathcal{N}} + \frac{1}{2}\frac{\mathcal{K}}{\mathcal{N}^3}\right)\left[f(\mathcal{N})\left(1 - \frac{\varepsilon}{\mathcal{N}}\right)\right]^{-1}, \\ f(\mathcal{N}) &= -3\left(\frac{\mathcal{N}}{\varepsilon}\right)^3\left[\ln\left(1 - \frac{\varepsilon}{\mathcal{N}}\right) + \frac{\varepsilon}{\mathcal{N}}\left(1 + \frac{\varepsilon}{2\mathcal{N}}\right)\right], \end{aligned}$$

$\mathcal{N} = r/R$ is the dimensionless radius, $\Theta(\mathcal{N})$ is the polar angle of the last open magnetic line, Φ_0 is the expression of the scalar potential in the vicinity of the star given by eq. (3.6) and $\xi = \theta/\Theta$, $\mathcal{K} = \varepsilon\mathcal{B}$, $\mathcal{B} = I/I_0$, $I_0 = MR^2$. These two functions H and f (MUSLIMOV; HARDING, 1997) contains the relativistic corrections which do not vanish for non-relativistic star. The other term of corrections is \mathcal{K} which vanish for non-relativistic ones. In the general expression for the potential, as explained by Morozova et al. (MOROZOVA; AHMEDOV; ZANOTTI, 2012) the compactness parameter ε that enters the definition of \mathcal{K} , shifts down the lines. This is will change the potential difference (the second item of the previous list that we discussed before).

It is important to note that the Goldreich-Julian charge is modified also (MOROZOVA; AHMEDOV; KAGRAMANOVA, 2008; MOROZOVA; AHMEDOV; ZANOTTI, 2010), implying a different energy-loss due to the change of mean free path of the charges (the first item of the previous list). The new mean free path of the curvature photons in the

magnetosphere is (MOROZOVA; AHMEDOV; ZANOTTI, 2012)

$$l_f = \frac{r_c}{\gamma_{\max}} = \left(\frac{8}{3B_0} \frac{R_{lc}^2}{R^3} \right)^3 \frac{RR_{lc}f^3(1)}{\mathcal{K}^3} \xi^{-2} (1 - \xi^2)^{-3}, \quad (3.13)$$

where $B_0 \simeq 2(P\dot{P}_{-15})^{1/2}10^{12}$ G, modifying the magnetic field strength to generate particles in the magnetosphere of the star.

Thus, using the consistent relativistic expression for the electromagnetic scalar potential, section 3.1.1, in the vicinity of the polar cap with a dependence on the aforementioned function $f(\epsilon)$, eq. (2.35), the new pair production condition can be written as

$$B_0 \gtrsim \left(\frac{\mathcal{K}}{f} \right) \left(\frac{P}{1 \text{ s}} \right)^{7/3} \left(\frac{R_s}{10 \text{ km}} \right)^{-3} 10^{12} \text{ G}. \quad (3.14)$$

3.2 Outer Gap Model

The second model of emission, named gap accelerator model, proposed by Cheng et al. (CHENG; HO; RUDERMAN, 1986a; CHENG; HO; RUDERMAN, 1986b), considers the production of the observed photons far away from the stellar surface, where the magnetic field lines are open. In this model, the energy is limited by a combination of curvature radiation and inverse Compton scattering. The mechanism relies on the acceleration of particles by an E_{\parallel} . This field can be screened out by the discharge of copious e^{\pm} created by γ -ray. The emitting particles move out of the gap from/towards the stellar surface and the production of e^{\pm} pairs feeds the necessary number of particles to sustain the gap (closure of the gap). Pair production is generated by at least two process: photon-photon or photon-magnetic field interaction which is effective only for strong magnetic fields (TAKATA; WANG; CHENG, 2010).

Zhang and Cheng (ZHANG; CHENG, 1997) have studied the gap mechanism using the photon-photon process between high-energy γ -rays and X-rays coming from the stellar surface. The pair production condition is estimated as:

$$E_X E_{\gamma} (1 - \cos \theta_{X\gamma}) \geq 2(mc^2)^2, \quad (3.15)$$

where $\theta_{X\gamma}$ is the angle between the directions of X and γ -rays. E_X is the energy of the soft-photons from the stellar surface and E_{γ} the energy of emitted γ -rays in the outer gap. In this case, the gap is sustained by an X-rays flux emitted from the star surface. These X photons are, in general, produced by a return current e^{\pm} which heat the stellar surface. In figure (3.1) we present a schematic representation of the process.

In the work of Viganò et al. (VIGANO *et al.*, 2015a), the assumptions, uncertainties

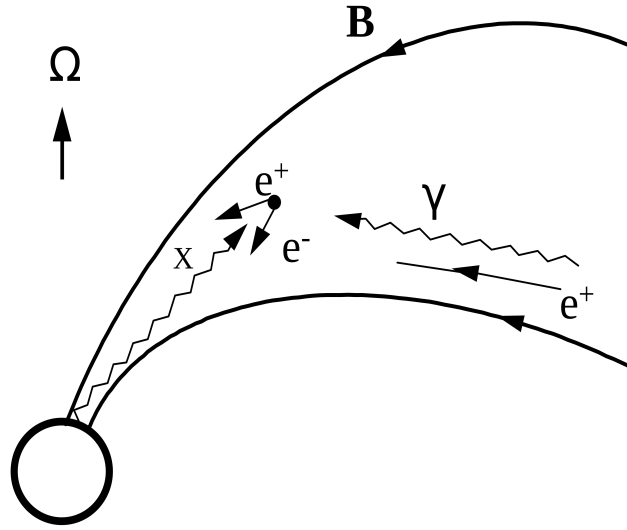


FIGURE 3.1 – Schematic representation of the gap mechanism. Interaction between X and γ -rays produces e^\pm which are sources for a return current towards the star surface, heating it and producing thermal X-ray. Figure from (ZHANG; CHENG, 1997).

and implications of outer gap model are explored. It was shown the relations among these quantities, summarized in the figure (3.2), where the yellow boxes indicate the elements for which the spectrum is more sensitive, and the green boxes the observable.

An important parameter considered in the outer gap model is the gap size/thickness or transfield fractional gap thickness f , this parametric quantity is related to the upper and lower boundaries of the gap (HIROTANI, 2006; VIGANO *et al.*, 2015a). Its definition is given by

$$f \equiv \frac{\theta_c - \theta_u}{\theta_c}, \quad (3.16)$$

where θ_u and θ_c are the magnetic colatitudes footpoints on the polar cap surface for the lower and upper boundary (VIGANO *et al.*, 2015a). The size of the outer gap is controlled by e^\pm production resulting from the interaction of thermal X-rays with primary γ -rays.

The parameter f is important in the description of electrodynamic radiation mechanism, since it controls the parallel electric field along the gap. E_{\parallel} is approximately given by (ZHANG; CHENG, 1997)

$$E_{\parallel} \approx \frac{Ba^2\Omega}{cr_c} \approx f^2 E_{\perp} \left(\frac{R_{lc}}{r_c} \right), \quad (3.17)$$

where a is related with the boundaries conditions in order to solve the Poisson equation (CHENG; HO; RUDERMAN, 1986a). As pointed out by Viganò *et al.* (VIGANO *et al.*, 2015a) the Eq. (3.17) is a simplification due to some approximations which arise from the intrinsic difficulties of the problem. Aimed to explore the E_{\parallel} dependencies with fewer

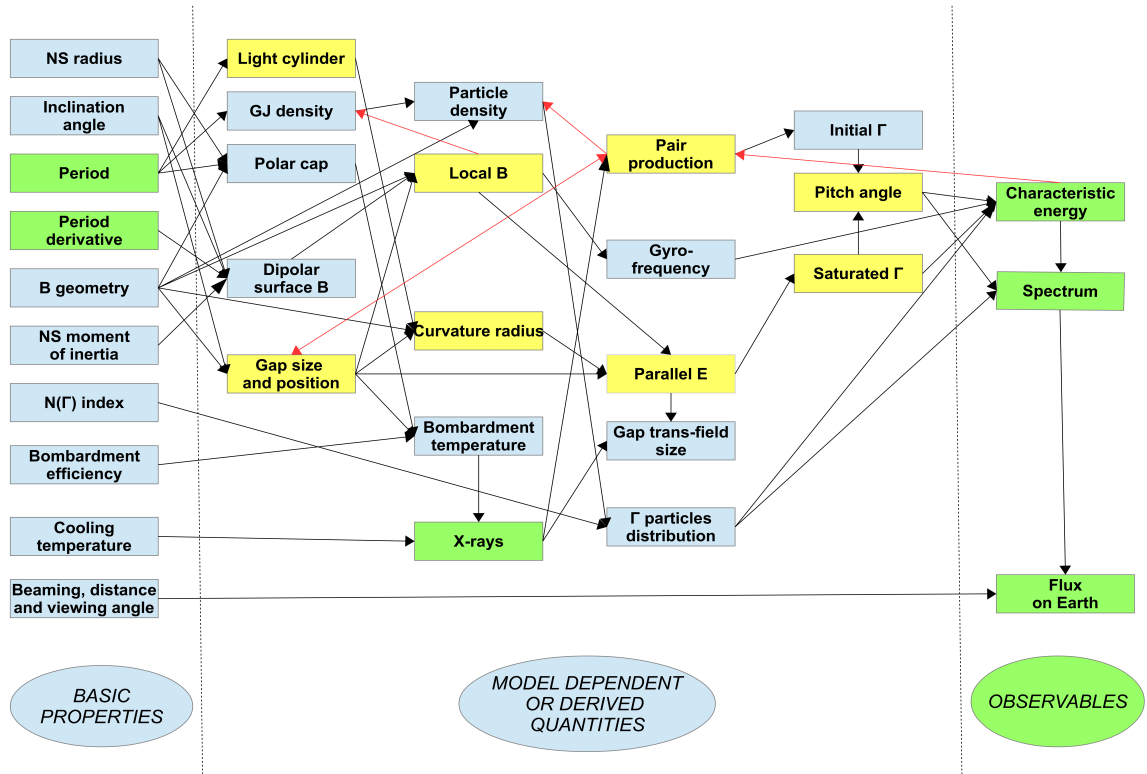


FIGURE 3.2 – Flow chart showing the characteristics/assumptions of the outer gap model. One can see that interdependence among the elements are quite complex. Figure from (VIGANO *et al.*, 2015a).

assumptions, they have considered E_{\parallel} as function of B , P and f , as well as with the geometry through the parameter χ , defined as

$$\chi \equiv \frac{a^2 q(q-1)}{R_{lc} r_c} \frac{B(r, \theta)}{B} \left(\frac{R}{R_{lc}} \right)^3, \quad (3.18)$$

where $q \equiv z/a$; $z \in [0, a]$. Considering also a screening factor κ , the above expression for the parallel electric field becomes

$$E_{\parallel} = \kappa \chi f^2 B \left(\frac{2\pi R}{cP} \right)^3. \quad (3.19)$$

Considering $\kappa = 1$ and $\chi = 1$ used by Zhang and Cheng's approach (ZHANG; CHENG, 1997), the associated potential drop in the gap is written as,

$$V = f^2 V_{\text{tot}}, \quad (3.20)$$

where V_{tot} is the total potential drop given by Eq. (3.6). Using the potential drop in the gap, it is possible to estimate the γ -ray luminosity considering the current flowing in the

gap I_{gap} ,

$$L_{\gamma} \sim I_{\text{gap}} V. \quad (3.21)$$

The current flow $I_{\text{gap}} \sim f I_{\text{GJ}}$, where I_{GJ} is the Goldreich-Julian current. Thus, as we can see, the parameter f plays a key role in the outer gap model.

Inverting the Eq. (3.19)

$$f = \sqrt{\frac{E_{\parallel}}{B\kappa\chi} \left(\frac{cP}{2\pi R} \right)^3}, \quad (3.22)$$

it is possible to estimate the death line according to the value of the E_{\parallel} needed to sustain the gap. As pointed by Viganò et al. (VIGANO *et al.*, 2015b) the constrains are strongly dependent on E_{\parallel} . That can be obtained by the equation of the Lorentz factor evolution,

$$mc^2 \frac{d\gamma}{dt} = eE_{\parallel}c - P_{\text{syn-curv}} - P_{\text{IC}} \quad (3.23)$$

where $P_{\text{syn-curv}}$ and P_{IC} are the energy-loss rates of the synchro-curvature radiation and inverse Compton process. One can obtain the electric field in the steady state, i.e., when the gain of energy by the electric field is equal to the energy loss by the synchrocurvature radiation (the inverse Compton radiation is smaller), that can be expressed as

$$eE_{\parallel}c - P_{\text{syn-curv}} = 0. \quad (3.24)$$

The synchrotron radiation is given by (JACKSON, 1975; CHENG; ZHANG, 1996),

$$P_{\text{syn}} = -\frac{2e^4 B^2 \sin^2 \alpha \gamma^2}{3m^2 c^3} \quad (3.25)$$

and curvature radiation given by (JACKSON, 1975; CHENG; ZHANG, 1996),

$$P_{\text{curv}} = -\frac{2e^2 c \gamma^4}{3r_c^2}. \quad (3.26)$$

If one considers a more general curvature characteristic energy $E_{\gamma} = 3\hbar c \gamma^3 / 2r_c$ given by Zhang and Cheng (CHENG; ZHANG, 1996) and combines it with Eq. (3.24) and Eq. (3.26) one obtains

$$E_{\parallel} = \left(\frac{2}{3} \right)^{7/3} \frac{e}{r_c^2} \left(\frac{r_c E_{\gamma}}{\hbar c} \right)^{4/3}. \quad (3.27)$$

The electric field relies on the specific choice of E_{γ} , the characteristic energy can be limited according the Eq. (3.15), and it was defined as (VIGANÒ *et al.*, 2015)

$$E_{\gamma} \equiv \frac{k_{\gamma}}{kT[\text{keV}]} \text{GeV}, \quad (3.28)$$

which takes in account the range $k_\gamma \sim [0.1 - 3.5]$ i.e., X-rays and γ are parameterized by the k_γ factor. The X-rays energies are associated with blackbody temperature. The first value in the range, $k_\gamma=0.1$, stands for low values of E_γ that corresponds to energetic X-ray photons with energy $E_X = 2.8 kT$. The upper value $k_\gamma=3.5$, indicates large values for E_γ that correspond to X-ray photons with $E_X = 0.75 kT$.

Writing the electric field in terms of the light cylinder and star period (VIGANÒ *et al.*, 2015), we can obtain

$$E_{\parallel} = \left(\frac{2}{3}\right)^{7/3} \frac{e}{c^2} \left(\frac{E_\gamma}{\hbar}\right)^{4/3} \left(\frac{2\pi R_{lc}}{Pr_c}\right)^{2/3}. \quad (3.29)$$

In this case E_{\parallel} involve a fixed T which is independent of P and B . Otherwise, the temperature will have a dependence on the mechanism associated with the thermal X-ray production through the parameter \mathcal{K}_h ,

$$E_{\parallel}(T_h) \propto \frac{1}{P^{4/9} B_{12}^{1/3}} \left(\frac{k_\gamma}{\mathcal{K}_h}\right)^{4/3} \left(\frac{R_{lc}}{r_c}\right)^{2/3}. \quad (3.30)$$

Considering these forms for the electric field we can write the gap size, eq. (3.22), for the case where the electric field depends on the period and radius of the star

$$f_t = a_t P^{7/6} B_{12}^{-1/2}, \quad (3.31)$$

the one which has a dependence on the temperature of the star

$$f_h = a_h P^{23/18} B_{12}^{-2/3}, \quad (3.32)$$

and their corresponding factors as (VIGANÒ *et al.*, 2015)

$$a_t = 3.6 \left(\frac{1}{R_6^3 \kappa \chi}\right)^{1/2} \left(\frac{k_\gamma}{kT[\text{keV}]}\right)^{2/3} \left(\frac{R_{lc}}{r_c}\right)^{1/3}, \quad (3.33a)$$

$$a_h = 7.0 \left(\frac{1}{R_6^3 \kappa \chi}\right)^{1/2} \left(\frac{k_\gamma}{\mathcal{K}_h}\right)^{2/3} \left(\frac{R_{lc}}{r_c}\right)^{1/3}. \quad (3.33b)$$

3.3 Constraining gamma emission

From eqs. (3.31) and (3.32) one can obtain the death lines for γ -rays: one for the case where the electric field depends on the period and radius (through a_t) and another which has a dependence on the temperature of the star (through a_h). The magnetic fields at the

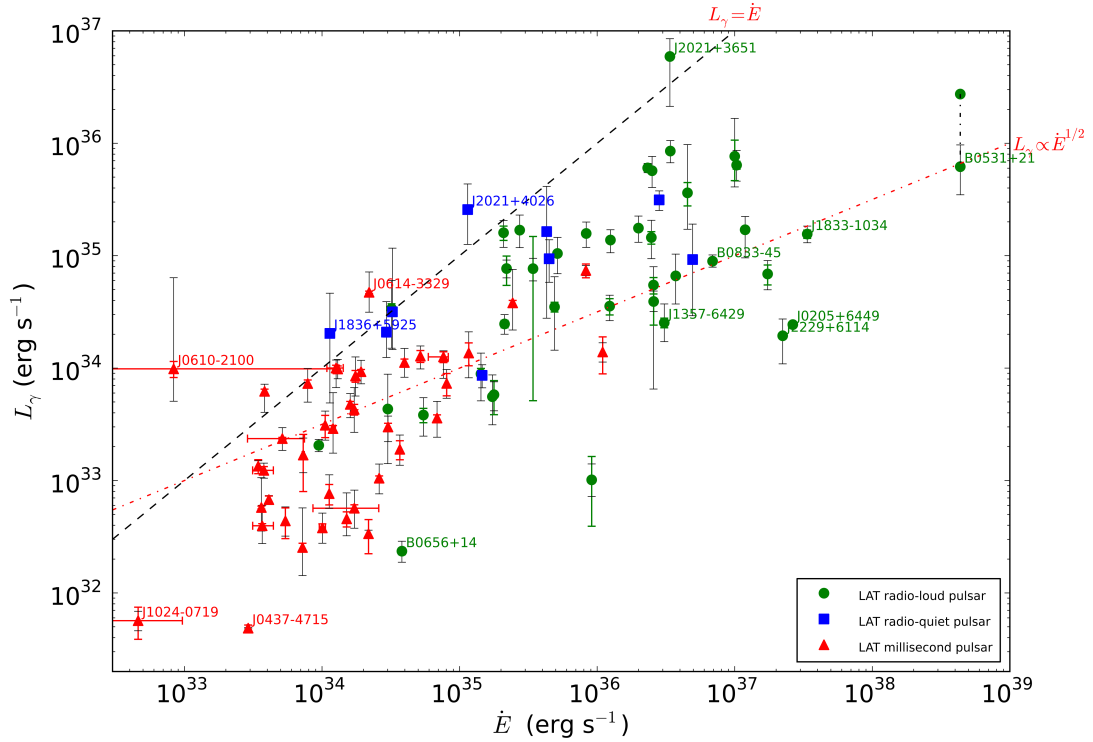


FIGURE 3.3 – γ -ray luminosity vs spindown luminosity. The upper line indicates 100% conversion of spindown into γ flux. The lower line, indicates a $L_\gamma \propto \sqrt{\dot{E}}$. Figure from (ABDO *et al.*, 2013).

light cylinder for these two cases are, respectively,

$$B_t^{\text{lc}} = \frac{10^{12}}{f^2 c^3} a_t^2 R^3 (2\pi)^3 P^{-2/3}, \quad (3.34)$$

$$B_h^{\text{lc}} = \frac{10^{12}}{f^{3/2} c^3} a_h^{3/2} R^3 (2\pi)^3 P^{-13/12}. \quad (3.35)$$

The models of γ emission predict different relations between the spindown and the γ -ray luminosity. Considering the astronomical observations, the γ -ray luminosity roughly seems to follow $L_\gamma \propto \dot{E}_{\text{rot}}^{1/2}$, see Figure (3.3).

In these descriptions, the γ -ray luminosity is only proportional to the GJ current, as pointed out in Eq. (3.21). It is known that the relation between the γ -luminosity and the spindown energy is not so well-defined for old γ -pulsars. Also, for non γ -pulsars the X-ray and optical bands seems to follow a different relation between the spindown energy and the luminosity (JOHNSON, 2012). Since the γ , X-ray and optical emissions are related, Kisaka and Tanaka proposed a model to investigate the efficiency in rotating powered pulsars (KISAKA; TANAKA, 2017). In their model, there is a $\gamma - \gamma$ scenario and the luminosity is described by

$$L_\gamma = \eta \dot{E}_{\text{rot}}, \quad (3.36)$$

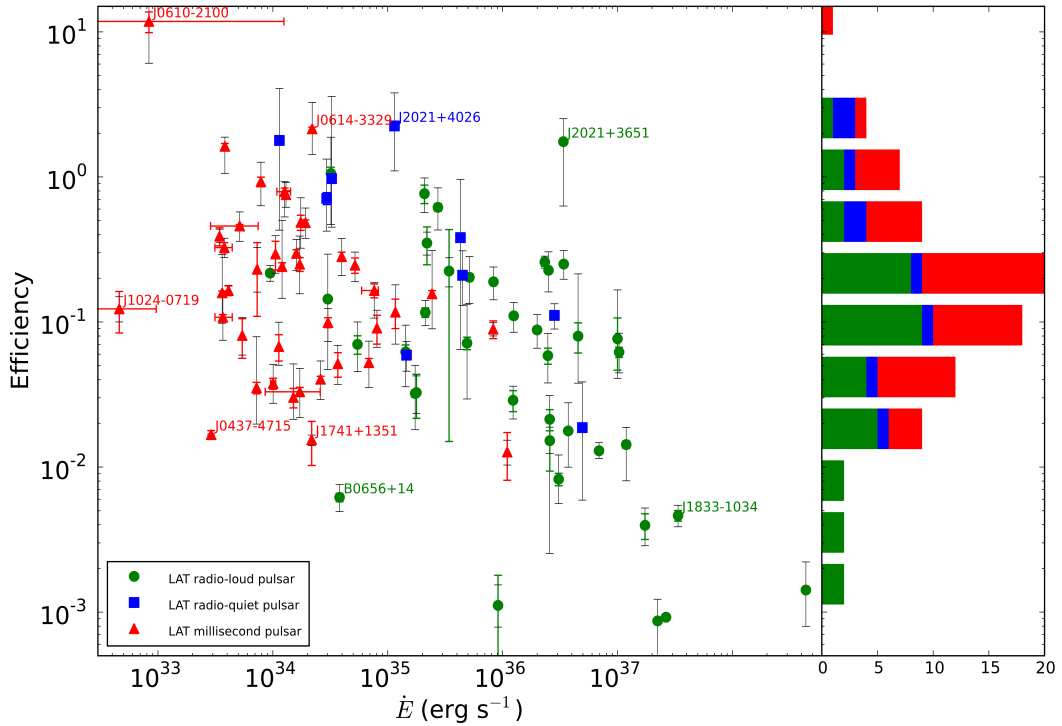


FIGURE 3.4 – γ -ray efficiency $\eta = L_\gamma / \dot{E}_{\text{rot}}$ vs spindown power. Figure from (ABDO *et al.*, 2013).

where the parameter η is the conversion efficiency, which must be smaller than 1. Thus, since in the outer gap model $L_\gamma \approx f^3 \dot{E}_{\text{rot}}$, we obtain f in terms of the efficiency,

$$f = \eta^{1/3}, \quad (3.37)$$

and consequently the death lines considering the efficiency of the pulsars.

Following the efficiency distribution in Fig. (3.4), we can see that η relies on around 10^{-1} for the majority of gamma pulsars. Thus, we are going to consider $f = 10^{-1/3}$ in the expressions for the dead lines given in eqs. (3.34) and (3.35). It is important to stress that our results do not depend too much on the value of f but depend strongly on the star radius.

We obtain the death lines, that depend on the black body temperature of the star surface, the photon energy, the radius of the light cylinder and the star radius. Thus, the size of the source affects considerably the possibility of a star to emit or not high energy radiation, and in particular, can help us to identify the nature of the SGRs/AXPs, if they are NSs or WDs.

3.3.1 Gamma emission of SGRs/AXPs as NSs

Using the radius from the mass-radius relationship obtained in section 2.3.4.3, and using the observed blackbody (minimum and maximum) temperature $\approx 0.12 - 0.59$ keV from (OLAUSEN; KASPI, 2014), for all SGRs/AXPs as NS, it is possible to estimate the range for a_t , eq. (3.33a), being written in table 3.1.

TABLE 3.1 – a_t values for SGRs/AXPs as NSs in terms of the radius of the star, blackbody temperature and γ energies E_γ .

	$R_{\min} [\approx 10 \text{ km}]$		$R [\approx 15 \text{ km}]$	
	$T_{\max} [0.59 \text{ keV}]$	$T_{\min} [0.12 \text{ keV}]$	$T_{\max} [0.59 \text{ keV}]$	$T_{\min} [0.12 \text{ keV}]$
$k_\gamma [0.1]$	$a_t = 5.74$	$a_t = 16.58$	$a_t = 3.13$	$a_t = 9.05$
$k_\gamma [3.5]$	$a_t = 61.36$	$a_t = 177.43$	$a_t = 33.50$	$a_t = 96.86$

In fig. 3.5 we have used a star radius of $R \approx 10$ km. For this radius the compactness is important, being necessary to use GR corrections for the magnetic field. We have used two values of k_γ , corresponding to different γ energies, the first value, $k_\gamma=0.1$, corresponds to low values of E_γ and energetic X-ray photons $E_X = 2.8 kT$, the continuous-lines; the second case, $k_\gamma=3.5$, corresponds to large values for E_γ and X-ray photons $E_X = 0.75 kT$, the dashed-lines. The left and the right-panel correspond to the maximum and minimum observed temperatures from the McGill catalog (OLAUSEN; KASPI, 2014), respectively. In these figures, we show the γ -rays pulsars according to “The second Fermi large area telescope catalog of gamma-ray pulsars” (ABDO *et al.*, 2013), which summarizes 117 high-confidence ≥ 0.1 GeV γ -pulsars. These pulsars are in three groups: millisecond pulsars, young radio-loud pulsars, and young radio-quiet pulsars. Are also shown, all the SGRs/AXPs (the squares and triangles), that we considered all as neutron star, among these, we highlight ten sources (the red ones), which have a waveband with persistent emission in soft- γ rays/hard X-rays (>10 keV) (OLAUSEN; KASPI, 2014). We have highlighted the three red squares and the red star which are considered NS and the red triangles WDs, according (COELHO *et al.*, 2017). From fig. 3.5a it is possible to see that the death line for $a_t = 5.74$, where the majority of milliseconds γ -pulsars are above the line, which means that they are able to emit in energetic X-rays and soft γ -rays. SGRs/AXPs are under the lines, being them unable to emit, the exception is the source PSR J1846-0258 which is above and soft gamma emission has been observed. In the same figure we have the second value of $a_t = 61.36$ which stands for the large values of E_γ . For this value the death line is shifted up and no pulsar should emit. The second figure, fig. 3.5b, shows the death lines for $a_t = 16.58$ and $a_t = 177.43$, the death lines are shifted up in comparison with fig. 3.5a, cutting the pulsar distribution in the middle for the lower a_t , i.e., only one half of them would be able to emit in soft γ -rays; for the highest value of a_t no one star should emit.

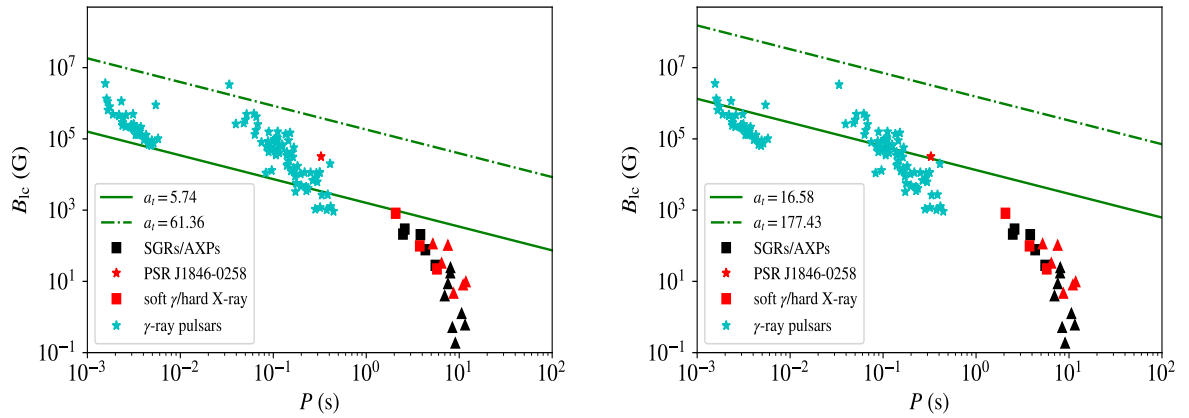
(a) Diagram for $a_t = 5.74$ and $a_t = 61.36$ (b) Diagram for $a_t = 16.58$ and $a_t = 177.43$

FIGURE 3.5 – $B - P$ diagram showing all γ -ray pulsars (cyan stars) from Abdo et al. (ABDO *et al.*, 2013) as well all SGRs/AXPs, we highlight the 10 sources (the red ones) with persistent emission in soft- γ /hard X-ray. In left panel it showed the death line for $a_t = 5.74$ (the green continuous line, which is for a temperature of 0.59 keV and $k_\gamma = 0.1$), where the majority of γ -pulsars are above the line, being able to emit in soft γ -rays, in this case the SRGs/AXPs should not emit, it is also showed the line for $a_t = 61.36$ (the green dashed-line, which is for a temperature of 0.59 keV and $k_\gamma = 3.5$), where all pulsars are below the line, being unable to emit high energy γ . In right panel it showed the death line for $a_t = 16.58$ (the green continuous line, which is for a temperature of 0.12 keV and $k_\gamma = 0.1$), where the death line cuts the pulsar distribution in the middle, being almost one half able to emit soft γ -rays; for the second case, $a_t = 177.43$ (the green dashed-line, which is for a temperature of 0.12 keV and $k_\gamma = 3.5$), again no one star should emit. In both cases we have considered the start radius of 10 km.

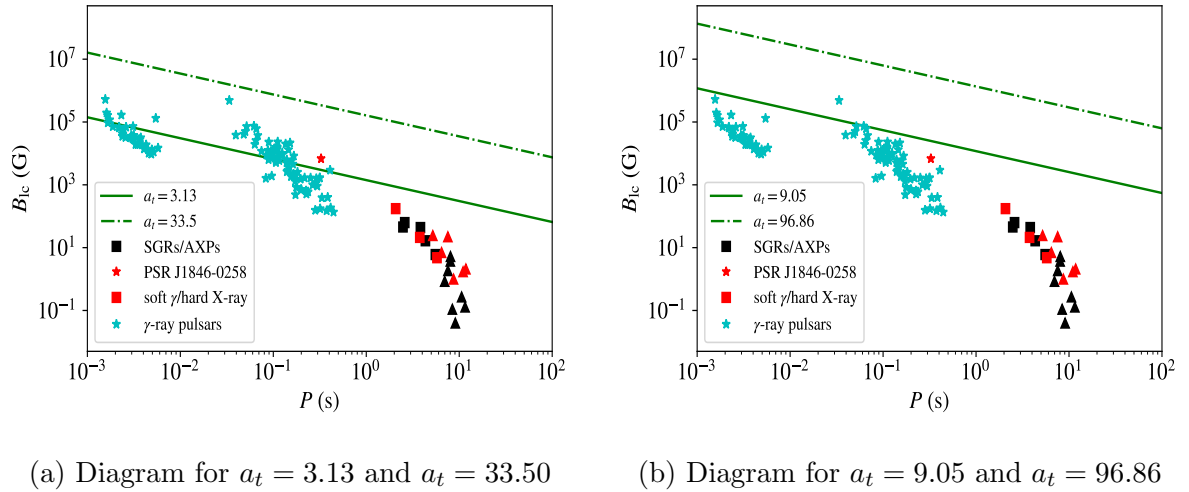


FIGURE 3.6 – $B - P$ diagram showing all γ -ray pulsars (cyan stars) from Abdo et al. (ABDO *et al.*, 2013) as well all SGRs/AXPs, we highlight the 10 sources (the red ones) with persistent emission in soft- γ /hard X-ray. In left panel it showed the death line for $a_t = 3.13$ (the green continuous line, which is for a temperature of 0.59 keV and $k_\gamma = 0.1$) and $a_t = 33.72$ (the green dashed-line, which is for a temperature of 0.59 keV and $k_\gamma = 3.5$), this figure is very similar to fig. 3.5b, where one half of the pulsars are above the line, being able to emit in γ -rays, the other half as well as the SGRs/AXPs should not emit. In right panel the lines are shifted up with $a_t = 9.05$ (the green continuous line, which is for a temperature of 0.12 keV and $k_\gamma = 0.1$) and $a_t = 96.86$ (the green dashed-line, which is for a temperature of 0.12 keV and $k_\gamma = 3.5$). The majority of the γ -pulsars were added below the line not emitting, the SGRs/AXPs should not emit as well. In both cases we have considered the start radius of 15 km.

Considering a star radius of $R \approx 15$ km, it is possible to obtain the figure fig. 3.6. For this radius it is not necessary to have GR corrections for the magnetic field, thus we have used the Newtonian magnetic field of eq. (2.32). The magnetic field in the light cylinder for these stars have decreased, as well as the new a_t , which in comparison with the previous case are almost one half lower. In fig. 3.6a we have the death line for $a_t = 3.13$ and $a_t = 33.50$, this figure is very similar to fig. 3.5b, where the down line cuts the pulsar distribution for the lowest line (the continuous green one) and one half should not emit. In fig. 3.6b the lines are shifted up and just only one γ -pulsar is above the lower line and the rest of them are below, not being able to emit even soft γ -rays. For both figures the SGRs/AXPs should not emit for any value of E_γ , for large values, any pulsars should not emit.

It seems unlikely that the model with the radius of $R \approx 15$ km represents the SGR/AXPs if we compare with the γ -pulsars.

TABLE 3.2 – a_h values for SGRs/AXPs as NSs in terms of the star radius and γ energies E_γ .

	R_{\min} [≈ 10 km]	R_{\max} [≈ 15 km]
k_γ [0.1]	$a_h = 8.81$	$a_h = 4.81$
k_γ [3.5]	$a_h = 94.28$	$a_h = 51.47$

If one considers the case where the electric field has a dependence on the mechanism of the X-ray generation, the case where we have the a_h factor, (3.33b). Using the radius of 10 km and 15 km, as in the previous case, it is estimated the range for a_h , which is shown in table 3.2.

For these a_h values, we show the death lines in fig. 3.7. In left-panel we have used a star radius of $R \approx 10$ km, whereas in fig. 3.7b a star radius of ≈ 15 km. As in the previous case, we have used the two values for the γ -rays. For the case $k_\gamma = 0.1$ we have $a_h = 8.81$ for the radius of 10 km and $a_h = 4.81$ for 15 km. For the higher energy, $k_\gamma = 3.5$, we have $a_h = 94.28$ and $a_h = 51.47$ for the radius of 10 km and 15 km, respectively. In fig. 3.7a we see that the majority of γ -pulsars are above the line for $a_h = 8.81$, inclusive few SGRs/AXPs, being able to emit in γ -rays. However the majority of millisecond pulsars are below being unable to emit soft γ -rays. There is also the line for $a_h = 94.28$, where only one pulsar should emit. The inclination of the curves are accentuated in comparison with the previous figures for a_t . In fig. 3.7b the lower death line, $a_h = 4.81$, cuts the pulsar distribution, being the majority below the lines. In the upper line, $a_h = 51.47$, all star are under the line.

This model seems unlikely that this one is more appropriate, as we can see the inclination of the lines does not agree with the distribution of the γ pulsars in the case of the radius of $R \approx 10$ km, which is closer to the fig. 3.5a. Due the inclination, the large majority of the millisecond pulsars are below. For the radius of $R \approx 15$ km the lines are up shifted.

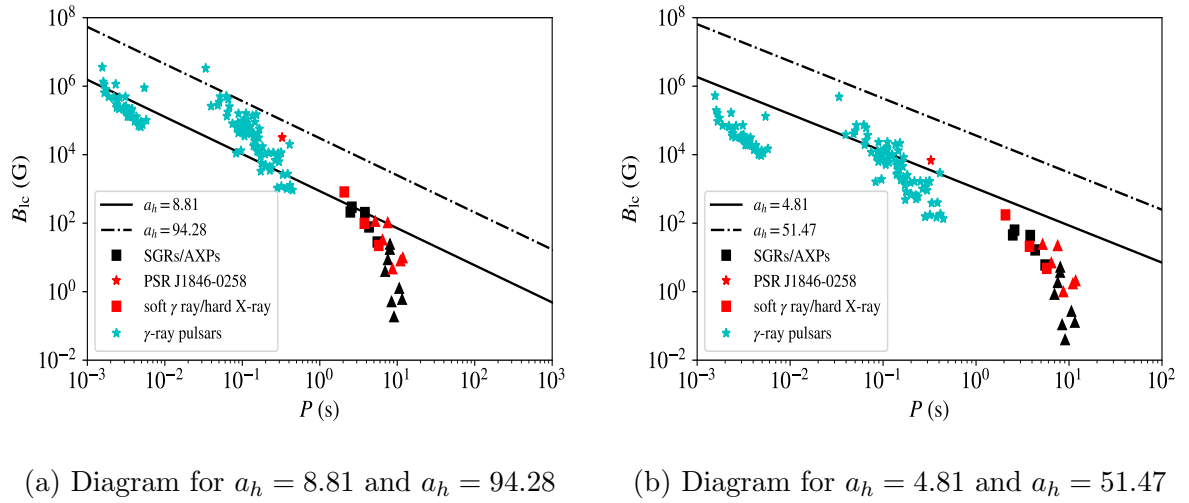


FIGURE 3.7 – $B - P$ diagram showing all γ -ray pulsars (cyan stars) from Abdo et al. (ABDO *et al.*, 2013) as well all SGRs/AXPs, we highlight the 10 sources (the red ones) with persistent emission in soft- γ /hard X-ray. In left panel it is showed the death line for $a_h = 8.81$, where the majority of the millisecond γ -pulsars are below the line, and majority of SGRs/AXPs as well, being unable to emit in γ -rays, it is also showed the line for $a_h = 94.28$, where only one pulsar should emit (we have used a star radius $R \approx 10$ km and $k_\gamma = 0.1$ and $k_\gamma = 3.5$ respectively). The inclination of the curves are accentuated in comparison with the previous images for a_t . In right panel it is showed the death line for $a_h = 4.81$ and $a_h = 51.47$ (corresponding to a radius of $R \approx 15$ km and $k_\gamma = 0.1$ and $k_\gamma = 3.5$ respectively), where the death line cuts the pulsar distribution, being the majority below the lines.

3.3.2 Gamma emission of SGRs/AXPs as WDs

Using the radius from the mass-radius relationship obtained in section 2.3.1.3 for WDs and the observed blackbody (minimum and maximum) temperature $\approx 0.12 - 0.59$ keV from (OLAUSEN; KASPI, 2014), we have estimated the range for the new a_t [see eq. (3.33)], considering SGRs/AXPs as WDs. The values are shown in table 3.3.

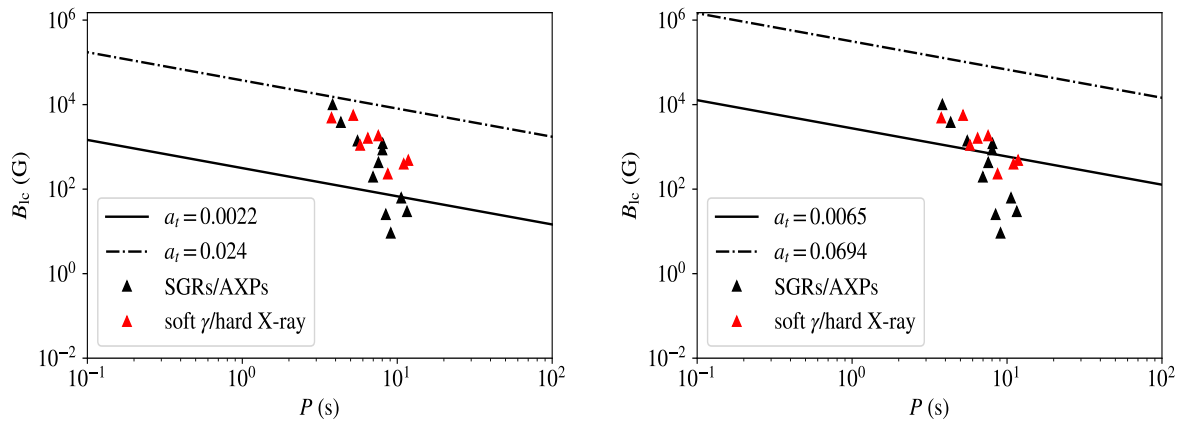
TABLE 3.3 – a_t values for SGRs/AXPs as WDs in terms of the radius of the star, blackbody temperature and γ energies E_γ .

	$R_{\min} [\approx 1.15 \times 10^3 \text{ km}]$		$R [\approx 3 \times 10^3 \text{ km}]$	
	$T_{\max} [0.59 \text{ keV}]$	$T_{\min} [0.12 \text{ keV}]$	$T_{\max} [0.59 \text{ keV}]$	$T_{\min} [0.12 \text{ keV}]$
$k_\gamma [0.1]$	$a_t = 0.0022$	$a_t = 0.0065$	$a_t = 0.0005$	$a_t = 0.0013$
$k_\gamma [3.5]$	$a_t = 0.0240$	$a_t = 0.0694$	$a_t = 0.0049$	$a_t = 0.0142$

From the WDs's a_t values, we obtain the death lines shown in figs. 3.8 and 3.9. We have used a minimum radius of $R \approx 1150$ km and maximum of $R \approx 3000$ km, consistent with our self-consistent calculation. These radii in combination with the inertial moment and mass, gave us the magnetic field on the light cylinder higher than for neutron star case, i.e., for some SGRs/AXPs as WDs, the magnetic fields in the light cylinder are larger since the distance between the light cylinder and the star surface is smaller.

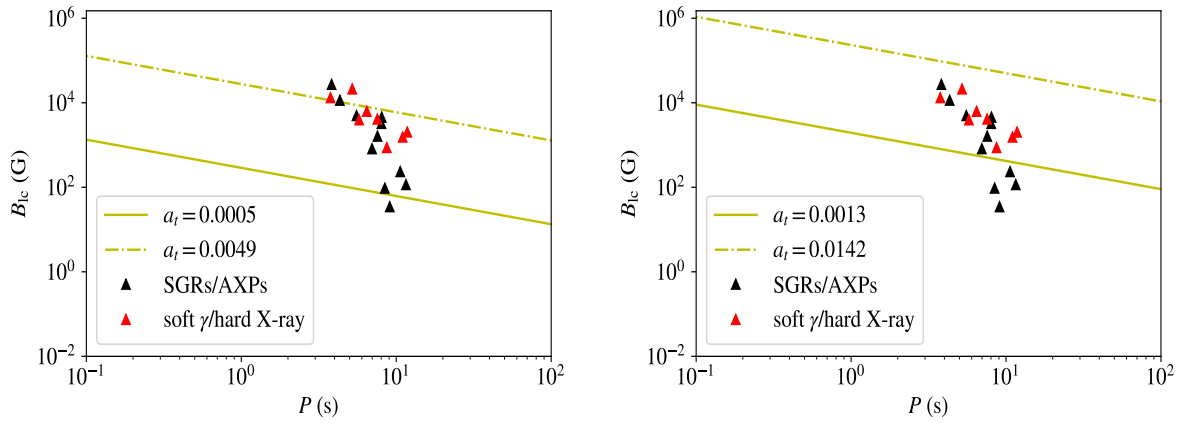
In fig. 3.8a it is showed the death line for $a_t = 0.0022$ and $a_t = 0.0240$, corresponding to the temperature of 0.59 keV and k_γ values of 0.1 and 3.5, respectively. As one can see, the death line for $a_t = 0.0022$ is under the WDs' middle distribution, meaning that some of them should emit γ -rays whereas 3 should not emit. For $a_t = 0.0240$ all stars are below i.e, any star should not emit. In fig. 3.8b it is showed the death line for $a_t = 0.0065$, where the death line cuts the stars' distribution in the upper middle, it is also showed the death line for $a_t = 0.0694$, where any star should not emit; these values of a_t are for a temperature of 0.12 keV and k_γ values of 0.1 and 3.5, respectively. For these two figures, we have considered the star radius of $\approx 1.15 \times 10^8$ cm and have highlighted the sources with persistent emission in soft- γ /hard X-ray (red triangles). As ones can see, for fig. 3.8a these sources are above the death-line for hard X/soft γ -rays ($k_\gamma = 0.1$).

In fig. 3.9a it is showed the death line for $a_t = 0.0005$ and $a_t = 0.0049$, corresponding to a temperature of 0.59 keV and k_γ values of 0.1 and 3.5, respectively. In this case the stars are above the first death line and some of them above the second one, i.e., all they should emit in the first case $k_\gamma = 0.1$ and few of them in the second case $k_\gamma = 3.5$. In fig. 3.9b it is showed the death line for $a_t = 0.0013$ and $a_t = 0.0142$, corresponding to a temperature of 0.12 keV and k_γ values of 0.1 and 3.5, respectively. The fig. 3.9b is similar to fig. 3.8a, about the emission possibility. The values of a_t correspond to a star radius of $\approx 3 \times 10^8$ cm.



(a) Diagram for $a_t = 0.0022$ and $a_t = 0.0240$ (b) Diagram for $a_t = 0.0065$ and $a_t = 0.0694$

FIGURE 3.8 – $B - P$ diagram showing the SGRs/AXPs as WDs, we highlight some sources (red triangles) with persistent emission in soft- γ /hard X-ray. In the left panel it is showed the death line for $a_t = 0.0022$ and $a_t = 0.0240$, corresponding to the temperature of 0.59 keV and k_γ values of 0.1 and 3.5, respectively. As one can see, the death line for $a_t = 0.0022$ is under the WDs' middle distribution, meaning that some of them should emit γ -rays whereas 3 should not emit. For $a_t = 0.0240$ all stars are below. i.e, any star should not emit. In right panel it is showed the death line for $a_t = 0.0065$, where the death line cuts the stars' distribution in the upper middle, it is also showed the death line for $a_t = 0.0694$, where any star should not emit; these values of a_t are for a temperature of 0.12 keV and k_γ values of 0.1 and 3.5, respectively. Here, we considered the star radius of $\approx 1.15 \times 10^8$ cm.



(a) Diagram for $a_t = 0.0005$ and $a_t = 0.0049$ (b) Diagram for $a_t = 0.0013$ and $a_t = 0.0142$

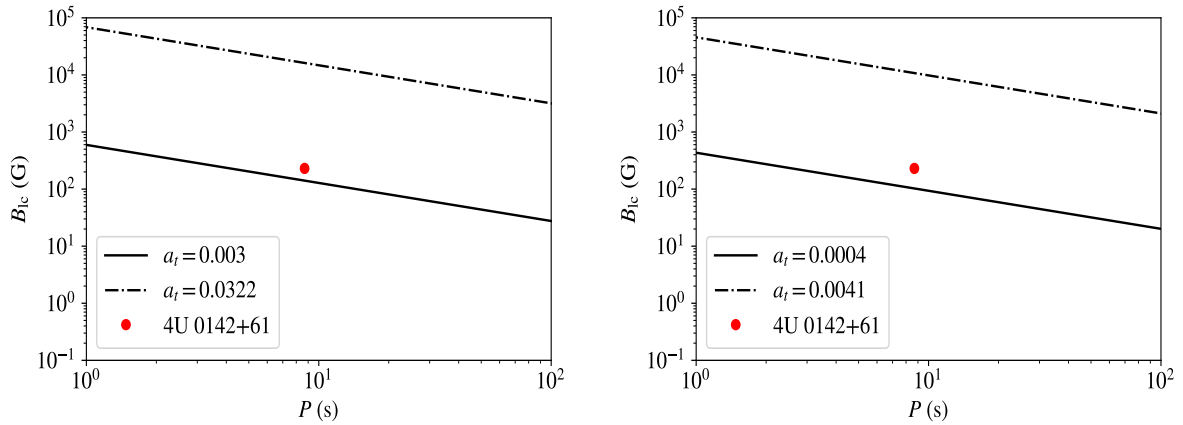
FIGURE 3.9 – $B-P$ diagram showing the SGRs/AXPs as WDs, highlighted some sources (red triangles) with persistent emission in soft- γ /hard X-ray. In the left panel it is showed the death line for $a_t = 0.0005$ and $a_t = 0.0049$, corresponding to a temperature of 0.59 keV and k_γ values of 0.1 and 3.5, respectively. In this case the stars are above the first death line and below the second one, i.e., they should emit only in the first case. In right panel it is showed the death line for $a_t = 0.0013$ and $a_t = 0.0142$, corresponding to a temperature of 0.12 keV and k_γ values of 0.1 and 3.5, respectively. The figure from the left panel is similar to fig. 3.8a, about the emission possibility. The values of a_t correspond to a star radius of $\approx 3 \times 10^8$ cm.

TABLE 3.4 – Possibles values for 4U 0142+61's a_t in terms of the radius of the star, blackbody temperature and γ energies E_γ .

	R_{\min} [$\approx 1.1564 \times 10^3$ km]	R [$\approx 3.99 \times 10^3$ km]
	T_{\max} [0.41 keV]	T_{\max} [0.41 keV]
k_γ [0.1]	$a_t = 0.0030$	$a_t = 0.0004$
k_γ [3.5]	$a_t = 0.0322$	$a_t = 0.0041$

Now we turn out to analyse the specific SGRs, named 4U 0142+61, which we already mentioned in section 2.2.1. Using its blackbody temperature 0.41 keV, from (OLAUSEN; KASPI, 2014) and the self-consistent massa-inertia-radius in order to compute the magnetic field, we obtain the a_t value for 4U 0142+61, showed in table 3.4.

For these a_t values, it is possible to have the death-lines for this specific source in fig. 3.10. We have considered the minimum radius of 1.15×10^3 km and a maximum of 3.99×10^3 km. For the lowest value of a_t in both cases, the source 4U 0142+61 should emit in hard X/soft γ -rays. For the case of high energy γ -rays, $k_\gamma = 3.5$, in both cases the star should not emit.



(a) Diagram for $a_t = 0.0003$ and $a_t = 0.0322$ (b) Diagram for $a_t = 0.0004$ and $a_t = 0.0041$

FIGURE 3.10 – $B - P$ diagram showing the source 4U 0142+61 which presents persistent emission in soft- γ /hard X-ray. In the left panel it is showed the death line for $a_t = 0.003$ and $a_t = 0.0322$, corresponding to k_γ values of 0.1 and 3.5, respectively and a radius of 1.150×10^3 . In this case the star is above the first death line and below the second one, i.e., it should emit only in the first case $k_\gamma = 0.1$. In right panel it is showed the death line for $a_t = 0.0004$ and $a_t = 0.0041$, corresponding to k_γ values of 0.1 and 3.5, respectively and a radius of $\approx 3.99 \times 10^3$ km, again, the star is above the first death line and below the second one.

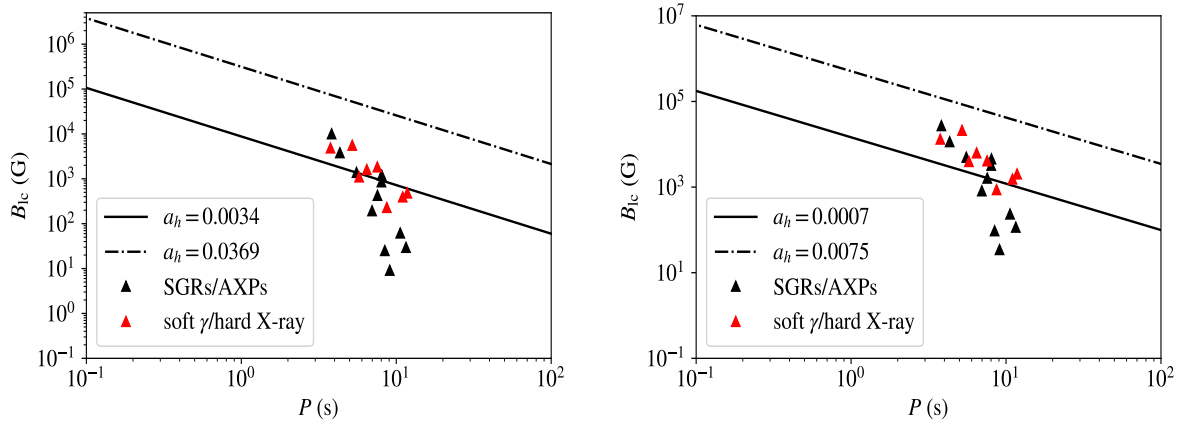
TABLE 3.5 – Possibles values a_h for SGRs/AXPs as WDs in terms of the star radius and γ energies E_γ .

	$R_{\min} [\approx 1.150 \times 10^3 \text{ km}]$	$R_{\max} [\approx 3000 \text{ km}]$
$k_\gamma [0.1]$	$a_h = 0.0034$	$a_h = 0.0007$
$k_\gamma [3.5]$	$a_h = 0.0369$	$a_h = 0.0075$

For the second model of γ -emission where the electric field depends on the temperature of the star, i.e., the case of a_h factor, eq. (3.33), considering the mass-radius relationship obtained in section 2.3.1.3, case where the SGRs/AXPs are considered as WDs, we have the factors a_h evaluated in table 3.5.

For these a_h values, we have the death lines in fig. 3.11. In the left panel we have used a star radius of ≈ 1150 km and in the right one a star radius of ≈ 3000 km. There were used two values of k_γ , corresponding to two values of the γ -rays energies. For the case of $k_\gamma = 0.1$ there are the values of $a_h = 0.0034$ for the radius of 1150 km and $a_h = 0.0007$ for the radius of 3000 km. For the case of $k_\gamma = 3.5$ there are, $a_h = 0.0369$ for the radius of 1150 km and $a_h = 0.0075$ for the radius of 3000 km. For both radius it is possible to see that the majority of stars are below the lines, being unable to emit in soft γ -rays/hard X-rays.

This second model needs a higher magnetic field on the light cylinder in order to produce pairs, seems unlikely that this model is appropriate to describe the sources.



(a) Diagram for $a_h = 0.0034$ and $a_h = 0.0369$ (b) Diagram for $a_h = 0.0007$ and $a_h = 0.0075$

FIGURE 3.11 – $B - P$ diagram showing all SGRs/AXPs as WDs, we highlight some sources (red triangles) with persistent emission in soft- γ /hard X-ray. In the left panel it is showed the death line for $a_h = 0.0034$, where the majority of γ -pulsars are below the line, being unable to emit in γ -rays, it is also showed the line for $a_h = 0.0369$, where all stars are below the death line. In right panel it is showed the death line for $a_h = 0.0007$ and $a_h = 0.0075$, where the first death line cuts the pulsar distribution, being the majority below the lines, in the second one, all stars are below the line.

TABLE 3.6 – Possibles values for a_h for 4U 0142+61 in terms of the star radius and γ energies E_γ .

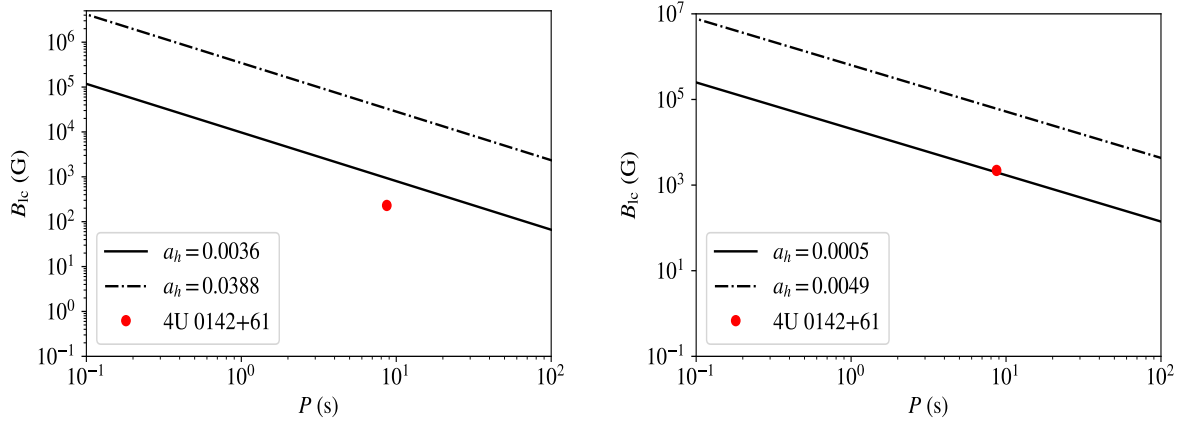
	R_{\min} [$\approx 1.1564 \times 10^3$ km]	R_{\max} [$\approx 3.99 \times 10^3$ km]
k_γ [0.1]	$a_h = 0.0036$	$a_h = 0.0005$
k_γ [3.5]	$a_h = 0.0388$	$a_h = 0.0049$

Now considering the specific case of 4U 0142+61 in this model, and considering its minimum and maximum radius, we obtain the values of a_h , shown in table 3.6.

From these a_h values, we obtain the death lines in fig. 3.12. As one can see in figs. 3.12a and 3.12b, for any value of a_h the star is in the death zone.

3.3.2.1 Bootstrapped pair production

Apart to the mechanism where the accelerated particles generate the high energy γ -rays by curvature radiation, there is another possibility where soft photons $\hbar\omega_s$ are boosted by inverse Compton scattering to produce primaries γ -rays $\gamma^2\hbar\omega_s$. These primaries pair interact with the soft ones, in general thermal X-rays coming from the surface, producing second pairs constrained by $\gamma^2\hbar\omega_s\hbar\omega_s \approx (mc^2)^2$ (CHEN; RUDERMAN, 1993) the synchrotron radiation of these secondary particles gives the spectrum. The importance of the inverse Compton scattering was broad studied (XIA *et al.*, 1985; DAUGHERTY; HARDING, 1989; DERMER, 1990; STURNER; DERMER; MICHEL, 1995). It was showed that



(a) Diagram for $a_h = 0.0036$ and $a_h = 0.0388$ (b) Diagram for $a_h = 0.0003$ and $a_h = 0.0029$

FIGURE 3.12 – $B - P$ diagram showing the source 4u 0142+61, which presents persistent emission in soft- γ /hard X-ray. In the left panel it is showed the death line for $a_h = 0.0036$ and $a_h = 0.0388$, the source is below of both death lines, being unable to emit. In the right panel it is showed the death line for $a_h = 0.0005$ and $a_h = 0.0049$, where again the source is close to the death zone.

this mechanism can generate photons more energetic and therefore have shorter mean free path to generate pairs than the curvature mechanism (ZHANG; QIAO, 1996; LUO, 1996).

The initial inverse Compton scattering limits the energy of the primary e^\pm to $\gamma mc^2 \sim (mc^2)^2 / \hbar \omega_s$. Because the maximum energy of secondary e^\pm is γmc^2 , the highest frequency synchrotron radiation from secondary e^\pm becomes (CHEN; RUDERMAN, 1993; LUO, 1996):

$$\omega_{\max} \sim \gamma \sin \theta \omega_B, \quad (3.38)$$

where $\omega_B = eB/mc$ and θ the angle between e^\pm and local B . There is a critical value, where the energy spectrum can be cut (CHEN; RUDERMAN, 1993),

$$\omega_c \sim \gamma \gamma_{\perp, c} \omega_B = \frac{\gamma_{\parallel}^3}{\omega_B^3} \left(\frac{mc^3 \omega}{e^2} \right)^2. \quad (3.39)$$

The typical frequency of the tertiary photons is

$$\omega_s \sim \frac{1}{\omega_B^3} \left(\frac{mc^3 \Omega}{e^2} \right)^2 \quad \text{valid only for } \omega_s \geq \omega_B. \quad (3.40)$$

From Eqs. (3.38), (3.39) and (3.40), we can obtain the critical frequency,

$$\omega_c \approx \gamma_{\parallel}^3 \frac{m^5 c^9}{e^7} \Omega^2 B^{-3}, \quad (3.41)$$

and the maximum synchrotron emission frequency,

$$\omega_{\max} \approx \frac{e^{15}}{\gamma_{\parallel} \hbar^2 m^9 c^{15}} \Omega^{-4} B^7. \quad (3.42)$$

If we consider $\omega_{\max} \approx \omega_c$, it is possible to obtain,

$$B_p = \left(\frac{P^{12} R^{-15} \gamma_{\parallel}^2 m^7 \hbar c^{27}}{e^{11} (2\pi)^{12}} \right)^{1/5}, \quad (3.43)$$

the term γ_{\parallel} can be inferred from observations and generally is taken as ~ 10 from the Vela pulsar (CHEN; RUDERMAN, 1993).

Now, taking $\omega_s \approx \omega_B$,

$$B_p = \left(\frac{m^3 c^{11} P^5 R^{-6}}{e^4 (2\pi)^5} \right)^{1/2}. \quad (3.44)$$

The condition (3.43) we label as “outer gap 1” and (3.44) as “outer gap 2”.

3.4 Constraining radio emission

3.4.1 Radio emission of SGRs/AXPs as NSs

The standard definition of death line implicitly assumes that pair formation is a necessary condition for pulsar radio emission and that pulsars become radio-quiet after crossing the death lines during their evolution from upper to above in the B - P diagram. This basic condition is enough but not sufficient to guarantee the radio emission, and functioning of radio pulsars may imply far more complex physical conditions (ZHANG, 2003).

Considering the dependence of the death lines on the R calculated self-consistently, as well as the magnetic field which considered I and R , eq. (3.9), (the Newtonian death line) and the death line, eq. (3.14), with corrections from GR for the NS, it is possible to draw the figs. 3.13 and 3.14, showing the death lines, the Newtonian and GR magnetic field as functions of the star radius. We have made a selection of 9 SGRs/AXPs that is pointed by (COELHO *et al.*, 2017) as potential rotation-powered neutron stars. These sources have large magnetic fields and are very similar to high- B pulsars, being strongly magnetized neutron stars, but with fields close to the critical field.

In fig. 3.13, we show 4 SGRs/AXPs which were observed in radio band. As we can see in fig. 3.13 these sources are above the death line of the polar cap model if one considers a huge radius and below of the 2 outer gap models i.e., the phenomenology is better described by the polar cap model in order to emit in radio.

This is different if we compare with other pulsars at least in γ band, where the data are in better agreement with outer gap models (RUBTSOV; SOKOLOVA, 2015). Polar cap models predict a super exponential cut-off in γ -ray spectra (VIGANO *et al.*, 2015a), due to the magnetic absorption on the surface, this is not observed (ABDO *et al.*, 2013).

From figure (3.13) we also see that the sources are very close to the death lines. This can indicate an explanation for the radio disappearance of two sources reported recently. According to (CAMILO *et al.*, 2016) the first one was XTE J1810-197, and more recently according to (SCHOLZ *et al.*, 2017) the source PSR J1622-4950 became radio quiet. The sources are approximating the death lines in the polar model, when the value of radius increases.

Secondly, in fig. 3.14 we consider the other 5 sources. These stars never showed radio emission. These sources have a similar behaviour of fig. 3.13, but a phenomenological way to better describe them is by Outer Gap models, where none of them would be a radio emitter.

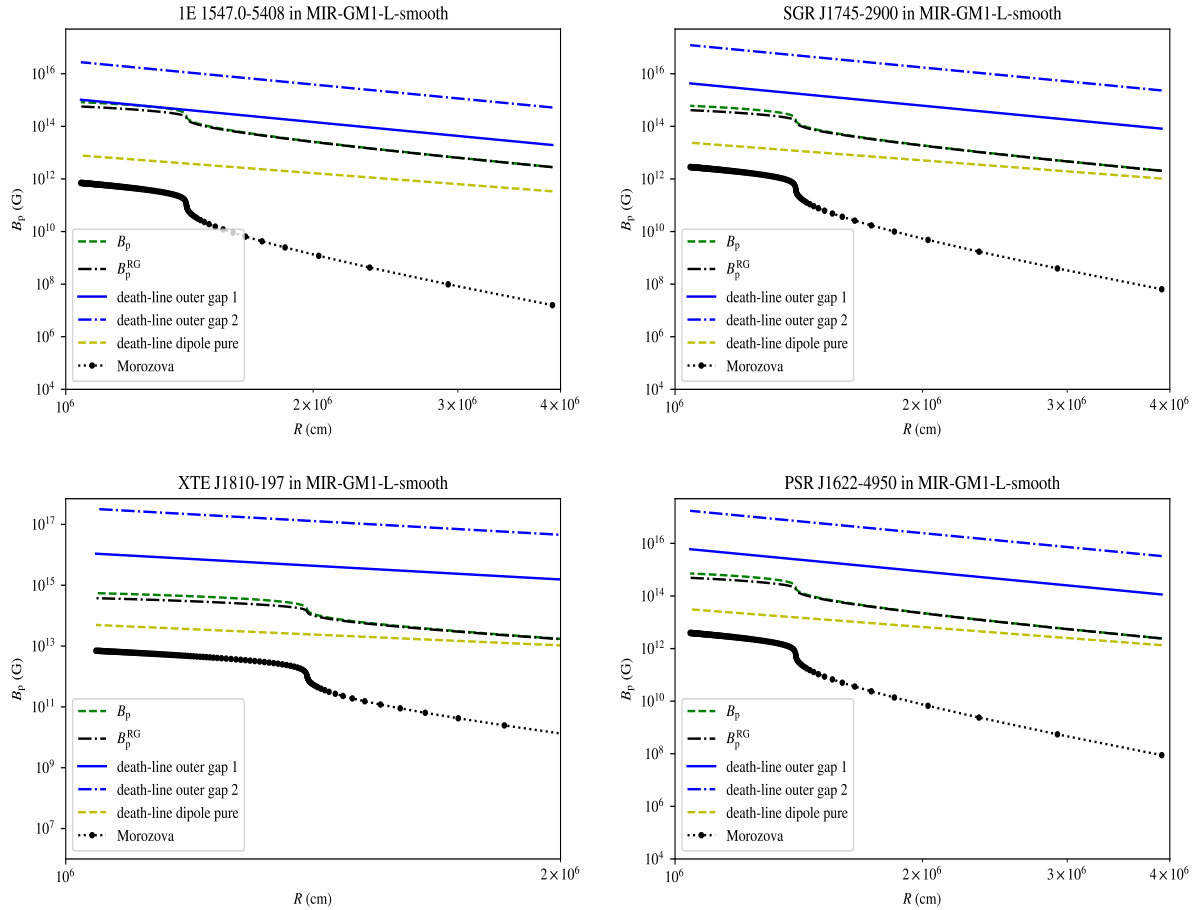


FIGURE 3.13 – Newtonian and relativistic magnetic fields for the GM1 equation of state as well as two polar caps: Newtonian, eq. (3.9), and relativistic, eq. (3.14), and outer gap death lines, eqs. (3.43) and (3.44). Here we highlight the four sources that show radio emission from observations. As we can see, these sources according the polar cap models should have radio emission, but according the Outer Gap models do not. Two sources a few years ago, were reported to have shown radio disappearance. The first according to (CAMILO *et al.*, 2016) was XTE J1810-197 (lower left), and more recently according (SCHOLZ *et al.*, 2017) the source PSR J1622-4950 (lower right) became radio quiet. One can see that the sources are approximating of the death lines of polar cap models, when the value of radius increase.

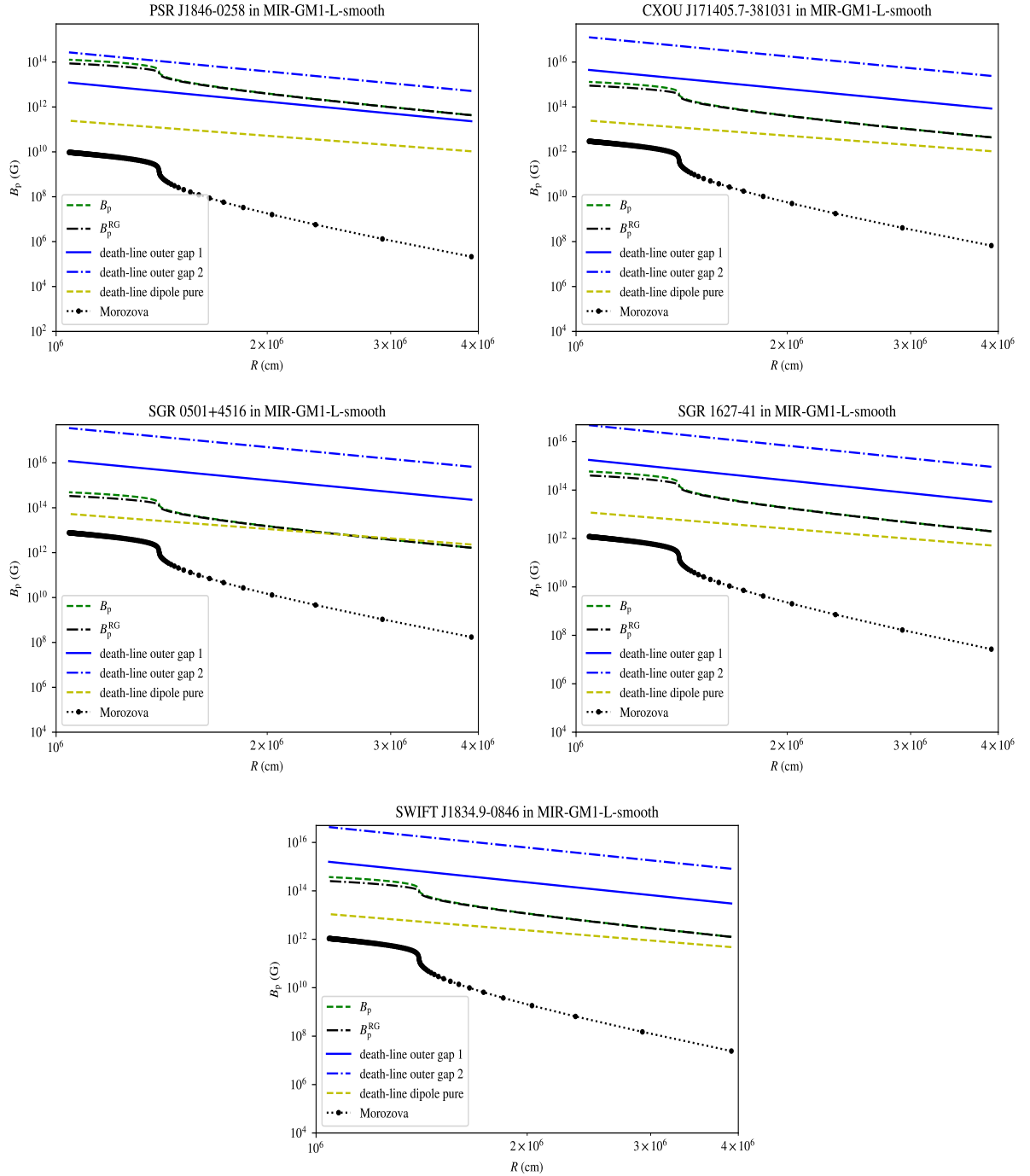


FIGURE 3.14 – Newtonian and relativistic magnetic fields for the GM1 equation of state as well as two polar caps: Newtonian, eq. (3.9), and relativistic, eq. (3.14), and outer gap death lines, eqs. (3.43) and (3.44). Here we highlight five sources that never showed radio emission from observations. These sources according the polar cap models may be radio emitter in disagreement with observations, within this, ones can discard polar cap models to describe these SGRs/AXPs. Outer Gap models should not have radio emission, which is in completely agreement with observations.

3.4.2 Radio emission of SGRs/AXPs as WDs

Now we turn to try understand SGRs/AXPs as white dwarfs pulsars in the context of models of emission. As we have mentioned, Usov (USOV, 1988; USOV, 1993) has shown that WD can produce pairs of electron-positron e^\pm in its magnetosphere like a neutron star pulsar and from observations the WD AR Scorpii shows emission in many aspects as the neutron stars pulsars.

Here we applied the model of polar cap in SGRs/AXPs described as WDs considering the case of a dipole pure (p1) [eq. (3.9)], magnetic field lines noticeably curved and curvature radius of 10^6 cm (p2) [eq. (3.10)] and the previous case, considering a polar cap area with the form $h \sim (B_p/B_s)^{1/2}R(R\Omega/c)^{1/2}$, being $B_s = B_q$ (p3) [eq. (3.11)].

In figure (3.15), we see that all sources SGRs/AXPs as WDs should be radio emitters while the two sources (AR Scorpii and AE Aquarii) should have emission only when the magnetic field lines are very curved. These WD pulsars show radio emission (MARSH *et al.*, 2016; IKHSANOV, 1998; ORURU; MEINTJES, 2014). As pointed by (GENG; ZHANG; HUANG, 2016), the number of particles observed emitting nonthermal optical of AR Sco's is significantly larger than the number that can be supplied by the WD itself. From this we can suggest that the electrons responsible by synchrotron radiation are supplied by the companion star's being different from neutron stars pulsars.

As we have shown, the particle density in the magnetosphere is smaller for white dwarfs in comparison with NS, being consistent with this interpretation.

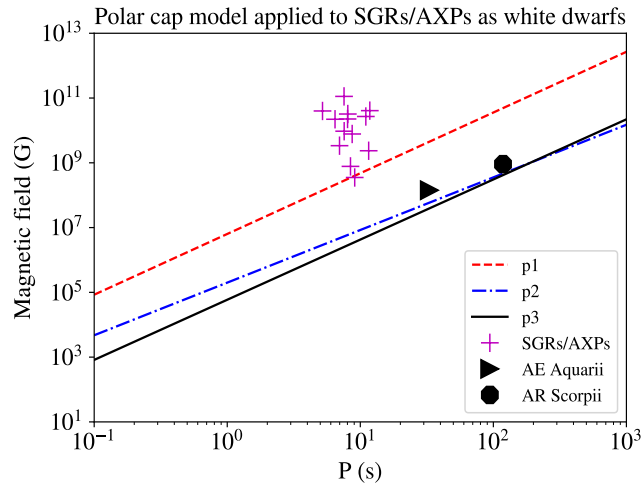


FIGURE 3.15 – Polar cap model applied to white dwarfs stars with the maximum mass of $\approx 1.39M_\odot$ and its respective radius ≈ 1.150 km. The two white dwarfs, AR Scorpii and AE Aquarii, with the masses $M = 1.29M_\odot$ and $M = 1.36M_\odot$ respectively and radii of $R \sim 10^8$ cm, are also presented. The death-lines were constructed using the radius of $R \sim 10^8$ cm.

Figure (3.16) shows the death line for SGRs/AXPs as WDs pulsars in the outer gap models. We see that almost all sources SGRs/AXPs are in the death zone, and they should be radio quiet. The two sources (AR Scorpii and AE Aquarii) should also not emit in radio, but observations show that these two stars have radio emission (MARSH *et al.*, 2016; IKHSANOV, 1998; ORURU; MEINTJES, 2014). However, as we comment before the origin of the radio emission for these two WDs - that are in binary systems - seems to come from particles of the companion that are accelerated by the WD in the outer magnetosphere, with a more complex mechanism than the ones discuss here in our emission models. Thus, the Outer Gap models seem to be more appropriate to describe the absence of radio emission in WD pulsars. These models consider the pair production far away of the star surface, since SGRs/AXPs are very slow, the value of magnetic field on their light cylinder is very weak to sustain pair production and to maintain a coherent radio flux.

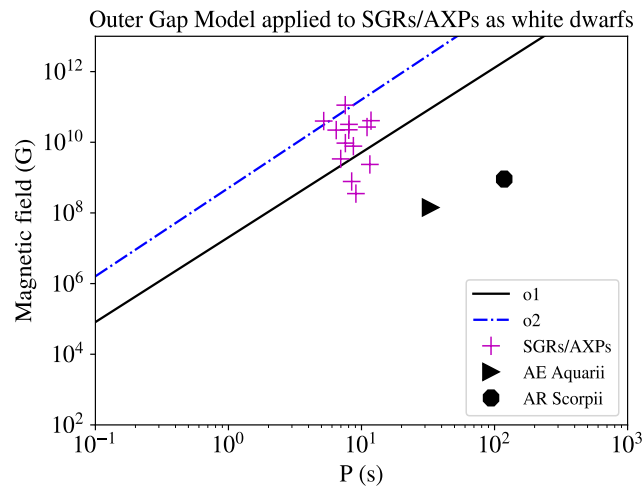


FIGURE 3.16 – Outer Gap Model applied to white dwarfs stars with the maximum mass of $\approx 1.39M_{\odot}$ and its respective radius ≈ 1.150 km. The two white dwarfs, AR Scorpii and AE Aquarii, with the masses $M = 1.29M_{\odot}$ and $M = 1.36M_{\odot}$ respectively and radii of $R \sim 10^8$ cm, are also presented. The death-lines were constructed using the radius of $R \sim 10^8$ cm.

4 Binary Compact Star Mergers: Gamma ray bursts, electromagnetic transients and gravitational waves

The discovery of a binary neutron star (NS) merger confirmed by LIGO/Virgo (the event GW170817) in both gravitational wave (GW) signal and electromagnetic entire wavelength (ABBOTT *et al.*, 2017a; ABBOTT *et al.*, 2017b; ABBOTT *et al.*, 2017c; GOLDSTEIN *et al.*, 2017), have shown the first direct evidence between this kind of merge and the short γ -ray bursts (SGRBs). These SGRBs have long been expected to be the result of neutron stars mergers (GOODMAN, 1986; NARAYAN; PACZYNSKI; PIRAN, 1992; PIRAN, 2005) and an engine to synthesize neutron-rich heavy elements (LATTIMER; SCHRAMM, 1974; EICHLER *et al.*, 1989). The breakthrough of the SGRB (ABBOTT *et al.*, 2017b) coincident with the event GW170817, as well as non-thermal emission, seems to confirm that some SGRBs arise from NS-NS merger. It is believed that they also can be the product of accretion onto a rapidly-spinning black hole or the merger of neutron star and stellar-mass black hole (NS-BH) (NARAYAN; PACZYNSKI; PIRAN, 1992; PIRAN, 2005). A novel interpretation (RUEDA *et al.*, 2018; RUEDA *et al.*, 2019), considers a possibility to have WD binary merge on this picture.

Electromagnetic spectrum counterpart is considered as an improvement to GWs signal (KOCHANNEK; PIRAN, 1993). It delivers an accurate source localization/redshift, reduces the degeneracies in GW parameter estimation (HUGHES; HOLZ, 2003); being a complementary piece of a such observed event (GROSSMAN *et al.*, 2014).

The γ -ray bursts are short and intense pulses of γ -rays (PIRAN, 2005) with the duration from a fraction to a hundred of seconds and isotropic luminosity of 10^{51-52} ergs/s. They are known to be the most electromagnetic luminous object in the sky. In general, their emissions are beamed and only part of it can be detected. They correspond the ones in our line of sight.

Although the event GW170817 possibly has confirmed that SGRBs are originated from compact binary merges, there are still some open issues to understand about its

nature. For example, the central engine requires physics models (strong gravity, high-density matter physics) different from the ones of the emission (collisionless, relativistic plasma shocks) (ROSSWOG, 2010). Though there are several works produced lately on this matter as well as regarding the gravitational wave event, the whole picture of this multi-messenger or at least in a multi-component picture it is not well understood.

Apart from the gravitational wave signal observed by LIGO/Virgo gravitational waves observatories, the merger was also observed (electromagnetically), two seconds later, by the Gamma-ray Burst Monitor (GBM) on board the Fermi-satellite (ABBOTT *et al.*, 2017b; GOLDSTEIN *et al.*, 2017) as well as with the optical-infrared-ultraviolet kilonova emission AT 2017gfo (COULTER *et al.*, 2017) for several days. The gravitational and electromagnetic spectrum have shown some discrepancies. The γ -ray observations have showed that the SGRB 170817A is not a usual SGRB, being weaker by three orders of magnitude if compared to the weakest SGRB emission seen before (GOTTLIEB *et al.*, 2018). Optical transient was measured approximately one day after the merger, and it was followed by a rapid fading of the luminosity (ARCAVI *et al.*, 2017). This rapid luminosity effect decreases hastily when compared to the supernova events, but still consistent with the predictions of kilonovae, as we will see. These discrepancies have raised some questions about the system itself (RUEDA *et al.*, 2018) and its characteristics, for instance, they were produced by a different mechanism than others SGRBs (!?). In a novel approach, we have shown that a WD-WD merge can produce optical and infrared emission resembling that one emitted from a kilonovae produced by NS-NS (RUEDA *et al.*, 2018). The fusion of white dwarfs cannot emit gravitational waves of the strength detected, as we will show in section 4.3, and according another work, the event would require (BELCZYNSKI *et al.*, 2018) extreme models. In addition to these inconsistencies, there were some issues about the chronological “predicition”, in general is said that LIGO detected first and after that the Fermi had detected, however, Fermi had sent first the notification to LIGO.

From the temporal and spatial coincidence of the gravitational wave signal of a binary neutron star merger and also from the short duration of γ -ray emissions it was concluded that the AT 2017gfo is a kilonova (ARCAVI *et al.*, 2017). In face of that, analytic studies and numerical simulations are being performed, for instance in (BROMBERG *et al.*, 2018; GOTTLIEB *et al.*, 2018; GOTTLIEB; NAKAR; PIRAN, 2018), to understand the open questions. From the temporal/spatial electromagnetic signal it has been also plausible to have white dwarfs mergers as “kilonova” (RUEDA *et al.*, 2019).

For the case of NS-NS merger perspective, there are two possibilities to explain the high energy low-luminosity: (1) The jet axis was slightly offset from our line of sight but close enough for γ -rays to be a component (off-axis model) (KATHIRGAMARAJU; DURAN; GIANNIOS, 2018); (2) our line of sight should be at a large angle from the jet axis, and the γ -rays were generated by a different mechanism (widely off-axis model)

(HALLINAN *et al.*, 2017).

A different approach concerning to NS-NS tries to explain the γ -ray, X-Ray, ultraviolet, optical, infrared and radio in a unique picture, it considers a mildly relativistic outflow in a wide angles and that propagates in the direction of observation (KASLIWAL *et al.*, 2017). This jet is generated by a cocoon (GOTTLIEB; NAKAR; PIRAN, 2018; GOTTLIEB *et al.*, 2018; BROMBERG *et al.*, 2018), the process is very different from regular SGRBs. The cocoon's interaction with the external medium can produce an afterglow over a wider angles (NAKAR; PIRAN, 2017; LAZZATI *et al.*, 2017a) generating a broad electromagnetic radiation. The cocoon/wide-angle emission was studied in an environment of baryons surrounding the merger (LAZZATI *et al.*, 2017b). In addition, Nakar and Piran (NAKAR; PIRAN, 2017), have considered the system under some assumptions, such as the cocoon being isotropic, but numerical simulations have shown that it is not the case. Therefore, it is worth to have self-consistent models, which successfully fits the observations (KASLIWAL *et al.*, 2017; HALLINAN *et al.*, 2017; GOTTLIEB *et al.*, 2018; MOOLEY *et al.*, 2018).

Aside from the nature/mechanism high energy puzzle, another point raised concerns about the standard interpretation of the AT 2017gfo as being powered by radioactive decay (LI *et al.*, 2018) i.e., the kilonova mechanism. The event showed a luminosity above the typical kilonovae values and a neutron-poor composition, invalidating previous numerical simulations. The source needs to be powered by some source (MATSUMOTO *et al.*, 2018), probably related to the engine of the γ -ray burst. Efforts are being done in to understand this energy difference as well as the exploration of their effects on the light curve. A first attempt (METZGER; THOMPSON; QUATAERT, 2018) considers a strongly magnetized hypermassive remnant NS¹, i.e., a magnetar with a lifetime of few seconds. The newborn NS generates a magnetized neutrino wind, which acts as the source to power the kilonova, explaining the blue component of the ejecta.

As shown by Rueda *et al.* (RUEDA *et al.*, 2018; RUEDA *et al.*, 2019) an alternative scenario is also plausible to the system, the idea relies on a WD-WD instead of a NS-NS merger. A WD-WD merger and an ejecta powered by fallback accretion onto one remain WD, is able to produce observational features in X and γ , as well as in optical, in agreement with the data of GRB 170817A/AT 2017gfo. The emission in the optical and infrared wavelengths is of the thermal character being due to the adiabatic cooling of WD-WD merger ejecta and by the fallback accretion (RUEDA *et al.*, 2019). The ejecta mass is about $10^{-3}M_{\odot}$ (DAN *et al.*, 2011; Lorén-Aguilar; ISERN; García-Berro, 2009) and the fallback may inject 10^{47-49} erg/s in the early times. This ejecta is powered in a completely different mechanisms with respect to the one in the kilonova from NS-NS, which are powered by radioactive decay through r-process of neutron-rich heavy atoms,

¹The magnetic field has an order of $\sim 10^{14}$ G

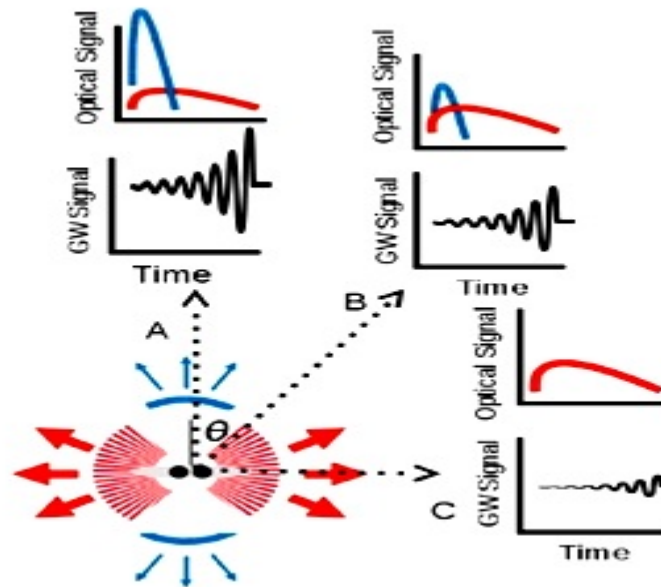


FIGURE 4.1 – Sketch of the possible geometry, emission region of the red and blue component and the gravitational wave signal considering a NS-NS merger. As we can see, depending on the sight of vision, we can observe different signals on the two spectra.

formed during the merger.

Polarimetry is a powerful tool that can be used to probe the emission process of these sources and the geometry. Considering the merger produced by a NS-NS fusion, according to Bulla et al. (BULLA *et al.*, 2019), AT 2017gfo can be interpreted as the combination of two ejecta constituents: One on the equatorial plane, the red component; and on the polar region, characterized by the blue component. From observations (NICHOLL *et al.*, 2017), it was revealed an optical excess fading over a timescale of a few days, going to a redder wavelength. Considering the system as NS-NS, in figure 4.1 we show the possible geometry of the system as well as the blue and red components, their evolution and the gravitational wave signal.

4.1 Gravitational emission from binary systems

Binary systems consisting of any objects radiate gravitational waves and as a result of radiation reaction the distance between the components of the binary decreases. On the gravitational spectrum side, the system will be characterized by an amplitude h , a flux F and luminosity L_{GW} .

4.1.1 Gravitational Radiation Luminosity

The flux F is defined as the gravitational radiation energy dE passing in an area dA of a sphere with radius r in a time dt and is given by (POSTNOV; YUNGELSON, 2014)

$$\frac{dE}{dAdt} \equiv F = \frac{c^3}{16\pi G} \left\langle \left(\frac{\partial \mathbf{h}_+}{\partial t} \right)^2 + \left(\frac{\partial \mathbf{h}_\times}{\partial t} \right)^2 \right\rangle. \quad (4.1)$$

The two time-dependent amplitudes $\mathbf{h}_{+,\times}$ give us two polarization components, characterizing the gravitational wave. At the distance r they are given by

$$\mathbf{h}_+ = \frac{G^{5/3}}{c^4} \frac{1}{r} 2 (1 + \cos^2 i) (\pi f_{\text{GW}} M)^{2/3} u \cos(2\pi f_{\text{GW}} t), \quad (4.2a)$$

$$\mathbf{h}_\times = \pm \frac{G^{5/3}}{c^4} \frac{1}{r} 4 \cos i (\pi f_{\text{GW}} M)^{2/3} u \sin(2\pi f_{\text{GW}} t), \quad (4.2b)$$

where u is the reduced mass², M is the mass of the system, f_{GW} the gravitational wave frequency, and i the system inclination angle. The detector on Earth will measure a linear combination of \mathbf{h}_+ and \mathbf{h}_\times .

The total power of gravitational radiation emitted by a binary system moving in an elliptic orbit, with two masses³ m_1 and m_2 , can be written as (PETERS; MATHEWS, 1963; PETERS, 1964)

$$\frac{dE}{dt} = \frac{8}{15} \frac{G^4}{c^5} \frac{m_1^2 m_2^2 (m_1 + m_2)}{\mathbf{a}^5 (1 - \mathbf{e}^2)^5} (1 + \mathbf{e} \cos \Psi)^4 [12(1 + \mathbf{e} \cos \Psi)^2 + \mathbf{e}^2 \sin^2 \Psi], \quad (4.3)$$

\mathbf{a} is the semimajor axis and \mathbf{e} the eccentricity of ellipse. Ψ is the angular velocity

$$\Psi = \frac{[G(m_1 + m_2)\mathbf{a}(1 - \mathbf{e}^2)]^{1/2}}{\mathfrak{d}^2},$$

where \mathfrak{d} is the orbit equation $\mathfrak{d} = \mathbf{a}(1 - \mathbf{e}^2)/(1 + \mathbf{e} \cos \Psi)$.

In average rate⁴ (FANG; RUFFINI, 1983)

$$\left\langle \frac{dE}{dt} \right\rangle = \frac{32}{5} \frac{G^4}{c^5} \frac{m_1^2 m_2^2 (m_1 + m_2)}{\mathbf{a}^5 (1 - \mathbf{e}^2)^{7/2}} \left(1 + \frac{73}{24} \mathbf{e}^2 + \frac{37}{96} \mathbf{e}^4 \right). \quad (4.4)$$

²Considering a system with two point masses m_1 and m_2 , $u = m_1 m_2 / M$

³Assuming that the source dimensions are small compared with the wavelength i.e., the quadrupole approximation.

⁴Plugging in it the value of the Hulse-Taylor binary pulsar: $\mathbf{a} = 1.95 \times 10^{11}$ cm, $m_1 = 1.441 M_\odot$, $m_2 = 1.383 M_\odot$, $\mathbf{e} = 0.617$ ones can obtain the power radiated 7.35×10^{31} erg/s. This is about 2% of the electromagnetic radiation of the Sun $P_\odot = 3.9 \times 10^{33}$ erg/s (BUONANNO, 2007).

We consider a circular orbit, as long as the radial velocity is smaller than the tangential one for the binary, following an adiabatic sequence of quasi-circular orbits, such as $\epsilon = 0$,

$$\left\langle \frac{dE}{dt} \right\rangle = -\frac{32 G^4 m_1^2 m_2^2 (m_1 + m_2)}{5 c^5 a^5}. \quad (4.5)$$

Using the total mass $M = m_1 + m_2$ and using Kepler's third law $a = (GM/\omega^2)^{1/3}$, we can rewrite Eq. (4.5) in terms of gravitational waves frequency $f_{\text{GW}} = 2f = \omega/\pi$,

$$\left\langle \frac{dE}{dt} \right\rangle = \frac{32 G^4 m_1^2 m_2^2 M}{5 c^5 \left(\frac{GM}{\omega^2}\right)^{5/3}} = \frac{32 G^4 m_1^2 m_2^2 M}{5 c^5 \left(\frac{GM}{(f_{\text{GW}}\pi)^2}\right)^{5/3}}. \quad (4.6)$$

If one considers the moment where the two stars enter into contact, namely at a distance $R = r_1 + r_2$ we can cut the gravitational wave emission in the frequency

$$f_c = \frac{1}{\pi} \left[\frac{GM}{(r_1 + r_2)^3} \right]^{1/2}. \quad (4.7)$$

The gravitational wave frequency increases as a function of time,

$$f_{\text{GW}}(t) = \frac{1}{\pi} \left(\frac{c^3}{G} \right)^{5/8} \left[\frac{5}{256} \frac{1}{uM^{2/3}} \frac{1}{t - t_0} \right]^{3/8}, \quad (4.8)$$

where t_0 is the time of coalescence. The frequency is a ‘‘chirrup’’, having a singularity at $t_s = t_0$.

4.1.2 Strain of Gravitational Radiation

The waves from large distances, are by the time they arrive at us, weak and plane-fronted. They can be described by the strain induced in an array of freely-moving particles in empty space (SCHUTZ, 1996). The wave changes the space between particles, i.e., the strain associated with the change δl of the distance l between two particles is the relative distance change, being proportional to the amplitude h of the gravitational wave that induces the strain

$$h = 2 \frac{\delta l}{l}.$$

For a fixed distance r and given f_{GW} , the amplitudes (4.2) are fully determined by $uM^{2/3} = \mathcal{M}^{5/3}$, where the definition

$$\mathcal{M} \equiv u^{3/5} M^{2/5} = \frac{(m_1 m_2)^{3/5}}{(m_1 + m_2)^{1/5}} \quad (4.9)$$

is called the “chirp mass” of the binary. Thus, the averaged GW amplitude is

$$h(f_{\text{GW}}, \mathcal{M}, r) = (\langle h_+^2 \rangle + \langle h_\times^2 \rangle)^{1/2} = \left(\frac{32}{5}\right)^{1/2} \frac{G^{5/3} \mathcal{M}^{5/3}}{c^4 r} (\pi f_{\text{GW}})^{2/3}. \quad (4.10)$$

4.1.2.1 Basic analysis concepts

Considering some signal $x(t)$, integrating $x^2(t)$ over some large period T and dividing by T , if it is stationary, then the time average of $x^2(t)$ is equal to its expectation value $\langle x^2 \rangle$, being possible to write as (CREIGHTON; ANDERSON, 2011)

$$\begin{aligned} \langle x^2 \rangle &= \lim_{T \rightarrow \infty} \frac{1}{T} \int_{-\infty}^{\infty} x_T^2(t) dt \\ &= \int_0^{\infty} S_x(f) df, \end{aligned} \quad (4.11)$$

where $S_x(f)$ is the power spectral density of the process $x(t)$.

The output of a gravitational wave detector is a time series $s(t)$ composed of: instrument noise $n(t)$ and the response to the gravitational signal $h(t)$ (CAMP; CORNISH, 2004)

$$s(t) = F^+(t)h_+(t) + F^\times(t)h_\times(t) + n(t). \quad (4.12)$$

The instrument response is a convolution of the antenna patterns F^+, F^\times with the two polarizations, for wavelengths that are large compared to the detector, the patterns are quadrupoles.

The information contained in the times series is represented by the Fourier domain as a strain amplitude spectral density $h(f) = \sqrt{S_s(f)}$, defined by the power spectral density $S_s(f) = \tilde{s}^*(f)\tilde{s}(f)$ of the Fourier transform of the time series

$$\tilde{s}(f) = \int_{-\infty}^{\infty} e^{-2\pi i f t} s(t) dt. \quad (4.13)$$

In the same way, is possible to define the noise power spectral density $S_n(f)$, the signal power spectral density $S_h(f)$ and the characteristic strain (CREIGHTON; ANDERSON, 2011)

$$h_c(f) = \sqrt{f S_s(f)}.$$

4.1.2.2 Gravitational wave spectrum

From Eq. (4.1), we can have the total energy flowing through an area dA as

$$\frac{dE}{dA} = \frac{c^3}{16\pi G} \int_{-\infty}^{\infty} dt \langle \dot{h}_+^2 + \dot{h}_\times^2 \rangle, \quad (4.14)$$

which in plane wave expansion and in the frequency domain can be written as (MAGGIORE, 2007)

$$\frac{dE}{dA} = \frac{\pi c^3}{2G} \int_0^{\infty} df f^2 \left(|\tilde{h}_+(f)|^2 + |\tilde{h}_\times(f)|^2 \right), \quad (4.15)$$

$$\frac{dE}{dA df} = \frac{\pi c^3}{2G} f^2 \left(|\tilde{h}_+(f)|^2 + |\tilde{h}_\times(f)|^2 \right) \equiv \frac{c^3}{G} \frac{\pi f^2}{2} S_h^2(f). \quad (4.16)$$

Integrating it over a sphere around the source, one finds the energy spectrum

$$\frac{dE}{df} = \frac{\pi c^3}{2G} f^2 r^2 \int d\Omega \left(|\tilde{h}_+(f)|^2 + |\tilde{h}_\times(f)|^2 \right), \quad (4.17)$$

which for the binary inspiral phase can be written as (FLANAGAN; HUGHES, 1998)

$$\frac{dE}{df_s} = \frac{1}{3} (\pi G)^{2/3} \mathcal{M}^{5/3} f_s^{-1/3}. \quad (4.18)$$

The gravitational wave strain written in terms of the gravitational wave spectrum is accordingly

$$h_c = \frac{1}{\pi d} \sqrt{\frac{1}{10} \frac{G}{c^3} \frac{dE}{df_s}}. \quad (4.19)$$

4.2 GRB subclasses and observational properties of NS-NS and NS-WD mergers

The detection announced by LIGO-Virgo Collaboration of the gravitational wave signal GW170817, at a luminosity distance of 40_{-14}^{+8} Mpc, considers the merging of a NS-NS binary. The best-constrained parameter from the GW170817 data is the binary chirp mass, $\mathcal{M} = 1.188_{-0.002}^{+0.004} M_\odot$. 90% confidence level of the total binary mass leads to the range $M = (2.73\text{--}3.29) M_\odot$. The lowest value, i.e. $M = 2.73 M_\odot$, corresponds to the case of equal-mass components, $m_1 = m_2 \equiv m = M/2 = 1.365 M_\odot$ (ABBOTT *et al.*, 2017b; LIGO Scientific Collaboration and Virgo Collaboration *et al.*, 2019).

As pointed out by the ICRANet's group in the following, different subclasses of short bursts from NS-NS mergers are possible, depending on whether they lead to a massive

neutron stars (MNS) or to a BH as remnant. (FRYER *et al.*, 2015; RUFFINI *et al.*, 2016):

- *Authentic short GRBs* (SGRBs): they occur when the NS-NS merger leads to a BH (RUFFINI *et al.*, 2015; RUFFINI *et al.*, 2016; MUCCINO *et al.*, 2013). These bursts have $E_{\text{iso}} \gtrsim 10^{52}$ erg (RUFFINI *et al.*, 2016; RUFFINI *et al.*, 2018).
- *Short γ -ray flashes* (SGRFs): they occur when the NS-NS merger leads to an MNS; i.e. there is no BH formation. These bursts have isotropic energy $E_{\text{iso}} \lesssim 10^{52}$ erg (RUFFINI *et al.*, 2016; RUFFINI *et al.*, 2018).

As mentioned, aside of γ -ray and X-ray emission, NS-NS mergers are expected to emit a kilonova in the infrared, optical and ultraviolet wavelengths, observable days after the merger (LI; PACZYŃSKI, 1998; BERGER; FONG; CHORNOCK, 2013; METZGER *et al.*, 2010). This signal comes from the decay neutron-rich material synthesized in the merger. The first kilonova associated with a short burst was established for GRB 130603B (TANVIR *et al.*, 2013; BERGER; FONG; CHORNOCK, 2013). With $E_{\text{iso}} \approx 2 \times 10^{51}$ erg (FONG *et al.*, 2013). The second association has been claimed for GRB 050709 (JIN *et al.*, 2016) which, with an $E_{\text{iso}} \approx 8 \times 10^{49}$ erg.

In addition to the above short bursts there is a subclass which show hybrid γ -ray properties between long and short bursts. These γ -ray flashes (GRFs) occur in a low-density circumburst medium (CBM), e.g. $n_{\text{CBM}} \sim 10^{-3}/\text{cm}^3$, and are not associated with supernovae (SNe) (VALLE *et al.*, 2006; CAITO *et al.*, 2009; RUFFINI *et al.*, 2016).

- *γ -ray flashes* (GRFs): they are thought to originate in NS-WD mergers (RUFFINI *et al.*, 2016; RUFFINI *et al.*, 2018). NS-WD binaries are notoriously common astrophysical systems (CADELANO *et al.*, 2015), possible evolutionary scenarios leading to these mergers have been investigated (FRYER *et al.*, 1999; LAZARUS *et al.*, 2014; TAURIS; HEUVEL; SAVONIJE, 2000). These bursts, which show an extended and softer emission, have $10^{51} \lesssim E_{\text{iso}} \lesssim 10^{52}$ erg. Only one NS-WD merger has been identified (CAITO *et al.*, 2009).

As we highlighted, GRB 170817A opens some questions: its very low energetic $E_{\text{iso}} \approx 5 \times 10^{46}$ erg (ABBOTT *et al.*, 2017a; ABBOTT *et al.*, 2017b; ABBOTT *et al.*, 2017c; GOLDSTEIN *et al.*, 2017) and the unprecedented details of the optical, infrared, radio and X-ray information of AT 2017gfo (ARCAVI *et al.*, 2017; COWPERTHWAITTE *et al.*, 2017; NICHOLL *et al.*, 2017). The observational features of GRB 170817A/AT 2017gfo lead us to consider the possibility of an additional subclass of GRBs produced in WD-WD mergers leading to the formation of a massive WD (RUEDA *et al.*, 2018; RUEDA *et al.*, 2019).

The WD-WD merger rate has been recently estimated in some works (MAOZ; HALLAKOUN, 2017; MAOZ; HALLAKOUN; BADENES, 2018; KALOGERA *et al.*, 2001), showing that some of them not lead to an Ia SNe.

The WD-WD mergers forming as remnant a central massive ($\sim 1.2\text{--}1.5 M_{\odot}$), highly magnetized ($10^9\text{--}10^{10}$ G), fast rotating ($P = 1\text{--}10$ s) WD, (RUEDA *et al.*, 2013) are interesting, because they can be an alternative explanation for the SGRs/AXPs origin (MALHEIRO; RUEDA; RUFFINI, 2012). Since there is no SN associated with GRB 170817A, the merger should not lead to an SN explosion (BECERRA *et al.*, 2018). The expected observable of these WD-WD mergers in the X and γ -rays, and in the optical and in the infrared wavelengths are suitable for the explanation of the GRB 170817A/AT 2017gfo association (RUEDA *et al.*, 2018; RUEDA *et al.*, 2019).

The name kilonova was coined in (METZGER *et al.*, 2010) to the optical transient produced in NS-NS mergers in view of their optical luminosity, $\sim 10^{41}$ erg/s, which is approximately 1000 times the one of novae, $\sim 10^{38}$ erg/s. This designation can be extended to the optical transient produced in WD-WD mergers. In this case the kilonova is not powered by the decay of r-process material but by the energy released by accretion onto the new WD formed in the merger (RUEDA *et al.*, 2018; RUEDA *et al.*, 2019).

In addition, it is interesting that the above mentioned physical properties (e.g. mass, rotation period and magnetic field) of the WD formed in the merger process correspond to the ones described by the WD model of SGRs/AXPs (MALHEIRO; RUEDA; RUFFINI, 2012; RUEDA *et al.*, 2013). Indeed, the WD-WD merger rate is high enough to explain the Galactic population of SGRs/AXPs.

4.3 Gravitational wave emission of NS-NS, NS-WD and WD-WD mergers

In this section I am going to present the gravitational wave calculations of NS-NS, NS-WD, WD-WD as a contribution to the novel interpretation (RUEDA *et al.*, 2018) of GW event 170817. In this new interpretation, we compared and contrasted the gravitational wave emission expected from GRBs and they observed electromagnetic emissions with the ones associated with GW170817 event.

Considering the gravitational counterpart, we have Fig. 4.2, where we show the gravitational wave source amplitude spectral density (ASD), $h_c(f)/\sqrt{f}$, together with the one-sided ASD of the Advanced LIGO detector's noise, $\sqrt{S_n}$ (ABBOTT *et al.*, 2018). The gravitational wave characteristic strain is $h_c = (1+z)\sqrt{(1/10)(G/c^3)dE/df_s/d_L(z)}$, where $d_L(z)$ is the luminosity distance to the source, $f = f_s/(1+z)$ and f_s are the

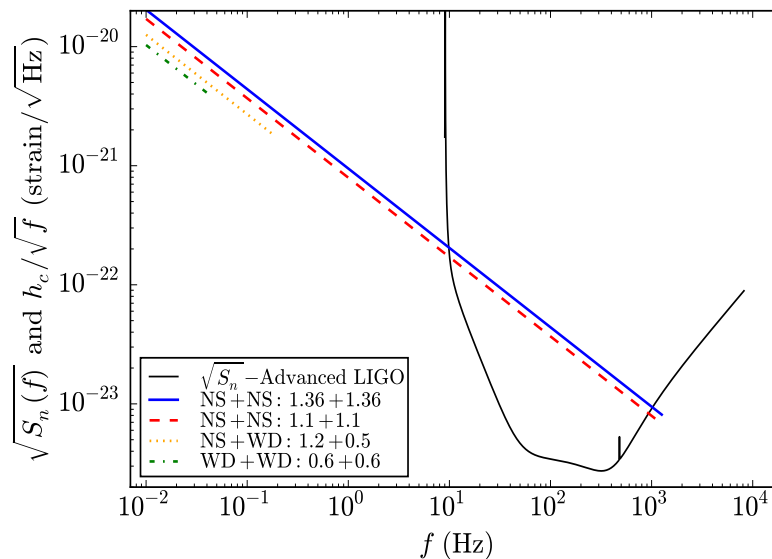


FIGURE 4.2 – Source ASD, $h_c(f)/\sqrt{f}$, together with the one-sided ASD of the Advanced LIGO detector’s noise, $\sqrt{S_n}$, for representative examples of S-GRBs (GRB 090510A-like), S-GRFs (GRB 130603B-like) and GRFs (GRB 060614-like). We have also included the expected ASD for a representative WD-WD binary. For the sake of the comparison all sources have been artificially assumed to be at a luminosity distance of 40 Mpc (cosmological redshift $z \approx 0.009$). For details of the gravitational wave emission of these binaries see (RUFFINI *et al.*, 2018).

gravitational wave frequency in the detector’s and in the source’s frame. For the luminosity distance we adopt a Λ CDM cosmology with $H_0 = 71 \text{ km s}^{-1}$, $\Omega_M = 0.3089$ and $\Omega_\Lambda = 0.6911$ (RIGAULT *et al.*, 2015). The spectrum of the binary inspiral phase is from the quadrupole formula (4.19). We cut, Eq. (4.7), the gravitational wave emission at the point where the two stars enter into contact. For the NS radii we use the mass-radius relation shown in (CIPOLLETTA *et al.*, 2015) obtained with the GM1 equation of state while, for the WDs, we use the mass-radius relation in (ROTONDO *et al.*, 2011) obtained with the relativistic Feynman-Metropolis-Teller equation of state.

To represent the emission of a SGRB is adopted the parameters of GRB 090510A, the first identified NS-NS merger leading to a BH (RUFFINI *et al.*, 2016). We use $m_1 = m_2 = 1.36 M_\odot$, consistent with the condition that the merging mass exceeds the NS critical mass in the case of the GM1 nuclear equation of state which, for a non-rotating NS, is $M_{\text{crit}} \approx 2.4 M_\odot$ (CIPOLLETTA *et al.*, 2015). For a SGRF, is assumed a GRB 130603B-like source with $m_1 = m_2 = 1.1 M_\odot$, consistent with the condition that the merged object is a massive but stable NS, consistent with the adopted NS critical mass value. For a GRF, a GRB 060614-like source, namely a NS-WD binary with $m_1 = 1.2 M_\odot$ and $m_2 = 0.5 M_\odot$ (CAITO *et al.*, 2009).

To compare and contrast the gravitational wave emission, we have located all the sources at a distance of $d = 40 \text{ Mpc}$, as the one of GW170817. The gravitational wave

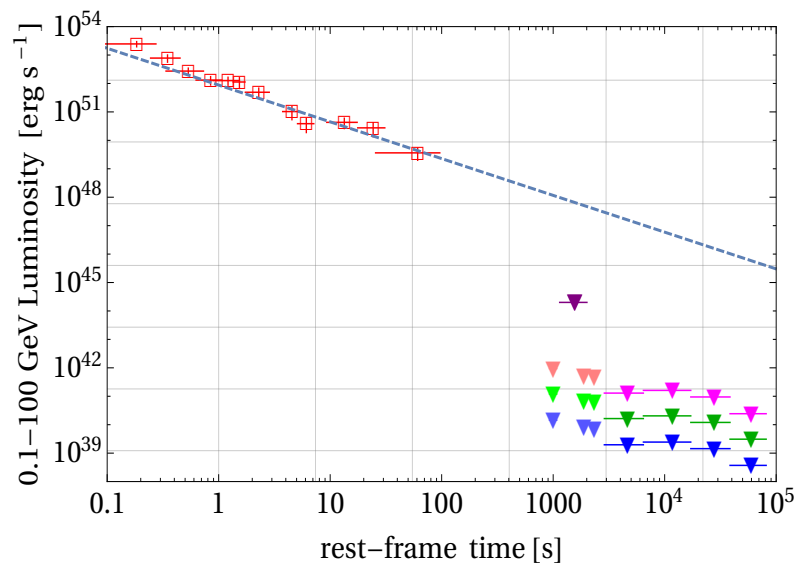


FIGURE 4.3 – Comparison of the rest-frame, 0.1–100 GeV band light-curve of GRB 090510A (red empty squares) with the corresponding observational upper limits of GRB 170817A (filled triangles). The dashed line indicates the power-law decay with slope index -1.29 ± 0.06 , observed in SGRBs (RUFFINI *et al.*, 2018). The purple triangle indicates the upper limit by Fermi-LAT of $9.7 \times 10^{43} \text{ erg s}^{-1}$ from 1151 to 2025 s from the Fermi trigger time. AGILE upper limits (pink, green and blue triangles) were calculated through extrapolation to the Fermi-LAT working energy band (0.1–100 GeV). We assume the spectral indices -2.0 (blue triangles), -1.0 (green triangles), -0.1 (pink triangles). The data of GRB 170817A were retrieved from (VERRECCHIA *et al.*, 2017).

emission associated with the inspiral phase of the NS-NS mergers (GRB 090510A-like and GRB 130603B-like) would be consistent, both in the characteristic strain and the spanned frequency range, with the ones of GW170817. Instead, the emission of NS-WD and WD-WD mergers is outside the Advanced LIGO frequency band. Details of the gravitational wave emission from these binaries are found in Ruffini *et al.* (RUFFINI *et al.*, 2018).

4.4 Comparison of the prompt, X-rays and optical light-curves of NS-NS and NS-WD mergers

In Rueda *et al.* (RUEDA *et al.*, 2018) we compared the electromagnetic emission of all these binaries, namely of SGRBs, SGRFs and GRFs, with the ones of GRB 170817A/AT 2017gfo. Summarized we have:

GeV emission.

A first general conclusion can be directly inferred for the absence in GRB 170817A of the GeV emission (COLLABORATION, 2017; VERRECCHIA *et al.*, 2017), GRB 170817A is not consistent with a SGRB, a NS-NS merger leading to a BH formation

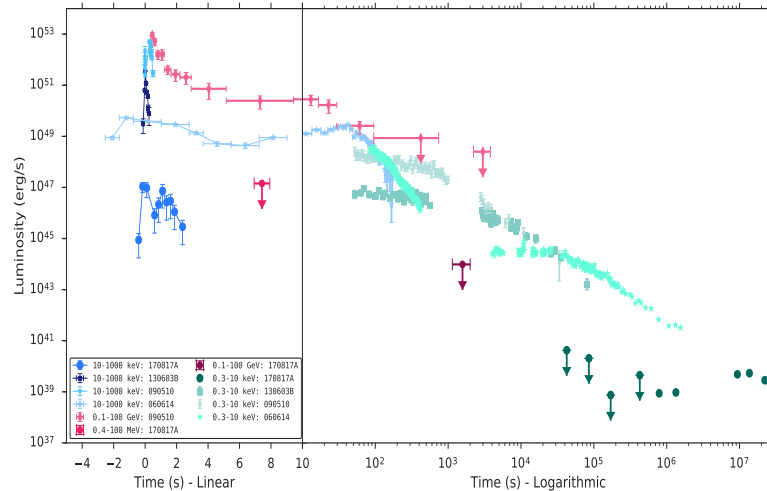


FIGURE 4.4 – Light-curves of GRBs 060614, 090510A, 130603 and 170817A in the cosmological rest-frame. We show the γ -ray (10–1000 keV) prompt and the X-ray (0.3–10 keV) emissions. The first 10 seconds are plotted in a linear scale and longer times in the logarithmic scale.

(see Fig. 4.3 and (RUFFINI *et al.*, 2018)). This conclusion is in agreement with the one obtained from the analysis of the γ -ray prompt emission and the X-ray emission (RUEDA *et al.*, 2018; RUEDA *et al.*, 2019).

γ -ray prompt emission.

Figure 4.4 shows the gamma-ray (10–1000 keV) prompt emission isotropic rest-frame light-curves of GRBs 090510, 130603B, 060614 and 170817A.

We can conclude that the gamma-ray prompt emission from GRB 170817A is not consistent with the one observed in GRBs 090510A, 130603B and 060614.

X-rays.

In addition, we also show in Fig. 4.4 the corresponding X-ray isotropic light-curves, in the rest-frame 0.3–10 keV energy band. It can be seen the overlapping of the light-curves at times $t \gtrsim 5000$ s from the BAT trigger (MELANDRI *et al.*, 2013). We recall that Ruffini *et al.* (RUFFINI *et al.*, 2013) have presented a first comparison of the X-ray light-curves of GRBs 090510A and 130603B. The match of the X-ray light-curves occurs irrespectively of their isotropic energies which differ up to a factor of ≈ 20 for instance in the case of GRB 130603B, $E_{\text{iso}} = 2.1 \times 10^{51}$ erg (FREDERIKS, 2013) and GRB 090510A, $E_{\text{iso}} = 3.95 \times 10^{52}$ erg (RUFFINI *et al.*, 2016).

We can see that the X-ray emission from GRB 170817A is not consistent with the one observed in GRBs 090510A, 130603B and 060614.

Optical and infrared.

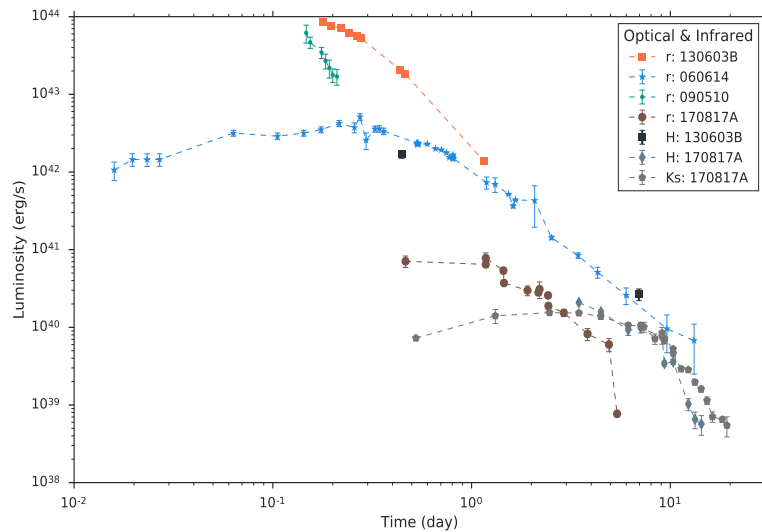


FIGURE 4.5 – Optical (r band) and infrared (H and Ks bands) light-curves of GRBs 060614, 090510A, 130603 and 170817A in the cosmological rest-frame.

We show in Fig. 4.5 the optical (r band) and infrared (H and Ks bands) light-curve of GRB 090510A (PASQUALE *et al.*, 2010; GUELZENZU *et al.*, 2012), GRB 130603B (TANVIR *et al.*, 2013; BERGER; FONG; CHORNOCK, 2013), GRB 060614 (CAITO *et al.*, 2009; YANG *et al.*, 2015), and GRB 170817A/AT 2017gfo (COULTER *et al.*, 2017; ARCAVI *et al.*, 2017; COWPERTHWAITTE *et al.*, 2017; NICHOLL *et al.*, 2017).

A kilonova emission had been associated with GRB 130603B (TANVIR *et al.*, 2013) and the similarity of this GRB in X-rays with GRB 090510A is consistent with the kilonova signature. This appears to be confirmed by Fig. 4.5. We can conclude (RUEDA *et al.*, 2018; RUEDA *et al.*, 2019) that all of these sources, SGRFs, SGRBs and GRFs, can produce a kilonova emission in line with the source AT 2017gfo, the kilonova associated with GRB 170817A.

Some above correlations of the electromagnetic emissions clearly originate from the traditional kilonova models based on ultra-relativistic regimes in NS-NS and NS-WD mergers pioneered in (LATTIMER *et al.*, 1977; EICHLER *et al.*, 1989; LI; PACZYŃSKI, 1998), following the classical work of (ARNETT, 1980; ARNETT, 1982).

The common asymptotic behavior at late times of the X-ray and optical emission of GRB 090510A (RUFFINI *et al.*, 2013) and GRB 130603B (TANVIR *et al.*, 2013) are a manifestation of a common synchrotron emission as recently outlined in (RUFFINI *et al.*, 2018). This approach is also supported by the parallel behavior of the optical and X-ray emission of GRB 060614 (see Figs. 4.4 and 4.5).

The contrast of the gamma and X-rays observational properties of GRB 170817A with respect to GRBs produced by NS-NS and NS-WD mergers has led us to consider the possibility of an additional subclass of GRBs produced by the merger of a still different

compact-star binary, a WD-WD merger, leading to a massive WD.

4.5 WD-WD mergers as an alternative mildly relativistic uncollimated emission for GRB 170817A-AT 2017gfo

The estimated WD-WD merger rate (MAOZ; HALLAKOUN, 2017; MAOZ; HALLAKOUN; BADENES, 2018; KALOGERA *et al.*, 2001) implies that 0.1% of WD-WD mergers can explain the GRB 170817A-like population for which a lower limit of (30–630) Gpc⁻³ yr⁻¹ has been recently obtained (ZHANG *et al.*, 2018).

The energy observed in gamma-rays in GRB 170817A, $E_{\text{iso}} \approx 3 \times 10^{46}$ erg, can originate from flares owing to the twist and stress of the magnetic field lines during the merger process: a magnetic energy of 2×10^{46} erg is stored in a region of radius 10^9 cm and magnetic field of 10^{10} G (MALHEIRO; RUEDA; RUFFINI, 2012).

The emission at optical and infrared wavelengths (see Fig. 4.6), can be explained from the adiabatic cooling of $10^{-3} M_{\odot}$ ejecta from the merger (Lorén-Aguilar; ISERN; García-Berro, 2009; DAN *et al.*, 2011) heated by fallback accretion onto the newly-formed WD (Lorén-Aguilar; ISERN; García-Berro, 2009). The ejecta becomes transparent at times $t \sim 1$ day with a peak bolometric luminosity of $L_{\text{bol}} \sim 10^{42}$ erg s⁻¹. The fallback accretion injects to the ejecta 10^{47-49} erg/s at early times and fall-off following a power-law behavior (Lorén-Aguilar; ISERN; García-Berro, 2009). The kilonovae from WD-WD mergers are therefore powered by a different mechanism with respect to the kilonovae from NS-NS mergers which are powered by the radioactive decay of r-process heavy material.

At times $t \sim 100$ –200 day, the ejecta are expected to become transparent to the X-rays leading to a luminosity of $\approx 10^{39}$ erg s⁻¹ as the one recently observed in GRB 170817A (see Fig. 4.4). At earlier times, the X-rays from fallback accretion are instead absorbed by the ejecta and are mainly transformed into kinetic energy then increasing the expansion velocity of the ejecta, from an initial non-relativistic value $0.01 c$ typical of the escape velocity from the WD, to a mildly relativistic velocity $0.1 c$. This mildly relativistic velocity is also consistent with the value derived from the evolution of blackbody spectra observed from ~ 0.5 day to ~ 7 day.

As we have mentioned in Sec. 4.2, the WD formed in the merger can become an SGR/AXP with mass up as $1.2 M_{\odot}$ (MALHEIRO; RUEDA; RUFFINI, 2012; RUEDA *et al.*, 2013). Thus, there is the possibility that, if a WD-WD merger produced GRB 170817A-AT 2017gfo, an SGR/AXP (a WD-pulsar) will show up in this sky position in the near future.

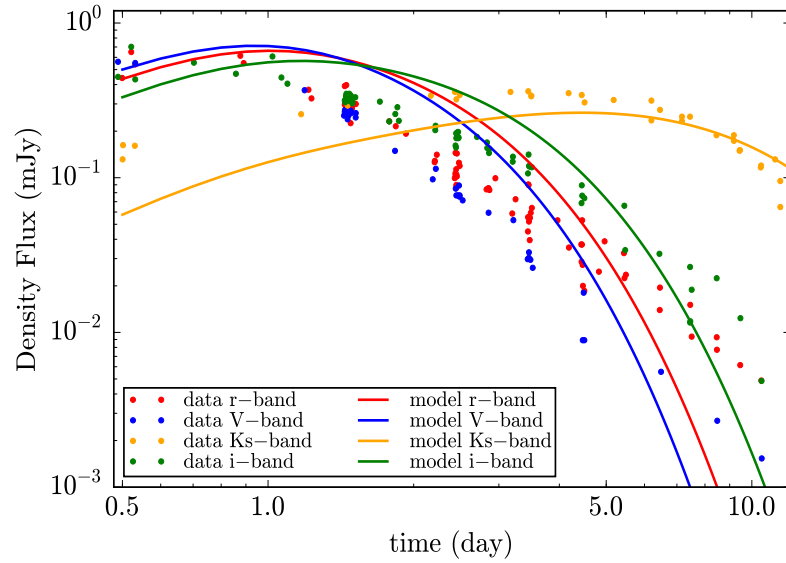


FIGURE 4.6 – Points: observed optical and infrared density flux of AT 2017gfo (COWPERTHWAITTE *et al.*, 2017; NICHOLL *et al.*, 2017). Solid curves: corresponding theoretical expectation from the cooling of $10^{-3} M_{\odot}$ of WD-WD merger ejecta heated by fallback accretion onto the newly-formed central WD.

As it is known, these events and their measurements have given us important information regarding the merger: relativistic jets, cocoon, radiation in a broad range (binary system of: NS-NS, NS-WD, WD-WD), being a fruitful field of exploration.

5 General conclusions

- The number of observed highly magnetized and massive white dwarfs have been increased in the last years, and self-consistent models with rotation and different EoSs have shown that we can have WD very massive and compact, rotating as fast as 1 s and they can be sources with magnetic field $\sim 10^{10}$ G.
- The discovery of the AR Scorpii in the last years has confirmed the hypothesis of WD pulsars, being the white dwarfs sources of high energy radiation as neutrons stars. The magnetic field of this source is up to 10^9 G. This source shares similarities with AE Aquarii, another white dwarf in a binary system which shows high energy emission.
- SGRs/AXPs are a new classe of pulsars and are in general considered as neutron stars. However, if one considers this, they will have huge magnetic field at least 100-1000 times larger than the "normal" neutron star pulsars, being slowly (there is no a satisfactory explanation by dynamo process). Apart from that, other phenomenological effects are also not well understood, e.g., in general the electromagnetic emission is higher than the rotational one. This is in contrast with the majority of pulsars, which are rotation powered pulsars.
- Apart from the interpretation of SGRs/AXPs as neutron star, there is another one, which considers a white dwarfs nature. In this interpretation some phenomenological effects are explained, as for the example the energy balance, i.e. the electromagnetic emission is lower than the rotational energy released. A recent possibility considers only some of them as NS. This is possible considering self-consistent models of NS instead of canonical parameters. These realistic models have shown the possibility to lower the values of magnetic fields and solve, for some of them, the energy balance. In general the classification is done considering the period of the source, being the NS the ones rapidly and the slowest are WD. Self-consistently mass-radius with realistic EoS and corrections from GR, decrease the value of magnetic field in SGRs/AXPs as NS, almost one order of magnitude. In this interpretation it is possible to describe these stars as rotation powered NS pulsars, instead of magnetar.

- Considering the SGRs/AXPs as WDs, is possible to perform a self-consistent model where the rotation is taken in account. Self-consistently mass-radius-moment of inertia for SGRs/AXPs as white dwarfs pointed out that properties of these sources are similar to those of massive white dwarfs observed.
- SGRs/AXPs understood as white dwarfs as well as the two observed white dwarfs pulsars (AE Aquarii and AR Scorpii, with $\sim 10^9$ G) can be sources able to accelerate ultra-high energy cosmic rays and are within of GZK limit.
- The models of electromagnetic emission studied have a dependence on the radius/temperature of the stars. This is due the influence of these quantities on the pair production and generation of γ -ray, X-ray and radio. The pair production defines the death zone, which is where the pulsars are unable to emit electromagnetic radiation. The death lines were constructed with observable such as period, temperature and with the mass, moment of inertia and radius calculated self-consistently.
- The death lines described with realistic configuration for NS are made for γ -rays, and we had observed that according the outer gap models for the SGRs/AXPs as NS, they should not emit hard X-rays/soft γ -rays. This is in contrast with the observation for some sources, where the persistent emission in hard X/soft γ are presented. If we consider the γ -pulsars observed using the parameters used for SGRs/AXPs as NS, these γ -pulsars are able to emit at least in soft- γ , so it is not possible that the SGRs/AXPs are NS pulsars according observations. Adding the polar cap model and analyzing only the nine sources which Coelho et al. (COELHO *et al.*, 2017) have considered as NS, we see that according this model, all sources should have condition for pair production and consequently γ /radio emission. However, this is verified only in four of them. Furthermore, this model predicts a super exponential cut-off in γ -ray spectra (VIGANO *et al.*, 2015a), due to the magnetic absorption on the surface. This is not observed (ABDO *et al.*, 2013; ABDO *et al.*, 2010). Considering the Outer Gap model, none of them would be radio emitter. This is partially in agreement, since radio emission has been observed in four of them. These conclusions are in accord with (RUBTSOV; SOKOLOVA, 2015) that had performed an analysis of the Fermi data, showing that outer gap models are in better agreement with data for γ -pulsars.

- The death lines to SGRs/AXPs as WDs are in agreement with observations when we consider the Outer Gap models. As we can see in this model, the sources are above the lines, being able to emit in soft gamma rays and hard X-rays, which is in agreement with the astronomical observations for SGRs/AXPs. The radio emission seems also to be explained by this model, as we can see from the results, where the sources are in the middle of the death zone, explaining the absence of radio emission in some of them. Considering the PC models, we also have the pair production satisfied, being the two models plausible for SGRs/AXPs as white dwarfs pulsars.
- Even if the event GW170817 had confirmed that short gamma rays bursts (SGRBs) are originated from compact binary merges, there are still some open issues to understand about its nature or mechanism involved in its physical environment. In a novel interpretation we raised the possibility to have a new subclass of SGRBs with a much less energetic and softer prompt emission in this scenario. This new WD-WD merger can be progenitors of massive and very fast WD. The WD formed in the merger process correspond to the ones described by the WD model of SGRs/AXPs. Thus, there is the possibility that, if a WD-WD merger produced GRB 170817A-AT 2017gfo, an SGR/AXP as a WD-pulsar will appear in this sky position in the near future.

Bibliography

GLENDENNING, N. K. **Compact Stars: Nuclear Physics, Particle Physics, and General Relativity**. 2. ed. New York: Springer-Verlag, 2000. (Astronomy and Astrophysics Library). 01397. ISBN 978-0-387-98977-8. 11

FRANZON, B.; SCHRAMM, S. Effects of strong magnetic fields and rotation on white dwarf structure. **Physical Review D**, v. 92, n. 8, p. 083006, out. 2015. 00028. 11, 15

CHANDRASEKHAR, S.; FERMI, E. Problems of Gravitational Stability in the Presence of a Magnetic Field. **The Astrophysical Journal**, v. 118, p. 116, jul. 1953. 00810. 11

COELHO, J. G. *et al.* Dynamical Instability of White Dwarfs and Breaking of Spherical Symmetry Under the Presence of Extreme Magnetic Fields. **The Astrophysical Journal**, v. 794, n. 1, p. 86, 2014. ISSN 0004-637X. 11, 15, 38

CHAMEL, N.; FANTINA, A. F.; DAVIS, P. J. Stability of super-Chandrasekhar magnetic white dwarfs. **Physical Review D**, v. 88, n. 8, p. 081301, out. 2013. 11, 15, 29

CHAMEL, N.; FANTINA, A. F. Electron capture instability in magnetic and nonmagnetic white dwarfs. **Physical Review D**, v. 92, n. 2, p. 023008, jul. 2015. 00000. 11

OTONIEL, E.; FRANZON, B.; MALHEIRO, M.; SCHRAMM, S.; WEBER, F. Very Magnetized White Dwarfs with Axisymmetric Magnetic Field and the Importance of the Electron Capture and Pycnonuclear Fusion Reactions for their Stability. **arXiv:1609.05994 [astro-ph]**, set. 2016. 00000. 11, 15

KEPLER, S. O. *et al.* Magnetic white dwarf stars in the Sloan Digital Sky Survey. **Monthly Notices of the Royal Astronomical Society**, v. 429, n. 4, p. 2934–2944, mar. 2013. ISSN 0035-8711. 00109. 11, 39

KEPLER, S. O. *et al.* New white dwarf stars in the Sloan Digital Sky Survey Data Release 10. **Monthly Notices of the Royal Astronomical Society**, v. 446, n. 4, p. 4078–4087, fev. 2015. ISSN 0035-8711. 00144. 11

FERRARIO, L.; de Martino, D.; GÄNSICKE, B. T. Magnetic White Dwarfs. **Space Science Reviews**, Springer Science+Business Media Dordrecht, v. 191, n. 1-4, p. 111–169, 2015. ISSN 15729672. 11, 16

- KEPLER, S. O.; ROMERO, A. D.; PELISOLI, I.; OURIQUE, G. White Dwarf Stars. **International Journal of Modern Physics: Conference Series**, v. 45, p. 1760023, jan. 2017. 00258. 11, 14
- MARSH, T. R. *et al.* A radio-pulsing white dwarf binary star. **Nature**, Nature Publishing Group, p. 1–15, 2016. ISSN 0028-0836. 00042. 11, 16, 17, 68, 69
- BUCKLEY, D. a. H.; MEINTJES, P. J.; POTTER, S. B.; MARSH, T. R.; GÄNSICKE, B. T. Polarimetric evidence of a white dwarf pulsar in the binary system AR Scorpii. **Nature Astronomy**, v. 1, n. 2, p. 0029, fev. 2017. ISSN 2397-3366. 00023. 11, 16, 17
- MEREGHETTI, S. *et al.* X-Ray and Optical Observations of the Unique Binary System Hd 49798/Rx J0648.0-4418. **The Astrophysical Journal**, v. 737, n. 2, p. 51, ago. 2011. ISSN 0004-637X. 11
- MEREGHETTI, S. *et al.* X-ray emission from the luminous O-type subdwarf HD 49798 and its compact companion. **Astronomy & Astrophysics**, v. 46, p. 1–5, 2013. 11, 23
- MALHEIRO, M.; RUEDA, J. A.; RUFFINI, R. SGRs and AXPs as Rotation-Powered Massive White Dwarfs. **Publications of the Astronomical Society of Japan**, v. 64, n. 3, jun. 2012. ISSN 0004-6264. 00073. 12, 19, 79, 84
- PACZYNSKI, B. X-ray pulsar 1E 2259 + 586 - A merged white dwarf with a 7 second rotation period? **The Astrophysical Journal Letters**, v. 365, p. L9–L12, dez. 1990. ISSN 0004-637X. 00101. 12, 19
- USOV, V. V. High-frequency emission of X-ray pulsar 1E 2259+586. **The Astrophysical Journal**, v. 410, p. 761–763, jun. 1993. ISSN 0004-637X. 00042. 12, 15, 30, 68
- USOV, V. V. Glitches in the X-ray pulsar 1E 2259+586. **The Astrophysical Journal**, v. 427, p. 984–986, jun. 1994. ISSN 0004-637X. 00035. 12
- COELHO, J. G.; MALHEIRO, M. Magnetic dipole moment of soft gamma-ray repeaters and anomalous X-ray pulsars described as massive and magnetic white dwarfs. **Publications of the Astronomical Society of Japan**, v. 66, p. 14, fev. 2014. ISSN 0004-6264. 00023. 12, 19
- LOBATO, R. V.; COELHO, J. G.; MALHEIRO, M. Radio pulsar death lines to SGRs/AXPs and white dwarfs pulsars. **AIP Conference Proceedings**, v. 1693, n. 1, p. 030003, dez. 2015. ISSN 0094-243X. 12, 18, 34
- LOBATO, R. V.; COELHO, J.; MALHEIRO, M. Particle acceleration and radio emission for SGRs/AXPs as white dwarf pulsars. **Journal of Physics: Conference Series**, v. 630, n. 1, p. 012015, 2015. ISSN 1742-6596. 12, 18, 34
- LOBATO, R. V.; MALHEIRO, M. Strong magnetic fields and SGRs/AXPs as white dwarf pulsar: A source of ultra-high energy cosmic rays. **Journal of Physics: Conference Series**, v. 706, n. 5, p. 052032, 2016. ISSN 1742-6596. 12, 34
- LOBATO, R. V.; MALHEIRO, M.; COELHO, J. G. Magnetars and white dwarf pulsars. **International Journal of Modern Physics D**, v. 25, n. 09, p. 1641025, jul. 2016. ISSN 0218-2718. 12, 19, 34

- MUKHOPADHYAY, B.; RAO, A. R. Soft gamma-ray repeaters and anomalous X-ray pulsars as highly magnetized white dwarfs. **Journal of Cosmology and Astroparticle Physics**, v. 2016, n. 05, p. 007, 2016. ISSN 1475-7516. 00000. 12
- LOBATO, R. V.; COELHO, J. G.; MALHEIRO, M. Ultra-high energy cosmic rays from white dwarf pulsars and the Hillas criterion. **Journal of Physics: Conference Series**, v. 861, n. 1, p. 012005, 2017. ISSN 1742-6596. 12, 34
- STURROCK, P. A. A Model of Pulsars. **The Astrophysical Journal**, v. 164, p. 529, mar. 1971. ISSN 0004-637X. 12, 41, 42
- RUDERMAN, M. A.; SUTHERLAND, P. G. Theory of pulsars - Polar caps, sparks, and coherent microwave radiation. **The Astrophysical Journal**, v. 196, p. 51–72, fev. 1975. ISSN 0004-637X. 12, 31, 41, 43
- ARONS, J.; SCHARLEMANN, E. T. Pair formation above pulsar polar caps - Structure of the low altitude acceleration zone. **The Astrophysical Journal**, v. 231, p. 854, ago. 1979. ISSN 0004-637X. 00737. 12, 41
- DAUGHERTY, J. K.; HARDING, A. K. Gamma-Ray Pulsars: Emission from Extended Polar CAP Cascades. **The Astrophysical Journal**, v. 458, p. 278, fev. 1996. ISSN 0004-637X. 00489. 12, 41
- CHENG, K. S.; HO, C.; RUDERMAN, M. Energetic radiation from rapidly spinning pulsars. I - Outer magnetosphere gaps. II - VELA and Crab. **The Astrophysical Journal**, v. 300, p. 500, jan. 1986. ISSN 0004-637X. 01357. 12, 41, 46, 47
- CHENG, K. S.; HO, C.; RUDERMAN, M. Energetic Radiation from Rapidly Spinning Pulsars. II. VELA and Crab. **The Astrophysical Journal**, v. 300, p. 522, jan. 1986. ISSN 0004-637X. 12, 41, 46
- ROMANI, R. W. Gamma-Ray Pulsars: Radiation Processes in the Outer Magnetosphere. **The Astrophysical Journal**, v. 470, p. 469, out. 1996. ISSN 0004-637X. 12, 41
- HIROTANI, K.; SHIBATA, S. One-dimensional electric field structure of an outer gap accelerator I. γ -ray production resulting from curvature radiation. **Monthly Notices of the Royal Astronomical Society**, v. 308, n. 1, p. 54–66, set. 1999. ISSN 0035-8711. 00077. 12, 41
- HIROTANI, K.; SHIBATA, S. One-dimensional electric field structure of an outer gap accelerator - II. γ -ray production resulting from inverse Compton scattering. **Monthly Notices of the Royal Astronomical Society**, v. 308, n. 1, p. 67–76, set. 1999. ISSN 0035-8711. 00046. 12, 41
- TAKATA, J.; WANG, Y.; CHENG, K. S. Outer gap accelerator closed by magnetic pair-creation process. **The Astrophysical Journal**, v. 715, n. 2, p. 1318–1326, abr. 2010. ISSN 0004-637X. 12, 41
- TONG, H.; SONG, L. M.; XU, R. X. Anomalous X-Ray Pulsars and Soft Gamma-Ray Repeater in the Outer Gap Model: Confronting Fermi Observations. **The Astrophysical Journal**, v. 738, n. 1, p. 31, 2011. ISSN 0004-637X. 12, 19, 41

- VIGANO, D.; TORRES, D. F.; HIROTANI, K.; PESSAH, M. E. An assessment of the pulsar outer gap model - I. Assumptions, uncertainties, and implications on the gap size and the accelerating field. **Monthly Notices of the Royal Astronomical Society**, v. 447, n. 3, p. 2631–2648, jan. 2015. ISSN 0035-8711. 12, 41, 46, 47, 48, 65, 87
- VIGANO, D.; TORRES, D. F.; HIROTANI, K.; PESSAH, M. E. An assessment of the pulsar outer gap model - II. Implications for the predicted γ -ray spectra. **Monthly Notices of the Royal Astronomical Society**, v. 447, n. 3, p. 2649–2657, jan. 2015. ISSN 0035-8711. 12, 41, 49
- VIGANÒ, D.; TORRES, D. F.; HIROTANI, K.; PESSAH, M. E. Compact formulae, dynamics and radiation of charged particles under synchro-curvature losses. **Monthly Notices of the Royal Astronomical Society**, v. 447, n. 2, p. 1164–1172, fev. 2015. ISSN 0035-8711. 00015. 12, 41, 49, 50
- RUEDA, J. A. *et al.* A White Dwarf Merger as Progenitor of the Anomalous X-Ray Pulsar 4U 0142+61? **The Astrophysical Journal Letters**, v. 772, n. 2, p. L24, 2013. ISSN 2041-8205. 00026. 12, 20, 79, 84
- GOODMAN, J. Are gamma-ray bursts optically thick? **The Astrophysical Journal Letters**, v. 308, p. L47–L50, set. 1986. ISSN 0004-637X. 00815. 12, 70
- NARAYAN, R.; PACZYNSKI, B.; PIRAN, T. Gamma-ray bursts as the death throes of massive binary stars. **The Astrophysical Journal**, v. 395, p. L83–L86, ago. 1992. ISSN 0004-637X. 01310. 12, 70
- PIRAN, T. The physics of gamma-ray bursts. **Reviews of Modern Physics**, v. 76, n. 4, p. 1143–1210, jan. 2005. 00000. 12, 70
- LATTIMER, J. M.; SCHRAMM, D. N. Black-hole-neutron-star collisions. **The Astrophysical Journal Letters**, v. 192, p. L145–L147, set. 1974. ISSN 0004-637X. 00445. 12, 70
- EICHLER, D.; LIVIO, M.; PIRAN, T.; SCHRAMM, D. N. Nucleosynthesis, neutrino bursts and γ -rays from coalescing neutron stars. **Nature**, v. 340, n. 6229, p. 126–128, jul. 1989. ISSN 1476-4687. 01639. 12, 70, 83
- RUEDA, J. A. *et al.* GRB 170817A-GW170817-AT 2017gfo and the observations of NS-NS, NS-WD and WD-WD mergers. **Journal of Cosmology and Astroparticle Physics**, v. 2018, n. 10, p. 006, 2018. ISSN 1475-7516. 00005. 12, 70, 71, 72, 78, 79, 81, 82, 83
- RUEDA, J. A. *et al.* Electromagnetic emission of white dwarf binary mergers. **Journal of Cosmology and Astroparticle Physics**, v. 2019, n. 03, p. 044–044, mar. 2019. ISSN 1475-7516. 00000. 12, 70, 71, 72, 78, 79, 82, 83
- KIPPENHAHN, R.; WEIGERT, A.; WEISS, A. **Stellar Structure and Evolution**. [S.l.]: Springer Science & Business Media, 2012. 02360. ISBN 978-3-642-30304-3. 14
- CHANDRASEKHAR, S. The Maximum Mass of Ideal White Dwarfs. **The Astrophysical Journal**, v. 74, p. 81, jul. 1931. ISSN 0004-637X. 00966. 14, 28

BECERRA, L.; RUEDA, J. A.; Lorén-Aguilar, P.; García-Berro, E. The Spin Evolution of Fast-rotating, Magnetized Super-Chandrasekhar White Dwarfs in the Aftermath of White Dwarf Mergers. **The Astrophysical Journal**, v. 857, n. 2, p. 134, abr. 2018. ISSN 0004-637X. 00004. 14, 79

WEINBERG, S. **Cosmology**. [S.l.]: OUP Oxford, 2008. ISBN 978-0-19-852682-7. 14

RIESS, A. G. *et al.* Observational Evidence from Supernovae for an Accelerating Universe and a Cosmological Constant. **The Astronomical Journal**, v. 116, n. 3, p. 1009–1038, set. 1998. ISSN 00046256. 14

PERLMUTTER, S. *et al.* Measurements of Omega and Lambda from 42 High-Redshift Supernovae. **The Astrophysical Journal**, v. 517, n. 2, p. 565, 1998. ISSN 0004-637X. 14

HOWELL, D. A. *et al.* The type Ia supernova SNLS-03D3bb from a super-Chandrasekhar-mass white dwarf star. **Nature**, v. 443, n. 7109, p. 308–311, set. 2006. ISSN 0028-0836. 14

SCALZO, R. A. *et al.* Nearby Supernova Factory Observations of SN 2007if: First Total Mass Measurement of a Super-Chandrasekhar-Mass Progenitor. **The Astrophysical Journal**, v. 713, n. 2, p. 1073, 2010. ISSN 0004-637X. 14

HICKEN, M. *et al.* The Luminous and Carbon-rich Supernova 2006gz: A Double Degenerate Merger? **The Astrophysical Journal Letters**, v. 669, n. 1, p. L17, 2007. ISSN 1538-4357. 14

YAMANAKA, M. *et al.* Early Phase Observations of Extremely Luminous Type Ia Supernova 2009dc. **The Astrophysical Journal Letters**, v. 707, n. 2, p. L118, 2009. ISSN 1538-4357. 14

TAUBENBERGER, S. *et al.* High luminosity, slow ejecta and persistent carbon lines: SN 2009dc challenges thermonuclear explosion scenarios. **Monthly Notices of the Royal Astronomical Society**, v. 412, n. 4, p. 2735–2762, abr. 2011. ISSN 0035-8711, 1365-2966. 14

SILVERMAN, J. M. *et al.* Fourteen months of observations of the possible super-Chandrasekhar mass Type Ia Supernova 2009dc. **Monthly Notices of the Royal Astronomical Society**, v. 410, n. 1, p. 585–611, jan. 2011. ISSN 0035-8711, 1365-2966. 14

DAS, U.; MUKHOPADHYAY, B. Violation of Chandrasekhar mass limit: The exciting potential of strongly magnetized white dwarfs. **International Journal of Modern Physics D**, v. 21, n. 11, p. 1242001, set. 2012. ISSN 0218-2718. 14, 15

DAS, U.; MUKHOPADHYAY, B. New Mass Limit for White Dwarfs: Super-Chandrasekhar Type Ia Supernova as a New Standard Candle. **Physical Review Letters**, v. 110, n. 7, p. 071102, fev. 2013. 14, 15

DAS, U.; MUKHOPADHYAY, B. Maximum mass of stable magnetized highly super-Chandrasekhar white dwarfs: Stable solutions with varying magnetic fields. **Journal of Cosmology and Astroparticle Physics**, v. 2014, n. 06, p. 050, 2014. ISSN 1475-7516. 00025. 14, 15

- MOLL, R.; RASKIN, C.; KASEN, D.; WOOSLEY, S. E. Type Ia Supernovae from Merging White Dwarfs. I. Prompt Detonations. **The Astrophysical Journal**, v. 785, n. 2, p. 105, 2014. ISSN 0004-637X. 00075. 14, 15
- RASKIN, C.; KASEN, D.; MOLL, R.; SCHWAB, J.; WOOSLEY, S. Type Ia Supernovae from Merging White Dwarfs. II. Post-merger Detonations. **The Astrophysical Journal**, v. 788, n. 1, p. 75, 2014. ISSN 0004-637X. 00041. 14, 15
- GVARAMADZE, V. V. *et al.* A massive white-dwarf merger product before final collapse. **Nature**, p. 1, maio 2019. ISSN 1476-4687. 00000. 15
- SCHWAB, J.; QUATAERT, E.; KASEN, D. The evolution and fate of super-Chandrasekhar mass white dwarf merger remnants. **Monthly Notices of the Royal Astronomical Society**, v. 463, n. 4, p. 3461–3475, dez. 2016. ISSN 0035-8711. 00039. 15
- JI, S. *et al.* The Post-merger Magnetized Evolution of White Dwarf Binaries: The Double-degenerate Channel of Sub-Chandrasekhar Type Ia Supernovae and the Formation of Magnetized White Dwarfs. **The Astrophysical Journal**, v. 773, n. 2, p. 136, 2013. ISSN 0004-637X. 00000. 15
- ROSSUM, D. R. van *et al.* Light Curves and Spectra from a Thermonuclear Explosion of a White Dwarf Merger. **The Astrophysical Journal**, v. 827, n. 2, p. 128, 2016. ISSN 0004-637X. 15
- DAS, U.; MUKHOPADHYAY, B. Strongly magnetized cold degenerate electron gas: Mass-radius relation of the magnetized white dwarf. **Physical Review D**, v. 86, n. 4, p. 042001, ago. 2012. 15
- DONG, J. M.; ZUO, W.; YIN, P.; GU, J. Z. Comment on New Mass Limit for White Dwarfs: Super-Chandrasekhar Type Ia Supernova as a New Standard Candle. **Physical Review Letters**, v. 112, n. 3, p. 039001, jan. 2014. 15
- NITYANANDA, R.; KONAR, S. Comment on Strongly magnetized cold degenerate electron gas: Mass-radius relation of the magnetized white dwarf. **Physical Review D**, v. 91, n. 2, p. 028301, jan. 2015. 00000. 15
- DAS, U.; MUKHOPADHYAY, B. Revisiting some physics issues related to the new mass limit for magnetized white dwarfs. **Modern Physics Letters A**, v. 29, n. 07, p. 1450035, mar. 2014. ISSN 0217-7323. 15
- LIU, H.; ZHANG, X.; WEN, D. One possible solution of peculiar type Ia supernovae explosions caused by a charged white dwarf. **Physical Review D**, v. 89, n. 10, p. 104043, maio 2014. 00013. 15
- CARVALHO, G. A.; ARBAÑIL, J. D. V.; MARINHO, R. M.; MALHEIRO, M. White dwarfs with a surface electrical charge distribution: Equilibrium and stability. **The European Physical Journal C**, v. 78, n. 5, p. 411, maio 2018. ISSN 1434-6052. 00000. 15
- BOSHKAYEV, K.; RUEDA, J. A.; RUFFINI, R.; SIUTSOU, I. On General Relativistic Uniformly Rotating White Dwarfs. **The Astrophysical Journal**, v. 762, n. 2, p. 117, 2013. ISSN 0004-637X. 15, 19, 26

- SUBRAMANIAN, S.; MUKHOPADHYAY, B. GRMHD formulation of highly super-Chandrasekhar rotating magnetized white dwarfs: Stable configurations of non-spherical white dwarfs. **Monthly Notices of the Royal Astronomical Society**, v. 454, n. 1, p. 752–765, nov. 2015. ISSN 0035-8711. 00000. 15
- CARVALHO, G.; MARINHO, R.; MALHEIRO, M. The importance of GR for the radius of massive white dwarfs. **AIP Conference Proceedings**, v. 1693, n. 1, p. 030004, dez. 2015. ISSN 0094-243X. 15, 26
- CARVALHO, G. A.; JR, R. M. M.; MALHEIRO, M. Mass-Radius diagram for compact stars. **Journal of Physics: Conference Series**, v. 630, n. 1, p. 012058, 2015. ISSN 1742-6596. 15, 26
- BERA, P.; BHATTACHARYA, D. Mass–radius relation of strongly magnetized white dwarfs: Dependence on field geometry, GR effects and electrostatic corrections to the EOS. **Monthly Notices of the Royal Astronomical Society**, v. 456, n. 3, p. 3375–3385, mar. 2016. ISSN 0035-8711. 15
- BECERRA, L.; BOSHKAYEV, K.; RUEDA, J. A.; RUFFINI, R. Time evolution of rotating and magnetized white dwarf stars. **Monthly Notices of the Royal Astronomical Society**, v. 487, n. 1, p. 812–818, jul. 2019. ISSN 0035-8711. 00000. 15
- Lynden-Bell, D.; OSTRIKER, J. P. On the Stability of Differentially Rotating Bodies. **Monthly Notices of the Royal Astronomical Society**, v. 136, n. 3, p. 293–310, jul. 1967. ISSN 0035-8711. 00000. 15
- OSTRIKER, J. P.; HARTWICK, F. D. A. Rapidly Rotating Stars.IV. Magnetic White Dwarfs. **The Astrophysical Journal**, v. 153, p. 797, set. 1968. 00000. 15
- OSTRIKER, J. P.; BODENHEIMER, P. Rapidly Rotating Stars. II. Massive White Dwarfs. **The Astrophysical Journal**, v. 151, p. 1089, mar. 1968. 00269. 15
- OSTRIKER, J. P.; MARK, J. W.-K. Rapidly rotating stars. I. The self-consistent-field method. **The Astrophysical Journal**, v. 151, p. 1075, mar. 1968. 00213. 15
- OSTRIKER, J. Possible Model for a Rapidly Pulsating Radio Source. **Nature**, v. 217, n. 5135, p. 1227, mar. 1968. 00048. 15
- OSTRIKER, J. P.; TASSOUL, J. L. On the Oscillations and Stability of Rotating Stellar Models. II. Rapidly Rotating White Dwarfs. **The Astrophysical Journal**, v. 155, p. 987, mar. 1969. 00076. 15
- HAMADA, T.; SALPETER, E. E. Models for Zero-Temperature Stars. **The Astrophysical Journal**, v. 134, p. 683, nov. 1961. ISSN 0004-637X. 00624. 15, 28
- SALPETER, E. E. Energy and Pressure of a Zero-Temperature Plasma. **The Astrophysical Journal**, v. 134, p. 669, nov. 1961. ISSN 0004-637X. 00000. 15, 28
- USOV, V. V. Generation of Gamma-Rays by a Rotating Magnetic White Dwarf. **Soviet Astronomy Letters**, v. 14, p. 258, mar. 1988. 00019. 15, 30, 68
- ZHANG, B.; GIL, J. GCRT J1745–3009 as a Transient White Dwarf Pulsar. **The Astrophysical Journal Letters**, v. 631, n. 2, p. L143, 2005. ISSN 1538-4357. 15

TERADA, Y. *et al.* Suzaku Discovery of Hard X-Ray Pulsations from a Rotating Magnetized White Dwarf, AEAquarii. **Publications of the Astronomical Society of Japan**, v. 60, n. 2, p. 387–397, abr. 2008. ISSN 0004-6264. 00000. 16, 18

ORURU, B.; MEINTJES, P. J. X-ray characteristics and the spectral energy distribution of AE Aquarii. **Monthly Notices of the Royal Astronomical Society**, v. 421, n. 2, p. 1557–1568, abr. 2012. ISSN 0035-8711. 16, 18

KATZ, J. I. AR Sco: A Precessing White Dwarf Synchronar? **The Astrophysical Journal**, v. 835, n. 2, p. 150, fev. 2017. ISSN 1538-4357. 17

TAKATA, J.; YANG, H.; CHENG, K. S. A Model for AR Scorpii: Emission from Relativistic Electrons Trapped by Closed Magnetic Field Lines of Magnetic White Dwarfs. **The Astrophysical Journal**, v. 851, n. 2, p. 143, dez. 2017. ISSN 1538-4357. 17

MARCOTE, B.; MARSH, T. R.; STANWAY, E. R.; PARAGI, Z.; BLANCHARD, J. M. Towards the origin of the radio emission in AR Scorpii, the first radio-pulsing white dwarf binary. **Astronomy & Astrophysics**, v. 601, p. L7, maio 2017. ISSN 0004-6361, 1432-0746. 00006. 17

STILLER, R. A. *et al.* High-time-resolution Photometry of AR Scorpii: Confirmation of the White Dwarf's Spin-down. **The Astronomical Journal**, v. 156, n. 4, p. 150, 2018. ISSN 1538-3881. 00001. 17

GENG, J.-J.; ZHANG, B.; HUANG, Y.-F. A MODEL OF WHITE DWARF PULSAR AR SCORPII. **The Astrophysical Journal**, v. 831, n. 1, p. L10, out. 2016. ISSN 2041-8213. 17, 29, 68

BESKROVNAYA, N. G.; IKHSANOV, N. R. AR Scorpii: A New White Dwarf in the Ejector State. **ASP**, v. 510, Stars: From Collapse to Collapse, p. 439, 2017. 00004. 17

de Jager, O. C.; MEINTJES, P. J.; O'DONOGHUE, D.; ROBINSON, E. L. The discovery of a brake on the white dwarf in AE Aquarii. **Monthly Notices of the Royal Astronomical Society**, v. 267, n. 3, p. 577–588, abr. 1994. ISSN 0035-8711. 00000. 18

IKHSANOV, N. R. The pulsar-like white dwarf in AE Aquarii. **Astronomy and Astrophysics**, v. 338, p. 521–526, out. 1998. ISSN 0004-6361. 00056. 18, 68, 69

ORURU, B.; MEINTJES, P. J. The Peculiar Binary System AE Aquarii from its Characteristic Multi-wavelength Emission. **EPJ Web of Conferences**, v. 64, p. 07003, 2014. ISSN 2100-014X. 00002. 18, 68, 69

CACERES, D. L.; de Carvalho, S. M.; COELHO, J. G.; de Lima, R. C. R.; RUEDA, J. A. Thermal X-ray emission from massive, fast rotating, highly magnetized white dwarfs. **Monthly Notices of the Royal Astronomical Society**, v. 465, n. 4, p. 4434–4440, nov. 2017. ISSN 0035-8711. 00005. 18, 30

BESKROVNAYA, N. G.; IKHSANOV, N. R. On the origin of the peculiar cataclysmic variable AEAquarii. **Advances in Space Research**, v. 55, n. 3, p. 787–790, fev. 2015. ISSN 0273-1177. 00000. 18

- MEINTJES, P. J. On the evolution of the nova-like variable AE Aquarii. **Monthly Notices of the Royal Astronomical Society**, v. 336, n. 1, p. 265–275, out. 2002. ISSN 0035-8711. 00000. 18
- MEREGHETTI, S. Pulsars and Magnetars. **Brazilian Journal of Physics**, v. 43, n. 5-6, p. 356–368, dez. 2013. ISSN 0103-9733. 00039. 18, 19, 21
- TUROLLA, R.; ZANE, S.; WATTS, A. L. Magnetars: The physics behind observations. A review. **Reports on Progress in Physics**, v. 78, n. 11, p. 116901, 2015. ISSN 0034-4885. 00002. 18, 19, 20, 21, 22, 23
- WOOSLEY, S. E.; WALLACE, R. K. The thermonuclear model for gamma-ray bursts. **The Astrophysical Journal**, v. 258, p. 716–732, jul. 1982. ISSN 0004-637X. 00000. 18
- LIVIO, M.; TAAM, R. E. Possible models for the high-energy transient GB790107. **Nature**, v. 327, n. 6121, p. 398–400, jun. 1987. ISSN 1476-4687. 00019. 18
- BLAES, O.; BLANDFORD, R.; GOLDREICH, P.; MADAU, P. Neutron starquake models for gamma-ray bursts. **The Astrophysical Journal**, v. 343, p. 839–848, ago. 1989. ISSN 0004-637X. 00139. 18
- KATZ, J. I.; TOOLE, H. A.; UNRUH, S. H. Yet another model of soft gamma repeaters. **The Astrophysical Journal**, v. 437, p. 727–732, dez. 1994. ISSN 0004-637X. 00040. 18
- DUNCAN, R. C.; THOMPSON, C. Formation of very strongly magnetized neutron stars - Implications for gamma-ray bursts. **The Astrophysical Journal**, v. 392, p. L9–L13, jun. 1992. ISSN 0004-637X. 02444. 18, 19
- THOMPSON, C.; DUNCAN, R. C. Neutron star dynamos and the origins of pulsar magnetism. **The Astrophysical Journal**, v. 408, p. 194–217, maio 1993. ISSN 0004-637X. 00885. 18, 19
- THOMPSON, C.; DUNCAN, R. C. The soft gamma repeaters as very strongly magnetized neutron stars - I. Radiative mechanism for outbursts. **Monthly Notices of the Royal Astronomical Society**, v. 275, n. 2, p. 255–300, jul. 1995. ISSN 0035-8711. 01410. 18, 19
- THOMPSON, C.; DUNCAN, R. C. The Soft Gamma Repeaters as Very Strongly Magnetized Neutron Stars. II. Quiescent Neutrino, X-Ray, and Alfvén Wave Emission. **The Astrophysical Journal**, v. 473, n. 1, p. 322, 1996. ISSN 0004-637X. 00000. 18, 19
- DUNCAN, R. C. Nature, Nurture or Not Sure? A Debate about SGRs and AXPs. **arXiv:astro-ph/0106041**, jun. 2001. 00007. 18, 19
- THOMPSON, C.; LYUTIKOV, M.; KULKARNI, S. R. Electrodynamics of Magnetars: Implications for the Persistent X-Ray Emission and Spin-down of the Soft Gamma Repeaters and Anomalous X-Ray Pulsars. **The Astrophysical Journal**, v. 574, n. 1, p. 332, 2002. ISSN 0004-637X. 00548. 18, 19
- THOMPSON, C. Nature of the soft gamma repeaters and anomalous X-ray pulsars. **Memorie della Societa Astronomica Italiana**, v. 73, p. 477–484, 2002. ISSN 0037-8720. 00012. 18, 19

- THOMPSON, C. Electrodynamics of Magnetars III: Pair Creation Processes in an Ultrastrong Magnetic Field and Particle Heating in a Dynamic Magnetosphere. **The Astrophysical Journal**, v. 688, p. 1258–1281, 2008. ISSN 0004-637X. 00034. 18, 19
- THOMPSON, C. Electrodynamics of Magnetars. IV. Self-Consistent Model of the Inner Accelerator with Implications for Pulsed Radio Emission. **Astrophysical Journal**, v. 688, n. 1996, p. 499–526, 2008. ISSN 0004-637X. 00033. 18, 19
- KASPI, V. M.; BELOBORODOV, A. M. Magnetars. **Annual Review of Astronomy and Astrophysics**, v. 55, n. 1, p. 261–301, 2017. 00057. 18, 19, 22
- REA, N. *et al.* A Low-Magnetic-Field Soft Gamma Repeater. **Science**, v. 330, n. 6006, p. 944–946, nov. 2010. ISSN 0036-8075, 1095-9203. 00235. 19
- ABDO, A. A. *et al.* Search for Gamma-ray Emission from Magnetars with the Fermi Large Area Telescope. **The Astrophysical Journal Letters**, v. 725, n. 1, p. L73, 2010. ISSN 2041-8205. 00045. 19, 87
- TONG, H.; SONG, L. M.; XU, R. X. Non-detection in a Fermi/LAT Observation of AXP 4U 0142+61: Magnetars? **The Astrophysical Journal Letters**, v. 725, n. 2, p. L196, 2010. ISSN 2041-8205. 19
- MORINI, M.; ROBBA, N. R.; SMITH, A.; van der Klis, M. EXOSAT observations of the supernova remnant G109.1-1.0 and the X-ray pulsar 1E 2259+586. **The Astrophysical Journal**, v. 333, p. 777–787, out. 1988. ISSN 0004-637X. 00064. 19
- KÜLEBI, B.; JORDAN, S.; EUCHNER, F.; GÄNSICKE, B. T.; HIRSCH, H. Analysis of hydrogen-rich magnetic white dwarfs detected in the Sloan Digital Sky Survey. **Astronomy & Astrophysics**, v. 506, n. 3, p. 1341–1350, nov. 2009. ISSN 0004-6361, 1432-0746. 00079. 19, 39
- WANG, Z.; CHAKRABARTY, D.; KAPLAN, D. L. A debris disk around an isolated young neutron star. **Nature**, v. 440, n. 7085, p. 772–775, abr. 2006. ISSN 1476-4687. 00274. 20
- KUIPER, L.; HERMSEN, W.; HARTOG, P. R. den; COLLMAR, W. Discovery of Luminous Pulsed Hard X-Ray Emission from Anomalous X-Ray Pulsars 1RXS J1708-4009, 4U 0142+61, and 1E 2259+586 by INTEGRAL and RXTE. **The Astrophysical Journal**, v. 645, n. 1, p. 556–575, jul. 2006. ISSN 0004-637X. 00000. 20, 22, 23
- OLAUSEN, S. A.; KASPI, V. M. The McGill Magnetar Catalog. **The Astrophysical Journal Supplement Series**, v. 212, n. 1, p. 6, 2014. ISSN 0067-0049. 00327. 20, 24, 25, 29, 30, 31, 53, 58, 60
- ALEKSIĆ, J. *et al.* Observations of the magnetars 4U 0142+61 and 1E 2259+586 with the MAGIC telescopes. **Astronomy & Astrophysics**, v. 549, p. A23, jan. 2013. ISSN 0004-6361, 1432-0746. 00003. 20
- HEWISH, A.; BELL, S. J.; PILKINGTON, J. D. H.; SCOTT, P. F.; COLLINS, R. A. Observation of a Rapidly Pulsating Radio Source. **Nature**, v. 217, n. 5130, p. 709, fev. 1968. ISSN 1476-4687. 01922. 20

- MANCHESTER, R. N.; HOBBS, G. B.; TEOH, A.; HOBBS, M. The Australia Telescope National Facility Pulsar Catalogue. **The Astronomical Journal**, v. 129, n. 4, p. 1993–2006, abr. 2005. ISSN 1538-3881. 00913. 20, 21
- KRISHNAN, V. V. *et al.* The UTMOST Survey for Magnetars, Intermittent pulsars, RRATs and FRBs I: System description and overview. **arXiv:1905.02415 [astro-ph]**, maio 2019. 00000. 20, 21, 24
- CAMILO, F. *et al.* Transient pulsed radio emission from a magnetar. **Nature**, v. 442, n. 7105, p. 892, ago. 2006. ISSN 1476-4687. 00387. 21
- CAMILO, F.; RANSOM, S. M.; HALPERN, J. P.; REYNOLDS, J. 1E 1547.0-5408: A Radio-emitting Magnetar with a Rotation Period of 2 Seconds. **The Astrophysical Journal**, v. 666, n. 2, p. L93–L96, ago. 2007. ISSN 1538-4357. 00275. 21
- CAMILO, F. *et al.* The Variable Radio-to-X-Ray Spectrum of the Magnetar XTE J1810–197. **The Astrophysical Journal**, v. 669, n. 1, p. 561, nov. 2007. ISSN 0004-637X. 00087. 21
- LEVIN, L. *et al.* A RADIO-LOUD MAGNETAR IN X-RAY QUIESCENCE. **The Astrophysical Journal**, v. 721, n. 1, p. L33–L37, ago. 2010. ISSN 2041-8205. 00148. 21
- SHANNON, R. M.; JOHNSTON, S. Radio properties of the magnetar near Sagittarius A* from observations with the Australia Telescope Compact Array. **Monthly Notices of the Royal Astronomical Society: Letters**, v. 435, n. 1, p. L29–L32, out. 2013. ISSN 1745-3925. 00000. 21
- MEREGHETTI, S. The strongest cosmic magnets: Soft gamma-ray repeaters and anomalous X-ray pulsars. **The Astronomy and Astrophysics Review**, v. 15, n. 4, p. 225–287, jul. 2008. ISSN 0935-4956, 1432-0754. 00659. 21, 22, 23
- REA, N.; PONS, J. A.; TORRES, D. F.; TUROLLA, R. THE FUNDAMENTAL PLANE FOR RADIO MAGNETARS. **The Astrophysical Journal**, v. 748, n. 1, p. L12, fev. 2012. ISSN 2041-8205. 00062. 21
- BARING, M. G.; HARDING, A. K. Radio-Quiet Pulsars with Ultrastrong Magnetic Fields. **The Astrophysical Journal Letters**, v. 507, n. 1, p. L55, set. 1998. ISSN 1538-4357. 00202. 21
- BARING, M. G.; HARDING, A. K. Photon Splitting and Pair Creation in Highly Magnetized Pulsars. **The Astrophysical Journal**, v. 547, n. 2, p. 929, fev. 2001. ISSN 0004-637X. 00175. 21
- REA, N.; TORRES, D. F. (Ed.). **High-Energy Emission from Pulsars and Their Systems: Proceedings of the First Session of the Sant Cugat Forum on Astrophysics**. Berlin Heidelberg: Springer-Verlag, 2011. (Astrophysics and Space Science Proceedings). 00088. ISBN 978-3-642-17250-2. 21
- IBRAHIM, A. I. *et al.* Discovery of a Transient Magnetar: XTE J1810-197. **The Astrophysical Journal**, v. 609, n. 1, p. L21–L24, maio 2004. ISSN 1538-4357. 00225. 21

- REA, N. *et al.* A STRONGLY MAGNETIZED PULSAR WITHIN THE GRASP OF THE MILKY WAY\textquotesingleS SUPERMASSIVE BLACK HOLE. **The Astrophysical Journal**, v. 775, n. 2, p. L34, set. 2013. ISSN 2041-8205. 00000. 21
- KASPI, V. M. *et al.* TIMING AND FLUX EVOLUTION OF THE GALACTIC CENTER MAGNETAR SGR J1745–2900. **The Astrophysical Journal**, v. 786, n. 2, p. 84, abr. 2014. ISSN 0004-637X. 00077. 21
- TONG, H.; YUAN, J.-P.; LIU, Z.-Y. Non-detection of pulsed radio emission from magnetar Swift J1834.9–0846: Constraint on the fundamental plane of magnetar radio emission. **Research in Astronomy and Astrophysics**, v. 13, n. 7, p. 835–840, jun. 2013. ISSN 1674-4527. 00004. 21
- HO, W. C. G. More than meets the eye: Magnetars in disguise. **Monthly Notices of the Royal Astronomical Society**, v. 429, n. 1, p. 113–118, fev. 2013. ISSN 0035-8711. 00008. 21
- MEREGHETTI, S. *et al.* Pulse Phase Variations of the X-Ray Spectral Features in the Radio-quiet Neutron Star 1E 1207-5209. **The Astrophysical Journal**, v. 581, n. 2, p. 1280–1285, dez. 2002. ISSN 0004-637X. 00105. 21
- KUIPER, L.; HERMSEN, W.; MENDEZ, M. Discovery of Hard Nonthermal Pulsed X-Ray Emission from the Anomalous X-Ray Pulsar 1E 1841-045. **The Astrophysical Journal**, v. 613, n. 2, p. 1173–1178, out. 2004. ISSN 0004-637X. 00153. 22
- MEREGHETTI, S.; GÖTZ, D.; MIRABEL, I. F.; HURLEY, K. INTEGRAL discovery of persistent hard X-ray emission from the Soft Gamma-ray Repeater SGR 1806–20. **Astronomy & Astrophysics**, v. 433, n. 2, p. L9–L12, abr. 2005. ISSN 0004-6361, 1432-0746. 00026. 22
- MOLKOV, S. *et al.* The broad-band spectrum of the persistent emission from SGR 1806-20. **Astronomy & Astrophysics**, v. 433, n. 2, p. L13–L16, abr. 2005. ISSN 0004-6361, 1432-0746. 00017. 22
- GÖTZ, D.; MEREGHETTI, S.; TIENGO, A.; ESPOSITO, P. Magnetars as persistent hard X-ray sources: INTEGRAL discovery of a hard tail in SGR 1900+14. **Astronomy & Astrophysics**, v. 449, n. 2, p. L31–L34, abr. 2006. ISSN 0004-6361, 1432-0746. 00037. 22
- ENOTO, T. *et al.* Soft and Hard X-Ray Emissions from the Anomalous X-Ray Pulsar 4U 0142+61 Observed with Suzaku. **Publications of the Astronomical Society of Japan**, v. 63, n. 2, p. 387–396, abr. 2011. ISSN 0004-6264. 00030. 22
- KASPI, V. M.; BOYDSTUN, K. ON THE X-RAY SPECTRA OF ANOMALOUS X-RAY PULSARS AND SOFT GAMMA REPEATERS. **The Astrophysical Journal**, v. 710, n. 2, p. L115–L120, jan. 2010. ISSN 2041-8205. 00042. 23
- HARTOG, P. R. den *et al.* INTEGRAL survey of the Cassiopeia region in hard X rays. **Astronomy & Astrophysics**, v. 451, n. 2, p. 587–602, maio 2006. ISSN 0004-6361, 1432-0746. 00018. 23

- WU, J. H. K. *et al.* Pulsed γ -ray emission from magnetar 1E 2259+586. **Journal of Astronomy and Space Sciences**, v. 30, n. 2, p. 83–85, 2013. ISSN 2093-5587. 00002. 23
- THOMPSON, C.; BELOBORODOV, A. M. High-Energy Emission from Magnetars. **The Astrophysical Journal**, v. 634, n. 1, p. 565–569, nov. 2005. ISSN 0004-637X. 00130. 23
- BARING, M. G.; GONTHIER, P. L.; HARDING, A. K. Spin-dependent Cyclotron Decay Rates in Strong Magnetic Fields. **The Astrophysical Journal**, v. 630, n. 1, p. 430–440, set. 2005. ISSN 0004-637X. 00044. 23
- BARING, M. G.; HARDING, A. K. Modeling the Non-Thermal X-ray Tail Emission of Anomalous X-ray Pulsars. **AIP Conference Proceedings**, v. 968, n. 1, p. 93–100, jan. 2008. ISSN 0094-243X. 00010. 23
- COELHO, J. G. *et al.* The rotation-powered nature of some soft gamma-ray repeaters and anomalous X-ray pulsars. **Astronomy & Astrophysics**, v. 599, p. A87, mar. 2017. ISSN 0004-6361, 1432-0746. 00008. 23, 24, 25, 35, 36, 37, 38, 40, 53, 65, 87
- GAVRIIL, F. P. *et al.* Magnetar-Like Emission from the Young Pulsar in Kes 75. **Science**, v. 319, n. 5871, p. 1802–1805, mar. 2008. ISSN 0036-8075, 1095-9203. 00213. 24
- CAMILO, F. *et al.* Radio Disappearance of the Magnetar XTE J1810-197 and Continued X-ray Timing. **The Astrophysical Journal**, v. 820, n. 2, p. 110, 2016. ISSN 0004-637X. 00019. 24, 65, 66
- SCHOLZ, P. *et al.* Spin-down Evolution and Radio Disappearance of the Magnetar PSR J1622-4950. **The Astrophysical Journal**, v. 841, n. 2, p. 126, jun. 2017. ISSN 1538-4357. 00007. 24, 65, 66
- SHAPIRO, S. L.; TEUKOLSKY, S. A. **Black Holes, White Dwarfs, and Neutron Stars: The Physics of Compact Objects**. [S.l.]: John Wiley & Sons, 2008. 03439. ISBN 978-3-527-61767-8. 26, 37
- ROTONDO, M.; RUEDA, J. A.; RUFFINI, R.; XUE, S. S. The self-consistent general relativistic solution for a system of degenerate neutrons, protons and electrons in β -equilibrium. **Physics Letters B**, v. 701, n. 5, p. 667–671, jul. 2011. ISSN 0370-2693. 26, 35
- CARVALHO, G. A.; MARINHO, R. M.; MALHEIRO, M. General relativistic effects in the structure of massive white dwarfs. **General Relativity and Gravitation**, v. 50, n. 4, abr. 2018. ISSN 0001-7701, 1572-9532. 00000. 26
- TOLMAN, R. C. Static Solutions of Einstein's Field Equations for Spheres of Fluid. **Physical Review**, v. 55, n. 4, p. 364–373, fev. 1939. 01665. 26, 35
- OPPENHEIMER, J. R.; VOLKOFF, G. M. On Massive Neutron Cores. **Physical Review**, v. 55, n. 4, p. 374–381, fev. 1939. 02827. 26, 35
- HARTLE, J. B. Slowly Rotating Relativistic Stars. I. Equations of Structure. **The Astrophysical Journal**, v. 150, p. 1005, dez. 1967. 00814. 26, 29

- WEBER, F. Strange quark matter and compact stars. **Progress in Particle and Nuclear Physics**, v. 54, n. 1, p. 193–288, mar. 2005. ISSN 0146-6410. 00596. 27
- WEBER, F. **Pulsars as Astrophysical Laboratories for Nuclear and Particle Physics**. [S.l.]: Routledge, 2017. 00490. ISBN 978-1-351-42095-2. 27, 28
- WEBER, F.; GLENDENNING, N. K.; WEIGEL, M. K. Structure and stability of rotating relativistic neutron stars. **The Astrophysical Journal**, v. 373, p. 579–591, jun. 1991. ISSN 0004-637X. 00088. 27
- WEBER, F.; GLENDENNING, N. K. Application of the improved Hartle method for the construction of general relativistic rotating neutron star models. **The Astrophysical Journal**, v. 390, p. 541–549, maio 1992. ISSN 0004-637X. 00137. 27
- GLENDENNING, N. K.; WEBER, F. Impact of frame dragging on the Kepler frequency of relativistic stars. **Physical Review D**, v. 50, n. 6, p. 3836–3841, set. 1994. 00054. 27
- BELVEDERE, R.; RUEDA, J. A.; RUFFINI, R. ON THE MAGNETIC FIELD OF PULSARS WITH REALISTIC NEUTRON STAR CONFIGURATIONS. **The Astrophysical Journal**, v. 799, n. 1, p. 23, jan. 2015. ISSN 0004-637X. 00019. 28, 36, 38
- LAI, D.; SHAPIRO, S. L. Cold equation of state in a strong magnetic field - Effects of inverse beta-decay. **The Astrophysical Journal**, v. 383, p. 745–751, dez. 1991. ISSN 0004-637X. 00000. 28
- CHAMEL, N. *et al.* Properties of the outer crust of strongly magnetized neutron stars from Hartree-Fock-Bogoliubov atomic mass models. **Physical Review C**, v. 86, n. 5, p. 055804, nov. 2012. 00000. 28
- CHAMEL, N.; MOLTER, E.; FANTINA, A. F.; ARTEAGA, D. P. Maximum strength of the magnetic field in the core of the most massive white dwarfs. **Physical Review D**, v. 90, n. 4, p. 043002, ago. 2014. 00000. 29
- HARTLE, J. B.; THORNE, K. S. Slowly Rotating Relativistic Stars. II. Models for Neutron Stars and Supermassive Stars. **The Astrophysical Journal**, v. 153, p. 807, set. 1968. ISSN 0004-637X. 00695. 29
- HARTLE, J. B.; THORNE, K. S. Slowly Rotating Relativistic Stars. III. Static Criterion for Stability. **The Astrophysical Journal**, v. 158, p. 719, nov. 1969. 00023. 29
- HARTLE, J. B. Slowly-Rotating Relativistic Stars.IV. Rotational Energy and Moment of Inertia for Stars in Differential Rotation. **The Astrophysical Journal**, v. 161, p. 111, jul. 1970. 00048. 29
- HARTLE, J. B.; THORNE, K. S.; CHITRE, S. M. Slowly Rotating Relativistic Stars.VI. Stability of the Quasiradial Modes. **The Astrophysical Journal**, v. 176, p. 177, ago. 1972. 00023. 29
- HARTLE, J. B. Slowly rotating relativistic stars. IIIA. The static stability criterion recovered. **The Astrophysical Journal**, v. 195, p. 203, jan. 1975. 00011. 29

- HARTLE, J. B.; MUNN, M. W. Slowly rotating relativistic stars. V. Static stability analysis of $n = 3/2$ polytropes. **The Astrophysical Journal**, v. 198, p. 467, jun. 1975. 00020. 29
- HARTLE, J. B.; FRIEDMAN, J. L. Slowly Rotating Relativistic Stars. VIII. Frequencies of the Quasi-Radial Modes of an $N = 3/2$ Polytrope. **The Astrophysical Journal**, v. 196, p. 653, mar. 1975. 00036. 29
- GOLDREICH, P.; JULIAN, W. H. Pulsar Electrodynamics. **The Astrophysical Journal**, v. 157, p. 869, ago. 1969. ISSN 0004-637X. 02766. 30, 42
- JACKSON, J. D. **Classical Electrodynamics**. [S.l.]: Wiley, 1975. 50016. ISBN 978-0-471-43132-9. 31, 37, 49
- PTITSYNA, K. V.; TROITSKY, S. V. Physical conditions in potential accelerators of ultra-high-energy cosmic rays: Updated Hillas plot and radiation-loss constraints. **Physics-Uspekhi**, v. 53, n. 7, p. 691–701, out. 2010. ISSN 1063-7869. 00083. 32
- HILLAS, A. M. The origin of ultra-high-energy cosmic rays. **Annual Review of Astronomy and Astrophysics**, v. 22, n. 1, p. 425–444, 1984. 32
- HILLAS, A. M. Where do 1019 eV cosmic rays come from? **Nuclear Physics B - Proceedings Supplements**, v. 136, n. 1-3 SPEC.ISS., p. 139–146, nov. 2004. ISSN 09205632. 00032. 32
- FERRARI, A.; RUFFINI, R. Theoretical Implications of the Second Time Derivative of the Period of the Pulsar NP 0532. **The Astrophysical Journal Letters**, v. 158, p. L71, nov. 1969. ISSN 0004-637X. 00000. 33, 38
- COELHO, J. G.; MALHEIRO, M. SIMILARITIES OF SGRs WITH LOW MAGNETIC FIELD AND WHITE DWARF PULSARS. **International Journal of Modern Physics: Conference Series**, v. 18, p. 96–100, jan. 2012. ISSN 2010-1945. 00009. 34
- COELHO, J. G.; MALHEIRO, M. SGRs and AXPs as white dwarf pulsars. In: . [S.l.]: AIP Publishing, 2013. v. 1520, p. 258–263. 00006. 34
- LOBATO, R. V.; MALHEIRO, M.; COELHO, J. G. SGRs/AXPs as white dwarf pulsars: Sources of ultra-high energetic photons with $E \sim 10^{21}$ eV. In: **The Fourteenth Marcel Grossmann Meeting**. [S.l.]: WORLD SCIENTIFIC, 2017. p. 4313–4318. ISBN 978-981-322-659-3. 34
- ZATSEPIN, G. T.; KUZ'MIN, V. A. Upper Limit of the Spectrum of Cosmic Rays. v. 4, p. 78, ago. 1966. ISSN 0021-3640. 34
- GREISEN, K. End to the cosmic-ray spectrum? **Physical Review Letters**, v. 16, n. 17, p. 748–750, abr. 1966. ISSN 00319007. 34
- BELVEDERE, R.; BOSHKAYEV, K.; RUEDA, J. A.; RUFFINI, R. Uniformly rotating neutron stars in the global and local charge neutrality cases. **Nuclear Physics A**, v. 921, p. 33–59, jan. 2014. ISSN 0375-9474. 00040. 35, 36
- RUEDA, J. A.; RUFFINI, R.; XUE, S. S. The Klein first integrals in an equilibrium system with electromagnetic, weak, strong and gravitational interactions. **Nuclear Physics A**, v. 872, n. 1, p. 286–295, dez. 2011. ISSN 0375-9474. 35

- BELVEDERE, R.; PUGLIESE, D.; RUEDA, J. A.; RUFFINI, R.; XUE, S.-S. Neutron star equilibrium configurations within a fully relativistic theory with strong, weak, electromagnetic, and gravitational interactions. **Nuclear Physics A**, v. 883, p. 1–24, jun. 2012. ISSN 0375-9474. 00099. 35
- BAYM, G.; PETHICK, C.; SUTHERLAND, P. The Ground State of Matter at High Densities: Equation of State and Stellar Models. **The Astrophysical Journal**, v. 170, p. 299, dez. 1971. ISSN 0004-637X. 01395. 35
- BAYM, G.; BETHE, H. A.; PETHICK, C. J. Neutron star matter. **Nuclear Physics A**, v. 175, n. 2, p. 225–271, nov. 1971. ISSN 0375-9474. 00829. 35
- BOGUTA, J.; BODMER, A. R. Relativistic calculation of nuclear matter and the nuclear surface. **Nuclear Physics A**, v. 292, n. 3, p. 413–428, dez. 1977. ISSN 0375-9474. 00109. 35
- LALAZISSIS, G. A.; KÖNIG, J.; RING, P. New parametrization for the Lagrangian density of relativistic mean field theory. **Physical Review C**, v. 55, n. 1, p. 540–543, jan. 1997. 00109. 35
- SUGAHARA, Y.; TOKI, H. Relativistic mean-field theory for unstable nuclei with non-linear σ and ω terms. **Nuclear Physics A**, v. 579, n. 3, p. 557–572, out. 1994. ISSN 0375-9474. 00080. 35
- GLENDENNING, N. K.; MOSZKOWSKI, S. A. Reconciliation of neutron-star masses and binding of the Λ in hypernuclei. **Physical Review Letters**, v. 67, n. 18, p. 2414–2417, out. 1991. 00000. 36
- MALHEIRO, M. *et al.* Possible rotation-power nature of SGRs and AXPs. **Journal of Physics: Conference Series**, v. 861, n. 1, p. 012003, 2017. ISSN 1742-6596. 00000. 37, 40
- HARDING, A. K. The neutron star zoo. **Frontiers of Physics**, v. 8, n. 6, p. 679–692, dez. 2013. ISSN 2095-0470. 00084. 37
- PARET, D. M.; HORVATH, J. E.; MARTINEZ, A. P. Anisotropic stellar structure equations for magnetized stars. **arXiv:1407.2280 [astro-ph]**, v. 15, n. 7, p. 975, 2014. ISSN 16744527. 00007. 38
- REZZOLLA, L.; AHMEDOV, B. J. Electromagnetic fields in the exterior of an oscillating relativistic star - I. General expressions and application to a rotating magnetic dipole. **Monthly Notices of the Royal Astronomical Society**, v. 352, n. 4, p. 1161–1179, ago. 2004. ISSN 00358711. 00056. 38
- MELROSE, D. B. A Generic Pulsar Radio Emission Mechanism. **Chinese Journal of Astronomy and Astrophysics**, v. 6, n. S2, p. 74, 2006. ISSN 1009-9271. 00011. 41
- MELROSE, D. B. The models for radio emission from pulsars—The outstanding issues. **Journal of Astrophysics and Astronomy**, v. 16, n. 2, p. 137–164, jun. 1995. ISSN 0973-7758. 00066. 41

- RUBTSOV, G.; SOKOLOVA, E. Blind search for radio-quiet and radio-loud gamma-ray pulsars with Fermi-LAT data. **Soviet Journal of Experimental and Theoretical Physics Letters**, v. 100, n. 11, p. 689–694, 2015. ISSN 10906487. 00002. 42, 65, 87
- ABDO, A. A. *et al.* FERMILARGE AREA telescope OBSERVATIONS OF THE VELA PULSAR. **The Astrophysical Journal**, v. 696, n. 2, p. 1084–1093, abr. 2009. ISSN 0004-637X. 00000. 42
- ABDO, A. A. *et al.* The Second Fermi Large Area Telescope Catalog of Gamma-Ray Pulsars. **The Astrophysical Journal Supplement Series**, v. 208, n. 2, p. 17, 2013. ISSN 0067-0049. 00208. 42, 51, 52, 53, 54, 55, 57, 65, 87
- GHOSH, P. **Rotation and Accretion Powered Pulsars**. [S.l.]: World Scientific, 2007. 00103. ISBN 978-981-02-4744-7. 42
- KRALL, N. A.; TRIVELPIECE, A. W. **Principles of Plasma Physics**. [S.l.]: McGraw-Hill, 1973. 04090. ISBN 978-0-07-035346-6. 42
- CHEN, K.; RUDERMAN, M. Pulsar death lines and death valley. **The Astrophysical Journal**, v. 402, p. 264–270, jan. 1993. ISSN 0004-637X. 00281. 43, 44, 62, 63, 64
- ZHANG, B. Radio Pulsar Death. **Acta Astronomica Sinica**, v. 44, p. 215–222, fev. 2003. ISSN 0001-5245. 00104. 44, 65
- ZHANG, B.; HARDING, A. K.; MUSLIMOV, A. G. Radio Pulsar Death Line Revisited: Is PSR J2144-3933 Anomalous? **The Astrophysical Journal**, v. 531, n. 2, p. L135–L138, mar. 2000. ISSN 0004637X. 00099. 44
- ZHANG, B.; HARDING, A. K. High Magnetic Field Pulsars and Magnetars: A Unified Picture. **The Astrophysical Journal**, v. 535, n. 1, p. L51–L54, maio 2000. ISSN 1538-4357. 00084. 44
- BESKIN, V. S. General Relativity Effects on Electrodynamical Processes in Radio Pulsars. **Soviet Astronomy Letters**, v. 16, p. 286, jul. 1990. 00000. 45
- MUSLIMOV, A. G.; TSYGAN, A. I. Influence of General Relativity Effects on Electrodynamics in the Vicinity of a Magnetic Pole of a Neutron Star. **Soviet Astronomy**, v. 34, p. 133, abr. 1990. ISSN 0038-5301. 00000. 45
- MOROZOVA, V. S.; AHMEDOV, B. J.; ZANOTTI, O. General relativistic magnetospheres of slowly rotating and oscillating magnetized neutron stars. **Monthly Notices of the Royal Astronomical Society**, v. 408, n. 1, p. 490–502, out. 2010. ISSN 0035-8711. 45
- MUSLIMOV, A. G.; TSYGAN, A. I. General relativistic electric potential drops above pulsar polar caps. **Monthly Notices of the Royal Astronomical Society**, v. 255, p. 61–70, mar. 1992. ISSN 0035-8711. 45
- MOROZOVA, V. S.; AHMEDOV, B. J.; ZANOTTI, O. Explaining radio emission of magnetars via rotating and oscillating magnetospheres of neutron stars. **Monthly Notices of the Royal Astronomical Society**, v. 419, n. 3, p. 2147–2155, jan. 2012. ISSN 0035-8711. 45, 46

- MUSLIMOV, A.; HARDING, A. K. Toward the Quasi-Steady State Electrodynamics of a Neutron Star. **The Astrophysical Journal**, v. 485, n. 2, p. 735–746, ago. 1997. ISSN 0004-637X. 00121. 45
- MOROZOVA, V. S.; AHMEDOV, B. J.; KAGRAMANOVA, V. G. General Relativistic Effects of Gravitomagnetic Charge on Pulsar Magnetospheres and Particle Acceleration in the Polar Cap. **The Astrophysical Journal**, v. 684, n. 2, p. 1359–1365, set. 2008. ISSN 0004-637X. 00019. 45
- TAKATA, J.; WANG, Y.; CHENG, K. S. Pulsar High Energy Emissions from Outer Gap Accelerator Closed by a Magnetic Pair-creation Process. **The Astrophysical Journal**, v. 715, n. 2, p. 1318, 2010. ISSN 0004-637X. 46
- ZHANG, L.; CHENG, K. S. High-Energy Radiation from Rapidly Spinning Pulsars with Thick Outer Gaps. **The Astrophysical Journal**, v. 487, n. 1, p. 370, 1997. ISSN 0004-637X. 46, 47, 48
- HIROTANI, K. Particle Accelerator in Pulsar Magnetospheres: Super-Goldreich-Julian Current with Ion Emission from the Neutron Star Surface. **The Astrophysical Journal**, v. 652, n. 2, p. 1475, 2006. ISSN 0004-637X. 00088. 47
- CHENG, K. S.; ZHANG, J. L. General Radiation Formulae for a Relativistic Charged Particle Moving in Curved Magnetic Field Lines: The Synchrocurvature Radiation Mechanism. **The Astrophysical Journal**, v. 463, p. 271, maio 1996. 00000. 49
- JOHNSON, T. J. Constraints on the Emission Geometries of Gamma-ray Millisecond Pulsars Observed with the Fermi Large Area Telescope. **arXiv:1209.4000 [astro-ph]**, set. 2012. 00000. 51
- KISAKA, S.; TANAKA, S. J. Efficiency of Synchrotron Radiation from Rotation-Powered Pulsars. **The Astrophysical Journal**, IOP Publishing, v. 837, n. 1, p. 1–16, 2017. ISSN 1538-4357. 00001. 51
- XIA, X. Y.; QIAO, G. J.; WU, X. J.; HOU, Y. Q. Inverse Compton scattering in strong magnetic fields and its possible application to pulsar emission. **Astronomy and Astrophysics**, v. 152, p. 93, nov. 1985. ISSN 0004-6361. 00000. 62
- DAUGHERTY, J. K.; HARDING, A. K. Comptonization of Thermal Photons by Relativistic Electron Beams. **The Astrophysical Journal**, v. 336, p. 861, jan. 1989. ISSN 0004-637X. 00070. 62
- DERMER, C. D. Compton Scattering in Strong Magnetic Fields and the Continuum Spectra of Gamma-Ray Bursts: Basic Theory. **The Astrophysical Journal**, v. 360, p. 197, set. 1990. ISSN 0004-637X. 00128. 62
- STURNER, S. J.; DERMER, C. D.; MICHEL, F. C. Magnetic Compton-induced Pair Cascade Model for Gamma-Ray Pulsars. **The Astrophysical Journal**, v. 445, p. 736, jun. 1995. ISSN 0004-637X. 00128. 62
- ZHANG, B.; QIAO, G. J. A study on pulsar inner-gap sparking comparing inverse Compton scattering and curvature radiation processes. **Astronomy and Astrophysics**, v. 310, p. 135, jun. 1996. 00008. 63

- LUO, Q. Compton Scattering Effect on Formation of Pulsar Polar Gaps. **The Astrophysical Journal**, v. 468, p. 338, set. 1996. 00029. 63
- ABBOTT, B. P. *et al.* Gravitational Waves and Gamma-Rays from a Binary Neutron Star Merger: GW170817 and GRB 170817A. **The Astrophysical Journal**, 2017. ISSN 2041-8213. 00490. 70, 78
- ABBOTT, B. P. *et al.* GW170817: Observation of Gravitational Waves from a Binary Neutron Star Inspiral. **Physical Review Letters**, v. 119, n. 16, p. 161101, out. 2017. ISSN 0031-9007. 00000. 70, 71, 77, 78
- ABBOTT, B. P. *et al.* Multi-messenger Observations of a Binary Neutron Star Merger. **The Astrophysical Journal**, v. 848, n. 2, p. L12, out. 2017. ISSN 2041-8205. 00000. 70, 78
- GOLDSTEIN, A. *et al.* An Ordinary Short Gamma-Ray Burst with Extraordinary Implications: Fermi -GBM Detection of GRB 170817A. **The Astrophysical Journal Letters**, v. 848, n. 2, p. L14, 2017. ISSN 2041-8205. 00000. 70, 71, 78
- KOCHANEK, C. S.; PIRAN, T. Gravitational Waves and gamma -Ray Bursts. **The Astrophysical Journal**, v. 417, p. L17, nov. 1993. ISSN 0004-637X. 00000. 70
- HUGHES, S. A.; HOLZ, D. E. Cosmology with coalescing massive black holes. **Classical and Quantum Gravity**, v. 20, n. 10, p. S65, abr. 2003. ISSN 0264-9381. 00046. 70
- GROSSMAN, D.; KOROBKIN, O.; ROSSWOG, S.; PIRAN, T. The long-term evolution of neutron star merger remnants – II. Radioactively powered transients. **Monthly Notices of the Royal Astronomical Society**, v. 439, n. 1, p. 757–770, mar. 2014. ISSN 0035-8711. 00143. 70
- ROSSWOG, S. Compact binary mergers: An astrophysical perspective. **arXiv:1012.0912 [astro-ph, physics:nucl-th]**, dez. 2010. 00005. 71
- COULTER, D. A. *et al.* Swope Supernova Survey 2017a (SSS17a), the optical counterpart to a gravitational wave source. **Science**, v. 358, n. 6370, p. 1556–1558, dez. 2017. ISSN 0036-8075, 1095-9203. 00176. 71, 83
- GOTTLIEB, O.; NAKAR, E.; PIRAN, T.; HOTOKEZAKA, K. A cocoon shock breakout as the origin of the γ -ray emission in GW170817. **Monthly Notices of the Royal Astronomical Society**, v. 479, n. 1, p. 588–600, set. 2018. ISSN 0035-8711. 00052. 71, 72
- ARCAVI, I. *et al.* Optical emission from a kilonova following a gravitational-wave-detected neutron-star merger. **Nature**, v. 551, n. 7678, p. 64–66, nov. 2017. ISSN 1476-4687. 00119. 71, 78, 83
- BELCZYNSKI, K. *et al.* Binary neutron star formation and the origin of GW170817. **arXiv:1812.10065 [astro-ph]**, dez. 2018. 71
- BROMBERG, O.; TCHEKHOVSKOY, A.; GOTTLIEB, O.; NAKAR, E.; PIRAN, T. The γ -rays that accompanied GW170817 and the observational signature of a magnetic jet breaking out of NS merger ejecta. **Monthly Notices of the Royal Astronomical Society**, v. 475, n. 3, p. 2971–2977, abr. 2018. ISSN 0035-8711. 00031. 71, 72

- GOTTLIEB, O.; NAKAR, E.; PIRAN, T. The cocoon emission – an electromagnetic counterpart to gravitational waves from neutron star mergers. **Monthly Notices of the Royal Astronomical Society**, v. 473, n. 1, p. 576–584, jan. 2018. ISSN 0035-8711. 00085. 71, 72
- KATHIRGAMARAJU, A.; DURAN, R. B.; GIANNIOS, D. Off-axis short GRBs from structured jets as counterparts to GW events. **Monthly Notices of the Royal Astronomical Society: Letters**, v. 473, n. 1, p. L121–L125, jan. 2018. ISSN 1745-3925. 00063. 71
- HALLINAN, G. *et al.* A radio counterpart to a neutron star merger. **Science**, v. 358, n. 6370, p. 1579–1583, dez. 2017. ISSN 0036-8075, 1095-9203. 00115. 72
- KASLIWAL, M. M. *et al.* Illuminating gravitational waves: A concordant picture of photons from a neutron star merger. **Science**, v. 358, n. 6370, p. 1559–1565, dez. 2017. ISSN 0036-8075, 1095-9203. 00227. 72
- NAKAR, E.; PIRAN, T. The Observable Signatures of GRB Cocoons. **The Astrophysical Journal**, v. 834, n. 1, p. 28, 2017. ISSN 0004-637X. 00000. 72
- LAZZATI, D.; DEICH, A.; MORSONY, B. J.; WORKMAN, J. C. Off-axis emission of short γ -ray bursts and the detectability of electromagnetic counterparts of gravitational-wave-detected binary mergers. **Monthly Notices of the Royal Astronomical Society**, v. 471, n. 2, p. 1652–1661, out. 2017. ISSN 0035-8711. 00000. 72
- LAZZATI, D. *et al.* Off-axis Prompt X-Ray Transients from the Cocoon of Short Gamma-Ray Bursts. **The Astrophysical Journal Letters**, v. 848, n. 1, p. L6, 2017. ISSN 2041-8205. 00000. 72
- MOOLEY, K. P. *et al.* Superluminal motion of a relativistic jet in the neutron-star merger GW170817. **Nature**, v. 561, n. 7723, p. 355, set. 2018. ISSN 1476-4687. 00034. 72
- LI, S.-Z.; LIU, L.-D.; YU, Y.-W.; ZHANG, B. What Powered the Optical Transient AT2017gfo Associated with GW170817? **The Astrophysical Journal Letters**, v. 861, n. 2, p. L12, 2018. ISSN 2041-8205. 00000. 72
- MATSUMOTO, T.; IOKA, K.; KISAKA, S.; NAKAR, E. Is the Macronova in GW170817 Powered by the Central Engine? **The Astrophysical Journal**, v. 861, n. 1, p. 55, 2018. ISSN 0004-637X. 00000. 72
- METZGER, B. D.; THOMPSON, T. A.; QUATAERT, E. A Magnetar Origin for the Kilonova Ejecta in GW170817. **The Astrophysical Journal**, v. 856, n. 2, p. 101, 2018. ISSN 0004-637X. 00000. 72
- DAN, M.; ROSSWOG, S.; GUILLOCHON, J.; Ramirez-Ruiz, E. PRELUDE TO A DOUBLE DEGENERATE MERGER: THE ONSET OF MASS TRANSFER AND ITS IMPACT ON GRAVITATIONAL WAVES AND SURFACE DETONATIONS. **The Astrophysical Journal**, v. 737, n. 2, p. 89, ago. 2011. ISSN 0004-637X. 00000. 72, 84

- Lorén-Aguilar, P.; ISERN, J.; García-Berro, E. High-resolution smoothed particle hydrodynamics simulations of the merger of binary white dwarfs. **Astronomy & Astrophysics**, v. 500, n. 3, p. 1193–1205, jun. 2009. ISSN 0004-6361, 1432-0746. 00000. 72, 84
- BULLA, M. *et al.* The origin of polarization in kilonovae and the case of the gravitational-wave counterpart AT 2017gfo. **Nature Astronomy**, v. 3, n. 1, p. 99, jan. 2019. ISSN 2397-3366. 00000. 73
- NICHOLL, M. *et al.* The Electromagnetic Counterpart of the Binary Neutron Star Merger LIGO/Virgo GW170817. III. Optical and UV Spectra of a Blue Kilonova from Fast Polar Ejecta. **The Astrophysical Journal Letters**, v. 848, n. 2, p. L18, 2017. ISSN 2041-8205. 00000. 73, 78, 83, 85
- POSTNOV, K. A.; YUNGELSON, L. R. The evolution of compact binary star systems. **Living Reviews in Relativity**, v. 17, 2014. ISSN 14338351. 74
- PETERS, P. C.; MATHEWS, J. Gravitational Radiation from Point Masses in a Keplerian Orbit. **Physical Review**, v. 131, n. 1, p. 435–440, jul. 1963. ISSN 0031-899X. 01053. 74
- PETERS, P. C. Gravitational Radiation and the Motion of Two Point Masses. **Physical Review**, v. 136, n. 4B, p. B1224–B1232, nov. 1964. ISSN 0031-899X. 01347. 74
- BUONANNO, A. Gravitational waves. **arXiv:0709.4682 [gr-qc]**, set. 2007. 04328. 74
- FANG, L. Z.; RUFFINI, R. **Basic Concepts in Relativistic Astrophysics**. [S.l.]: World Scientific Publishing Company, 1983. 00000. ISBN 978-981-310-413-6. 74
- SCHUTZ, B. F. Gravitational-wave sources. **Classical and Quantum Gravity**, v. 13, n. 11A, p. A219, 1996. ISSN 0264-9381. 00109. 75
- CREIGHTON, J. D. E.; ANDERSON, W. G. **Gravitational-Wave Physics and Astronomy: An Introduction to Theory, Experiment and Data Analysis**. 1 edition. ed. Weinheim, Germany: Wiley-VCH, 2011. 00000. ISBN 978-3-527-40886-3. 76
- CAMP, J. B.; CORNISH, N. J. GRAVITATIONAL WAVE ASTRONOMY. **Annual Review of Nuclear and Particle Science**, v. 54, n. 1, p. 525–577, dez. 2004. ISSN 0163-8998, 1545-4134. 00030. 76
- MAGGIORE, M. **Gravitational Waves: Volume 1: Theory and Experiments**. Oxford: OUP Oxford, 2007. 00000. ISBN 978-0-19-857074-5. 77
- FLANAGAN, É. É.; HUGHES, S. A. Measuring gravitational waves from binary black hole coalescences. I. Signal to noise for inspiral, merger, and ringdown. **Physical Review D**, v. 57, n. 8, p. 4535–4565, abr. 1998. 00632. 77
- LIGO Scientific Collaboration and Virgo Collaboration *et al.* Properties of the Binary Neutron Star Merger GW170817. **Physical Review X**, v. 9, n. 1, p. 011001, jan. 2019. 00000. 77
- FRYER, C. L.; OLIVEIRA, F. G.; RUEDA, J. A.; RUFFINI, R. Neutron-Star–Black-Hole Binaries Produced by Binary-Driven Hypernovae. **Physical Review Letters**, v. 115, n. 23, p. 231102, dez. 2015. 00000. 78

RUFFINI, R. *et al.* ON THE CLASSIFICATION OF GRBs AND THEIR OCCURRENCE RATES. **The Astrophysical Journal**, v. 832, n. 2, p. 136, nov. 2016. ISSN 0004-637X. 00000. 78

RUFFINI, R. *et al.* GRB 140619B: A SHORT GRB FROM A BINARY NEUTRON STAR MERGER LEADING TO BLACK HOLE FORMATION. **The Astrophysical Journal**, v. 808, n. 2, p. 190, ago. 2015. ISSN 0004-637X. 00000. 78

RUFFINI, R. *et al.* GRB 090510: A GENUINE SHORT GRB FROM A BINARY NEUTRON STAR COALESCING INTO A KERR–NEWMAN BLACK HOLE. **The Astrophysical Journal**, v. 831, n. 2, p. 178, nov. 2016. ISSN 0004-637X. 00018. 78, 80, 82

MUCCINO, M.; RUFFINI, R.; BIANCO, C. L.; IZZO, L.; PENACCHIONI, A. V. GRB 090227B: THE MISSING LINK BETWEEN THE GENUINE SHORT AND LONG GAMMA-RAY BURSTS. **The Astrophysical Journal**, v. 763, n. 2, p. 125, jan. 2013. ISSN 0004-637X. 00000. 78

RUFFINI, R. *et al.* On the Rate and on the Gravitational Wave Emission of Short and Long GRBs. **The Astrophysical Journal**, v. 859, n. 1, p. 30, maio 2018. ISSN 0004-637X. 00000. 78, 80, 81, 82

LI, L.-X.; PACZYŃSKI, B. Transient Events from Neutron Star Mergers. **The Astrophysical Journal Letters**, v. 507, n. 1, p. L59, 1998. ISSN 1538-4357. 00527. 78, 83

BERGER, E.; FONG, W.; CHORNOCK, R. AN r-PROCESS KILONOVA ASSOCIATED WITH THE SHORT-HARD GRB 130603B. **The Astrophysical Journal**, v. 774, n. 2, p. L23, ago. 2013. ISSN 2041-8205. 00281. 78, 83

METZGER, B. D. *et al.* Electromagnetic counterparts of compact object mergers powered by the radioactive decay of r-process nuclei. **Monthly Notices of the Royal Astronomical Society**, v. 406, n. 4, p. 2650–2662, ago. 2010. ISSN 0035-8711. 00000. 78, 79

TANVIR, N. R. *et al.* A ‘kilonova’ associated with the short-duration γ -ray burst GRB 130603B. **Nature**, v. 500, n. 7464, p. 547–549, ago. 2013. ISSN 1476-4687. 00527. 78, 83

FONG, W. *et al.* SHORT GRB 130603B: DISCOVERY OF A JET BREAK IN THE OPTICAL AND RADIO AFTERGLOWS, AND A MYSTERIOUS LATE-TIME X-RAY EXCESS. **The Astrophysical Journal**, v. 780, n. 2, p. 118, dez. 2013. ISSN 0004-637X. 00127. 78

JIN, Z.-P. *et al.* The Macronova in GRB 050709 and the GRB-macronova connection. **Nature Communications**, v. 7, p. 12898, set. 2016. ISSN 2041-1723. 00000. 78

VALLE, M. D. *et al.* An enigmatic long-lasting γ -ray burst not accompanied by a bright supernova. **Nature**, v. 444, n. 7122, p. 1050, dez. 2006. ISSN 1476-4687. 00420. 78

CAITO, L. *et al.* GRB060614: A “fake” short GRB from a merging binary system. **Astronomy & Astrophysics**, v. 498, n. 2, p. 501–507, maio 2009. ISSN 0004-6361, 1432-0746. 00000. 78, 80, 83

- CADELANO, M. *et al.* OPTICAL IDENTIFICATION OF He WHITE DWARFS ORBITING FOUR MILLISECOND PULSARS IN THE GLOBULAR CLUSTER 47 TUCANAE. **The Astrophysical Journal**, v. 812, n. 1, p. 63, out. 2015. ISSN 0004-637X. 00000. 78
- FRYER, C. L.; WOOSLEY, S. E.; HERANT, M.; DAVIES, M. B. Merging White Dwarf/Black Hole Binaries and Gamma-Ray Bursts. **The Astrophysical Journal**, v. 520, n. 2, p. 650–660, ago. 1999. ISSN 0004-637X. 00168. 78
- LAZARUS, P. *et al.* Timing of a young mildly recycled pulsar with a massive white dwarf companion. **Monthly Notices of the Royal Astronomical Society**, v. 437, n. 2, p. 1485–1494, jan. 2014. ISSN 0035-8711. 00023. 78
- TAURIS, T. M.; HEUVEL, E. P. J. van den; SAVONIJE, G. J. Formation of Millisecond Pulsars with Heavy White Dwarf Companions: Extreme Mass Transfer on Subthermal Timescales. **The Astrophysical Journal**, v. 530, n. 2, p. L93–L96, fev. 2000. ISSN 1538-4357. 00129. 78
- COWPERTHWAITTE, P. S. *et al.* The Electromagnetic Counterpart of the Binary Neutron Star Merger LIGO/Virgo GW170817. II. UV, Optical, and Near-infrared Light Curves and Comparison to Kilonova Models. **The Astrophysical Journal Letters**, v. 848, n. 2, p. L17, 2017. ISSN 2041-8205. 78, 83, 85
- MAOZ, D.; HALLAKOUN, N. The binary fraction, separation distribution and merger rate of white dwarfs from SPY. **Monthly Notices of the Royal Astronomical Society**, v. 467, n. 2, p. 1414–1425, maio 2017. ISSN 0035-8711. 00027. 79, 84
- MAOZ, D.; HALLAKOUN, N.; BADENES, C. The separation distribution and merger rate of double white dwarfs: Improved constraints. **Monthly Notices of the Royal Astronomical Society**, v. 476, n. 2, p. 2584–2590, maio 2018. ISSN 0035-8711. 00019. 79, 84
- KALOGERA, V.; NARAYAN, R.; SPERGEL, D. N.; TAYLOR, J. H. The Coalescence Rate of Double Neutron Star Systems. **The Astrophysical Journal**, v. 556, n. 1, p. 340–356, jul. 2001. ISSN 0004-637X. 00190. 79, 84
- ABBOTT, B. P. *et al.* Prospects for observing and localizing gravitational-wave transients with Advanced LIGO, Advanced Virgo and KAGRA. **Living Reviews in Relativity**, v. 21, n. 1, p. 3, abr. 2018. ISSN 1433-8351. 00479. 79
- RIGAULT, M. *et al.* CONFIRMATION OF A STAR FORMATION BIAS IN TYPE Ia SUPERNOVA DISTANCES AND ITS EFFECT ON THE MEASUREMENT OF THE HUBBLE CONSTANT. **The Astrophysical Journal**, v. 802, n. 1, p. 20, mar. 2015. ISSN 0004-637X. 00091. 80
- CIPOLLETTA, F.; CHERUBINI, C.; FILIPPI, S.; RUEDA, J. A.; RUFFINI, R. Fast rotating neutron stars with realistic nuclear matter equation of state. **Physical Review D - Particles, Fields, Gravitation and Cosmology**, v. 92, n. 2, p. 1–14, 2015. ISSN 15502368. 00044. 80
- ROTONDO, M.; RUEDA, J. A.; RUFFINI, R.; XUE, S.-S. Relativistic Feynman-Metropolis-Teller theory for white dwarfs in general relativity. **Physical Review D**, v. 84, n. 8, p. 084007, out. 2011. 00053. 80

- VERRECCHIA, F. *et al.* AGILE Observations of the Gravitational-wave Source GW170817: Constraining Gamma-Ray Emission from an NS–NS Coalescence. **The Astrophysical Journal**, v. 850, n. 2, p. L27, nov. 2017. ISSN 2041-8205. 00000. 81
- COLLABORATION, L. a. T. Fermi-LAT observations of the LIGO/Virgo event GW170817. out. 2017. 00003. 81
- MELANDRI, A. *et al.* GRB 130603B: Swift detection of a bright short burst. **GRB Coordinates Network, Circular Service, No. 14735, #1 (2013)**, v. 4735, p. 1, 2013. 00021. 82
- RUFFINI, R. *et al.* GRB 130603B: Analogy with GRB 090510A and possible connection with a supernova. **GRB Coordinates Network, Circular Service, No. 14913, #1 (2013)**, v. 4913, p. 1, 2013. 00001. 82, 83
- FREDERIKS, D. GRB 130603B: Rest-frame energetics in gamma-rays. **GRB Coordinates Network, Circular Service, No. 14772, #1 (2013)**, v. 4772, p. 1, 2013. 00004. 82
- PASQUALE, M. D. *et al.* SWIFTANDFERMIOBSERVATIONS OF THE EARLY AFTERGLOW OF THE SHORT GAMMA-RAY BURST 090510. **The Astrophysical Journal**, v. 709, n. 2, p. L146–L151, jan. 2010. ISSN 2041-8205. 00000. 83
- GUELBENZU, A. N. *et al.* The late-time afterglow of the extremely energetic short burst GRB 090510 revisited. **Astronomy & Astrophysics**, v. 538, p. L7, fev. 2012. ISSN 0004-6361, 1432-0746. 00001. 83
- YANG, B. *et al.* A possible macronova in the late afterglow of the long–short burst GRB 060614. **Nature Communications**, v. 6, p. 7323, jun. 2015. ISSN 2041-1723. 00159. 83
- LATTIMER, J. M.; MACKIE, F.; RAVENHALL, D. G.; SCHRAMM, D. N. The decompression of cold neutron star matter. **The Astrophysical Journal**, v. 213, p. 225–233, abr. 1977. ISSN 0004-637X. 00000. 83
- ARNETT, W. D. Analytic solutions for light curves of supernovae of Type II. **The Astrophysical Journal**, v. 237, p. 541–549, abr. 1980. ISSN 0004-637X. 00201. 83
- ARNETT, W. D. Type I supernovae. I - Analytic solutions for the early part of the light curve. **The Astrophysical Journal**, v. 253, p. 785–797, fev. 1982. ISSN 0004-637X. 00916. 83
- RUFFINI, R. *et al.* A GRB Afterglow Model Consistent with Hypernova Observations. **The Astrophysical Journal**, v. 869, n. 2, p. 101, dez. 2018. ISSN 0004-637X. 00003. 83
- ZHANG, B.-B. *et al.* A peculiar low-luminosity short gamma-ray burst from a double neutron star merger progenitor. **Nature Communications**, v. 9, n. 1, p. 447, jan. 2018. ISSN 2041-1723. 00035. 84

Appendix A - Publications list

A.1 Published papers

1. José D. V. Arbañil, G. A. Carvalho, R. V. Lobato, R. M. Marinho, and M. Malheiro. Extra dimensions' influence on the equilibrium and radial stability of compact objects with a linear equation of state. **Physical Review D** (2019), 100(2):024035, July 2019. 00000. arXiv:1907.07661 [gr-qc].
2. Ronaldo V. Lobato, G. A. Carvalho, A. G. Martins, and P. H. R. S. Moraes. Energy nonconservation as a link between $f(R, T)$ gravity and noncommutative quantum theory. **The European Physical Journal Plus** (2019) 134: 132. arXiv:1803.08630 [gr-qc, hep-th, math-ph], March 2018. 00000.
3. J. A. Rueda, R. Ruffini, Y. Wang, Y. Aimuratov, U. Barres de Almeida, C. L. Bianco, Y. C. Chen, R. V. Lobato, C. Maia, D. Primorac, R. Moradi, and J. F. Rodriguez. GRB 170817A-GW170817-AT 2017gfo and the observations of NS-NS, NS-WD and WD-WD mergers. **Journal of Cosmology and Astroparticle Physics**, 2018(10):006, 2018. 00000. arXiv:1802.10027 [astro-ph.HE, gr-qc].
4. G. A. Carvalho, R. V. Lobato, P. H. R. S. Moraes, José D. V. Arbañil, E. Otoniel, R. M. Marinho, and M. Malheiro. Stellar equilibrium configurations of white dwarfs in the $f(R, T)$ gravity. **The European Physical Journal C**, 77(12), December 2017. arXiv:1706.03596 [gr-qc, astro-ph.SR, hep-th, nucl-th].
5. P. H. R. S. Moraes, R. A. C. Correa, and R. V. Lobato. Analytical general solutions for static wormholes in $f(R, T)$ gravity. **Journal of Cosmology and Astroparticle Physics**, 2017(07):029, 2017. arXiv:1701.01028 [gr-qc, hep-th].
6. Ronaldo V. Lobato, Manuel Malheiro, and Jaziel G. Coelho. Magnetars and white dwarf pulsars. **International Journal of Modern Physics D**, 25(09):1641025, July 2016. arXiv:1603.00870 [astro-ph.HE, astro-ph.SR].

A.2 Proceedings

1. P. H. R. S. Moraes, J. D. V. Arbañil, G. A. Carvalho, R. V. Lobato, E. Otoniel, R. M. Marinho Jr., and M. Malheiro. Compact Astrophysical Objects in $f(R, T)$ gravity. **Proceedings of the XIV Hadron Physics 2018** arXiv:1806.04123 [gr-qc], June 2018.
2. Lobato, R.V., Coelho, J.G. and Malheiro, M., 2017. Ultra-high energy cosmic rays from white dwarf pulsars and the Hillas criterion. **Journal of Physics: Conference Series** (Vol. 861, No. 1, p. 012005). IOP Publishing.
3. Ronaldo V. Lobato, Manuel Malheiro, and Jaziel G. Coelho (2017) SGRs/AXPs as white dwarf pulsars: Sources of ultra-high energetic photons with $E \sim 10^{21}$ eV. **The Fourteenth Marcel Grossmann Meeting, WORLD SCIENTIFIC**: pp. 4313-4318.
4. M. Malheiro, R. M. Marinho, R. V. Lobato, and J. G. Coelho (2017) Are ultra-magnetized white dwarfs stable?. **The Fourteenth Marcel Grossmann Meeting, WORLD SCIENTIFIC**: pp. 4363-4371.
5. Otoniel, E., Lobato, R.V., Malheiro, M., Franzon, B., Schramm, S. and Weber, F., 2017. White Dwarf Pulsars and Very Massive Compact Ultra Magnetized White Dwarfs. **International Journal of Modern Physics: Conference Series** (Vol. 45, p. 1760024). World Scientific Publishing Company.
6. Malheiro, M., Coelho, J.G., Cáceres, D.L., de Lima, R.C.R., Lobato, R.V., Rueda, J.A. and Ruffini, R., 2017, June. Possible rotation-power nature of SGRs and AXPs. **Journal of Physics: Conference Series** (Vol. 861, No. 1, p. 012003). IOP Publishing.
7. Lobato, R.V. and Malheiro, M., 2016, April. Strong magnetic fields and SGRs/AXPs as white dwarf pulsar: a source of ultra-high energy cosmic rays. **Journal of Physics: Conference Series** (Vol. 706, No. 5, p. 052032). IOP Publishing.
8. Lobato, R.V., Coelho, J.G. and Malheiro, M., 2015, December. Radio pulsar death lines to SGRs/AXPs and white dwarfs pulsars. **AIP Conference Proceedings** (Vol. 1693, No. 1, p. 030003). AIP Publishing.
9. Lobato, R.V., Coelho, J. and Malheiro, M., 2015. Particle acceleration and radio emission for SGRs/AXPs as white dwarf pulsars. **Journal of Physics: Conference Series** (Vol. 630, No. 1, p. 012015). IOP Publishing.

FOLHA DE REGISTRO DO DOCUMENTO

1. CLASSIFICAÇÃO/TIPO <p style="text-align: center;">TD</p>	2. DATA <p style="text-align: center;">15 de Julho de 2019</p>	3. REGISTRO N° <p style="text-align: center;">DCTA/ITA/TD-015/2019</p>	4. N° DE PÁGINAS <p style="text-align: center;">114</p>
5. TÍTULO E SUBTÍTULO: <p>SGRs/AXPs and binary star mergers: electromagnetic and gravitational emission</p>			
6. AUTOR(ES): <p>Ronaldo Vieira Lobato</p>			
7. INSTITUIÇÃO(ÕES)/ÓRGÃO(S) INTERNO(S)/DIVISÃO(ÕES): <p>Instituto Tecnológico de Aeronáutica - ITA</p>			
8. PALAVRAS-CHAVE SUGERIDAS PELO AUTOR: <p>Radiation mechanisms: non-thermal, Radio lines: general - pulsars, Stars: kinematics, Binaries: close - stars, Stars: neutron - supernovae and supernova remnants</p>			
9. PALAVRAS-CHAVE RESULTANTES DE INDEXAÇÃO: <p>Estrelas anãs; Raios gama; Estrela de nêutrons; Campos magnéticos; Radiofrequência; Astrofísica; Física.</p>			
10. APRESENTAÇÃO: (X) Nacional () Internacional <p>ITA, São José dos Campos. Curso de Doutorado. Programa de Pós-Graduação em Física. Área de Física Nuclear. Orientador: Prof. Dr. Manuel Máximo Bastos Malheiro de Oliveira; coorientadores: Prof. Dr. Jorge Armando Rueda Hernández; Prof. Dr. Jaziel Goulart Coelho. Defesa em 08/07/2019. Publicada em 2019</p>			
11. RESUMO: <p>In this work, we discuss the white dwarf pulsars found recently and the massive and magnetic white dwarfs reported in the few years. We make the reference of the possibility of some soft γ repeaters (SGRs) and anomalous X-ray pulsars (AXPs) being part of this class of white dwarfs pulsars. Using self-consistently models which consider the sources' rotation and a realistic EoS, we estimate the mass, radius and moment of inertia of these sources as white dwarfs (WD). We also review them as neutrons stars (NS) with self-consistently models estimating the radius in both cases. We investigated these sources as WDs and NSs within of the context of high energy emission, studying hard X-ray, γ and radio band. The pair condition with realist parameters is calculated and the death lines for the electromagnetic radiation are obtained for γ production and consequently for radio emission. We have shown that the size of the source, i.e. the radius of the star R, and the ratio between it and the light cylinder R_{lc}, are important scales to understand the electromagnetic emission in these models. We conclude that the observed electromagnetic emission for soft gamma rays and the absence of radio radiation are better understood in a description of SGRs/AXPs as white dwarf pulsars, where this ratio between R_{lc} and R is 100 times smaller than in the case of magnetars. This fact, allows us to conclude that for SGRs/AXPs as white dwarfs the magnetic field in the light cylinder is 100 times more intense than as neutron stars, thus facilitating the emission in hard X-rays and soft gamma rays. We also study the properties of binary systems composed of NS-NS, WD-NS, WD-WD analyzing the event GW170817, trying to understand the nature and mechanism of the high energy emission of this event. We analyzed in particular the electromagnetic emission of a new type of two white dwarf merger (WD-WD), which may be the progenitor of very massive, fast and magnetic white dwarfs. We show that the gravitational wave received in the GW170817 event as a result of a fusion of neutron stars, is not compatible with the observed electromagnetic counterpart, that seems come from a WD-WD merger.</p>			
12. GRAU DE SIGILO: <p style="text-align: center;">(X) OSTENSIVO () RESERVADO () SECRETO</p>			